Thermoresponsive Nanocapsules with Suitable Mechanical Properties for Skin Hydration

Inaugural-Dissertation

to obtain the academic degree

Doctor rerum naturalium (Dr. rer. nat.)

submitted to the Department of Biology, Chemistry, Pharmacy of Freie Universität Berlin

by

Ernesto Rafael Osorio Blanco

Berlin

2020

I hereby declare that the submitted thesis is my own work and was prepared without the aid of other sources than the ones cited and acknowledged. This work has not been submitted to any other prior doctoral procedure.

Ernesto Rafael Osorio Blanco Berlin, den 26.06.2020

The following PhD thesis was carried out from January 2017 until May 2020 in the research group of Prof. Dr. Marcelo Calderón at the department of Biology, Chemistry, Pharmacy in the Freie Universität Berlin.

1st Reviewer: Prof. Dr. Marcelo Calderón

2nd Reviewer: Prof. Dr. Rainer Haag

Date of thesis defense: September 18th 2020

Acknowledgements

I would like to use this opportunity to express my gratitude to my mentor and doctoral father, **Prof. Dr. Marcelo Calderón**, who not only gave me the opportunity to conduct my doctoral thesis in his research group, but also provided me with excellent guidance and mentorship. I want to explicitly thank him for creating a nurturing, friendly research environment in which I was allowed to grow personally and professionally. In addition, I would like to thank him for all the vital lessons taught in research and on life and for all the life-long fun memories.
I would like to use this opportunity to express my gratitude towards **Prof. Dr. Rainer Haag** for being the co-referee of this doctoral thesis and for mentoring me after my research group moved to Spain. I want to explicitly thank him for allowing me to use his laboratories and equipment, as well as for making me feel part of the AG Haag family.

I would like to thank the Collaborative Research Center 1112 of the SFB 1112, as well as the Dahlem Research School for their financial support throughout my doctoral thesis.

I am grateful for the people who worked on the Collaborative Research Center 1112 for the outstanding collaborations, which are fundamental for this work:
Dr. Fiorenza Rancan for the great scientific discussions and outstanding collaboration.
Prof. Dr. Sarah Hedtrich and Prof. Dr. Daniel Klinger for their mentorship during the first years of this doctoral work.
Prof. Dr. Eckart Rühl, Prof. Dr. Annika Vogt, Prof. Dr. Martina Meinke, Prof. Dr. Ulrike Alexiev, Dr. André Klossek, Pin Dong, Johannes Stellmacher.

I am deeply honored to have had the opportunity to work during part of my doctoral thesis in Polymat. For this, I am thankful to Prof. Dr. Marcelo Calderón for opening this incredible possibility and to Prof. Dr. José M. Asua for letting me use his laboratories as well as mentoring me during my stay. My gratitude goes to his group, for helping me adapt to a new culture and learn new techniques. I would like to thank Dr. Nicholas Ballard and Dr. Alexandre Simula for their guidance. A special eskerrik asko goes to Dr. Nikolaos Politakos, Dr. Adrián Badia, Dr. Sebastian Dron, Dr. Elodie Limousin, Dr. Boris Bizet, Fabian Wenzel, Justine Elgoyhen, and metal eskerrik asko go to Adrián Pérez López.

I would also like to thank Prof. Dr. Alejandro Müller and Dr. Oihane Sanz for their friendship and great introduction into the gastronomy of the bask country.

I would like to thank Dr. Jose Luis Cuéllar-Camacho and Dr. Christoph Böttcher for teaching me state-of-the-art techniques for characterizing my nanoparticles.

I am especially thankful for the outstanding guidance and support of my subgroup leader Dr. Julián Bergueiro Álvarez. His thoughtful suggestions and guidance were fundamental for my professional and personal growth.

I would like to thank all the members of the Calderón group for helping create a relaxed, fun work-atmosphere during my doctoral work. I would like to thank the German branch of the Calderón group for all the fun times: Dr. Julián Bergueiro Álvarez, Dr. Stefanie Wedepohl, Dr. Catalina Biglione, Dr. Enrico Miceli, Dr. Gregor Nagel, Dr. Laura Voßen, Dr. Mazdak Asadian Birjand, Dr. Michael Giulbudagian, Dr. Emanuel Glitscher, Dr. Loryn Theune, Dr. Lydia Bouchet, Dr. Mrityunjoy Kar, Dr. Lucila Navarro. I would also like to thank the Spanish branch of the Calderón Group for the exciting new beginning and the pintxo potes: Dr. Neha Tiwari, Huiyi Wang (aka Tracy), David Esporrín Ubieto and Oliver Wolfgang Etzold.

I am very grateful to the former and present members of the Haag group for welcoming me with open arms. A special mention goes to: Dr. Wiebke Fischer, Dr. Carlo Fasting, Dr. Stefanie Wedepohl, Dr. Luis Cuéllar-Camacho, Dr. Christoph Schlaich, Dr. Mathias Dimde, Dr. Magda Ferraro, Dr. Ehsan Mohammadifar, Dr. Olaf Wagner, Dipl.-SpOec. Eike Ziegler, Ann-Cathrin Schmitt, Felix Reisbeck, Paria Pouyan, Michaël Kulka, Isabelle Heing-Becker and Daniel Braatz.

Special thanks go to my office and coffee group, those little reality breaks were a great source of energy: Dr. Stefanie Wedepohl, Dr. Mathias Dimde, Dr. Gregor Nagel, Dr. Loryn Theune, Dr. Emanuel Glitscher, Dr. Enrico Miceli, Dr. Olaf Wagner, Dr. Ehsan Mohammadifar, Felix Reisbeck, Daniel Braatz, Mariam Cherri and Ann-Cathrin Schmitt.

I would like to thank team Venezuela: Dr. Daniel Martinez-Tong, Dr. Daniel Arismendi (aka Dani 1 & Dani 2) and Erick Gerlach Rill; team la France: Dr. Elodie Limousin, Dr. Boris Bizet, Dr. Alexandre Simula and Justine Elgoyhen; team pumping and eating Brüder: Dr. Enrico Miceli, Fabian Wenzel and Pedro von Braunmühl, and team inglorious: Dr. Boris Bizet, Dr. Philip Scott and Guus Engels for their wonderful friendship and support.

I am very grateful for the support and love of my family. Despise all the obstacles and the long distance, the unconditional love of my parents gave me strength.

Above all, I want to thank my wife and partner in crime Paulina Osorio Samardakiewicz for her love and support. I would not be here without you and I am the luckiest person to be able to share my life with you.

Abstract

The skin is the largest organ of the human body. It fulfills various functions, such as preventing the loss of salts and fluids as well as regulates the body temperature. In addition, the skin acts as a highly complex and effective biological barrier, hindering the penetration of harmful substances (feature mostly attributed to the stratum corneum; SC). Overcoming the SC represents a great challenge in dermal and transdermal therapies, leading to the development of multiple strategies to enable the permeation of therapeutics across the skin. Using penetration enhancers (chemical or physical) has proven to increase the penetration of therapeutics. Nevertheless, the use of penetration enhancers exposes a great risk, as they can lead to permanent damage on the skin, reducing its barrier efficiency and resulting in the intrusion of harmful substances, which can result in inflammation.

Nanoparticle based dermal and transdermal drug delivery approaches represent promising tools to deliver drugs to the target site, while reducing or eliminating side effects. It has been found that soft nanoparticles can induce skin hydration and subsequently deliver therapeutics into the skin. Due to their high surface area, tunable sizes, easy functionalization (*in situ* or post-synthetic) and large encapsulation capacities, nanocapsules (NCs) represent a promising strategy for topical drug delivery. NCs are generally defined as hollow nanoparticles composed of a cross-linked shell surrounding a core forming space. Herein, we aim to synthesize soft thermoresponsive nanocapsules (tNCs) to induce skin hydration, thus enabling the skin penetration of high molecular compounds. For this purpose, NCs with a thermoresponsive shell and a void of 100 nm diameter, were synthesized. These NCs can shrink or swell upon a thermal trigger, which can be used to induce the release of water and or other encapsulated molecules in a controlled fashion. The tNCs were built using silica nanoparticles as sacrificial templates (to ensure the reproducibility or their core) in a seeded precipitation polymerization. Different ratios of poly(*N*-isopropylacrylamide) (PNIPAM) and poly(*N*-isopropylmethacrylamide) (PNIPMAM) were employed as thermoresponsive polymers and either *N,N*'-methylenebisacrylamide (BIS) as cross-linker or dendritic polyglycerol (dPG) as macrocross-linker were utilized to build the tNCs' shell.

Firstly, the effect of the synthesis on the mechanical properties of the tNCs was investigated. For this purpose, a comprehensive study was performed to investigate the mechanical properties of well-known (PNIPAM-BIS) thermoresponsive nanoparticles. In the study,

nanogels, nanogels with a hard core and nanocapsules were investigated below and above the volume phase transition temperature (temperature at which the particles change from a swollen state to a collapsed state) (VPTT) using nanoparticle tracking analysis (NTA), cryogenic-electron microscopy/electron tomography, and atomic force microscopy (AFM) in liquid. It could be shown, that the different structure of the particles affects their thermoresponsive behavior. Moreover, outstanding thermomechanical changes were found for the NCs (Young modulus changes from kPa to GPa upon crossing the VPTT). These findings underline the importance of fully characterizing the particles as their thermomechanical properties could enhance or limit their further applications. Additionally, these results were used to rationally design novel tNCs to induce skin hydration using dPG to introduce non-thermoresponsive domains within the shell; thus, leading to flexible materials even above the VPTT. By varying the ratio between PNIPAM and PNIPMAM, the VPTT, as well as the shell density, could be controlled. Next, the interactions and effects of tNCs on the stratum corneum were investigated using fluorescence microscopy, high resolution microscopy, and stimulated Raman spectromicroscopy. It could be shown, that the thermoresponsive properties of the tNCs could increase skin hydration. Finally, the potential of the NCs as penetration enhancer was assessed by using Atto Oxa12 NHS ester (a high molecular weight dye) as a model drug. It could be demonstrated, that the NCs increased the penetration of Atto Oxa12 in comparison to an aqueous formulation and a solution of the dye in 30% DMSO. This thesis demonstrates that both material properties and core-nanoarchitecture can considerably affect the thermomechanical properties of soft nanoparticles. In addition, it could be proven that the dPG-based tNCs cause skin hydration and that their thermoresponsive features can further enhance the hydration of the skin. Moreover, this work underlines the outstanding potential of tNCs to act as penetration enhancers for high molecular weight compounds by inducing skin hydration.

Kurzzusammenfassung

Die Haut ist das größte Organ des menschlichen Körpers. Sie erfüllt verschiedene Funktionen, z. B. die Verhinderung des Verlusts von Salzen und Flüssigkeiten sowie die Regulierung der Körpertemperatur. Darüber hinaus wirkt die Haut als hochkomplexe und wirksame biologische Barriere, die das Eindringen von Schadstoffen verhindert (ein Merkmal, das hauptsächlich dem *Stratum Corneum* zugeschrieben wird; SC). Die Überwindung des SC stellt eine große Herausforderung für dermale und transdermale Therapien dar und führte zur Entwicklung mehrerer Strategien, um das Eindringen von Therapeutika in die Haut zu ermöglichen. Um die Penetration von Therapeutika zu verbessern, werden sogenannte penetrationsverstärker (chemisch oder physikalisch) eingesetzt. Ihre Verwendung stellt jedoch ein großes Risiko dar, da sie permanente Schäden an der Haut erzeugen können. Außerdem kann durch die Verwendung von Penetrationsverstärkern die Barriereeffizienz der Haut verringert werden und dadurch das Eindringen von Schadstoffen ermöglichen, die zu Entzündungen führen können.

Auf Nanopartikeln basierende dermale und transdermale Wirkstofftransporter stellen vielversprechende Werkzeuge dar, um Arzneimittel an die Zielstelle zu transportieren und dadurch Nebenwirkungen zu reduzieren oder zu eliminieren. Es wurde festgestellt, dass weiche Nanopartikel die Haut hydrieren und dadurch den Transport von Therapeutika in die Haut ermöglichen können. Nanokapseln (NCs) sind aufgrund ihrer großen Oberfläche, einstellbaren Größen, einfachen Funktionalisierung (*in situ* oder postsynthetisch) und großen Verkapselungskapazitäten eine vielversprechende Strategie für den topischen Wirkstofftransport. Nanokapseln werden im Allgemeinen als hohle Nanopartikel definiert, die aus einer vernetzten Hülle bestehen, die einen Kernbildungsraum umgibt. In der vorliegenden Arbeit wollen wir weiche thermoresponsive Nanokapseln (tNCs) synthetisieren, um die Haut zu hydrieren und so das Eindringen hochmolekularer Verbindungen in die Haut zu ermöglichen. Zu diesem Zweck wurden NCs mit einer thermoresponsiven Hülle und einem Hohlraum von etwa 100 nm Durchmesser synthetisiert. Diese NCs können nach einem thermischen Stimulus schrumpfen oder anschwellen, wodurch die Freisetzung von Wasser und anderen eingekapselten Molekülen auf kontrollierte Weise induziert werden kann. Die

tNCs wurden unter Verwendung von Silika-Nanopartikeln als Opfertemplat (um die Reproduzierbarkeit des Kerns zu gewährleisten) in einer angeimpften Fällungspolymerisation hergestellt. Verschiedene Verhältnisse von Poly (*N*-isopropylacrylamid) (PNIPAM) und Poly (*N*-isopropylmethacrylamid) (PNIPMAM) wurden als thermoresponsive Polymere verwendet und *N, N*'-Methylenbisacrylamid (BIS) oder dendritisches Polyglycerol (dPG) wurden als Vernetzer bzw. als Makrovernetzer verwendet, um die Schale der tNCs zu aufzubauen.

Zunächst wurde der Einfluss einiger Syntheseparameter auf die mechanischen Eigenschaften der tNCs untersucht. Zu diesem Zweck wurde eine umfassende Studie durchgeführt, um die mechanischen Eigenschaften bekannter (PNIPAM-BIS) thermoresponsiver Nanopartikel zu analysieren. Nanogele, Nanogele mit einem harten Kern und tNCs wurden unterhalb und oberhalb der Volumen-Phasenübergangs-Temperatur (Temperatur, bei der die Partikel von einem gequollenen Zustand in einen kollabierten Zustand übergehen) (VPTT) mithilfe von Nanopartikel-Tracking-Analyse (NTA), Kryoelektronenmikroskopie/Elektronentomographie und Rasterkraftmikroskopie (AFM) in Lösung untersucht. Es konnte gezeigt werden, dass die unterschiedlichen Architekturen das thermoresponsive Verhalten der Partikel beeinflusst. Darüber hinaus wurden herausragende thermomechanische Änderungen für die NCs gefunden (Young-Modul-Änderungen von kPa zu GPa beim Überqueren der VPTT). Diese Ergebnisse unterstreichen die Bedeutung einer vollständigen Charakterisierung der Partikel, da ihre thermomechanischen Eigenschaften ihre weiteren Anwendungen verbessern oder einschränken könnten. Zusätzlich wurden diese Ergebnisse verwendet, um neuartige tNCs zu entwerfen, um die Haut zu hydrieren. Dafür wurde dPG eingesetzt, um nicht-thermoresponsive Bereiche innerhalb der Schale einzuführen, wodurch die Synthese von flexiblen Partikeln auch oberhalb der VPTT möglich werden sollte. Durch Variation des Verhältnisses zwischen PNIPAM und PNIPMAM konnten die VPTTs sowie die Vernetzungsdichte der Schalen gesteuert werden. Als nächstes wurden die Wechselwirkungen und Wirkungen von tNCs auf das SC unter Verwendung von Fluoreszenzmikroskopie, hochauflösender Mikroskopie und stimulierter Raman-Spektromikroskopie untersucht. Es konnte gezeigt werden, dass die thermoresponsiven Eigenschaften der tNCs die Hydrierung der Haut erhöhen können. Schließlich wurde das Potenzial der tNCs als Penetrationsverstärker unter Verwendung von Atto Oxa12 NHS-Ester (einem Farbstoff mit hohem Molekulargewicht) als Modellwirkstoff bewertet. Es konnte

gezeigt werden, dass die tNCs die Penetration von Atto Oxa12 im Vergleich zu einer wässrigen Formulierung und einer Lösung des reinen Farbstoffs in 30% DMSO erhöhten.

Diese Arbeit zeigt, dass sowohl die Materialeigenschaften als auch die Nanoarchitektur des Kerns die thermomechanischen Eigenschaften weicher Nanopartikel erheblich beeinflussen können. Darüber hinaus konnte nachgewiesen werden, dass die auf dPG basierenden tNCs die Haut hydrieren können und dass ihre thermoresponsiven Eigenschaften die Feuchtigkeitsversorgung der Haut weiter verbessern können. Darüber hinaus unterstreicht diese Arbeit das herausragende Potenzial von tNCs, als Penetrationsverstärker für Verbindungen mit hohem Molekulargewicht zu wirken.

Table of Contents:

1 Introduction

Due to its good accessibility and large surface area, the skin is regarded as an attractive administration route in drug delivery.[1] It has been demonstrated, that by applying therapeutic agents directly on the skin, side effects can be minimized as well as patient compliance can be improved.[2] The main challenge for both topical and transdermal therapies is to overcome the skin as a physical barrier.[3] Among the diverse functions of the skin, perhaps the most important one is to hinder the intrusion of harmful substances from the environment into the human body. This feature is mostly attributed to the stratum corneum (SC).[4,5] Overcoming the SC is one of the greatest challenges in topical and transdermal drug delivery. Although both drug delivery strategies are applied on the skin, their concepts and effects are different. Topical drug delivery induces a localized effect, increasing the total amount of drugs on the skin as well as reducing undesired side effects. Using topical drugs eliminates the need for systemically administered drug therapies. Contrary to topical drug delivery, transdermal drug delivery is utilized to induce a systemic effect. In this type of therapy, the skin is regarded solely as the entry for therapeutics into the body. Despite their different goals, in both topical and transdermal therapies overcoming the SC is crucial and directly affects the efficacy of the therapy.

1.1 General Structure of the Skin

The skin can be divided in mainly two layers: epidermis and dermis (**Figure 1**).

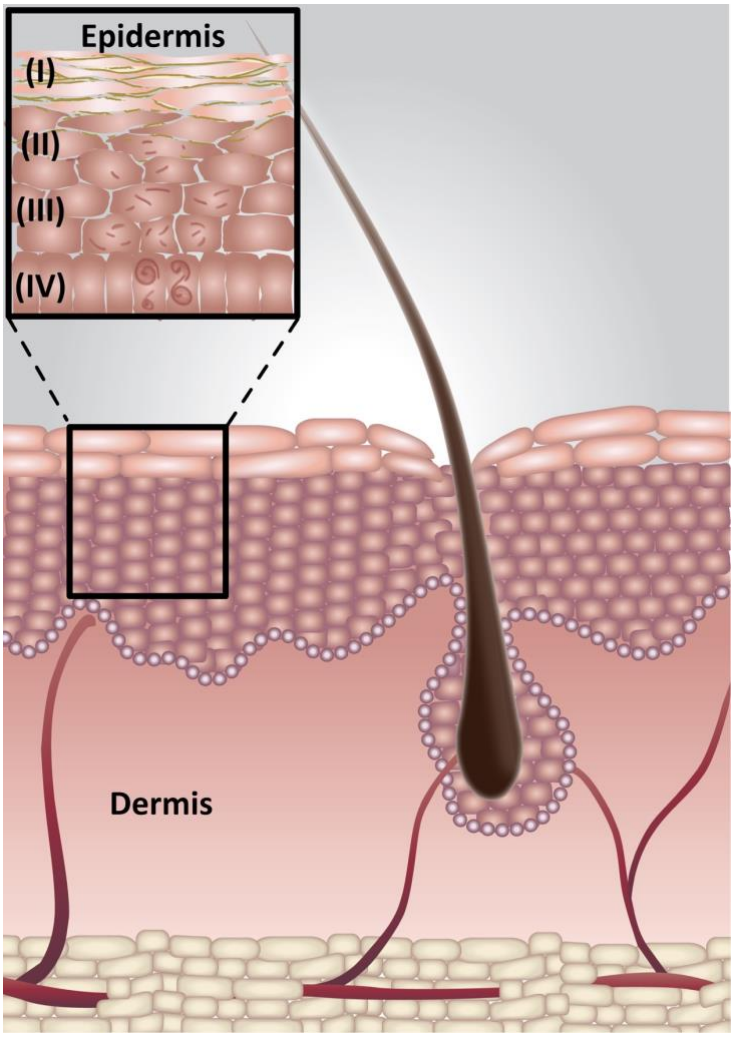

Figure 1: The skin layers and the subdivisions of the epidermis: (I) stratum corneum, (II) stratum granulosum, (III) stratum spinosum and (IV) stratum basale.

The **epidermis** is the outermost layer of the skin, only interrupted by hair follicles and sweat glands. As it is hindering the loss of water/salts as well as the intrusion of foreign agents into the skin, it has important protective functions. The epidermis is comprised of five different layers (Table 1); the deepest layer (stratum basale) is where keratinocytes originate and migrate towards the skin surface, while undergoing different biological modifications such as increasing keratinization (**Figure 1, inlet**).[6,7]

Table 1: Layers of the stratum corneum and their characteristics.

Epidermis layer	Characteristics
(IV) Stratum basale	Deepest layer of the epidermis; place of origin of keratinocytes.
(III) Stratum spinosum	Keratinocytes flatten and become prickle like (spiny cells).
(II) Stratum granulosum	Beginning of keratinization and start of the apoptosis of the keratinocytes. Cells produce granules of keratohyalin, which later becomes keratin.
Stratum lucidum	Only present in thick skin (e.g. soles of the feet). Cells are flattened, lack nucleus and cannot be distinguished from each other.
(I) Stratum corneum	Outermost layer of the epidermis. Comprised of proteins (mainly keratin), lipids and dead keratinocytes. The dead keratinocytes are renewed periodically (usually every 28 days in healthy skin) in a process denominated desquamation.

The **dermis** is the largest part of the skin. It is located directly beneath the epidermis and its main role is to provide structural support to the skin.[8] The dermis comprises of both collagen and elastin, embedded in a gel-like substance which is rich in hyaluronic acid (ground substance).[9] Moreover, the dermis contains blood vessels and hair follicles, which not only transport nutrients to the epidermis, but also absorb components through the skin into the systemic circulation.[8,9]

1.2 Penetration Routes

The stratum corneum (SC) selectively discriminates the substances (small molecules and micro/ nanoparticles) that can permeate through or into the skin. Three main permeation routes are described: intracellular, intercellular and through the hair follicle (**Figure 2**).[10] The **intracellular route** is the most direct and fast pathway for a substance to permeate the skin; however, this pathway is very challenging as the particle needs to overcome the lipophilic and lipophobic structures within the skin cells.[11] The **intercellular route** is one of the most common skin permeation mechanisms, wherein the penetrating substance crosses the SC by

diffusion between the cells. It has been proposed, that for this pathway, the penetrating particle needs to be flexible.[12] Rigid substances (e.g. rigid particles) have been found to rather stay on the surface of the SC as they are not flexible enough for the intercellular pathway.[13] For rigid particles the preferred route for penetrating the skin is *via* the hair follicle; however, hair follicle penetration has been found to be highly dependent on the size and rigidity of the particles.[14] Calderón et al. synthesized nanogels with different sizes and studied their hair follicle penetration. Nanogels with sizes between 300 nm and 500 nm exhibited effective hair follicle penetration.[15]

The limitations imposed by the barrier function of the SC lead to the investigation and development of compounds that can increase the penetration across the skin, so-called penetration enhancers.

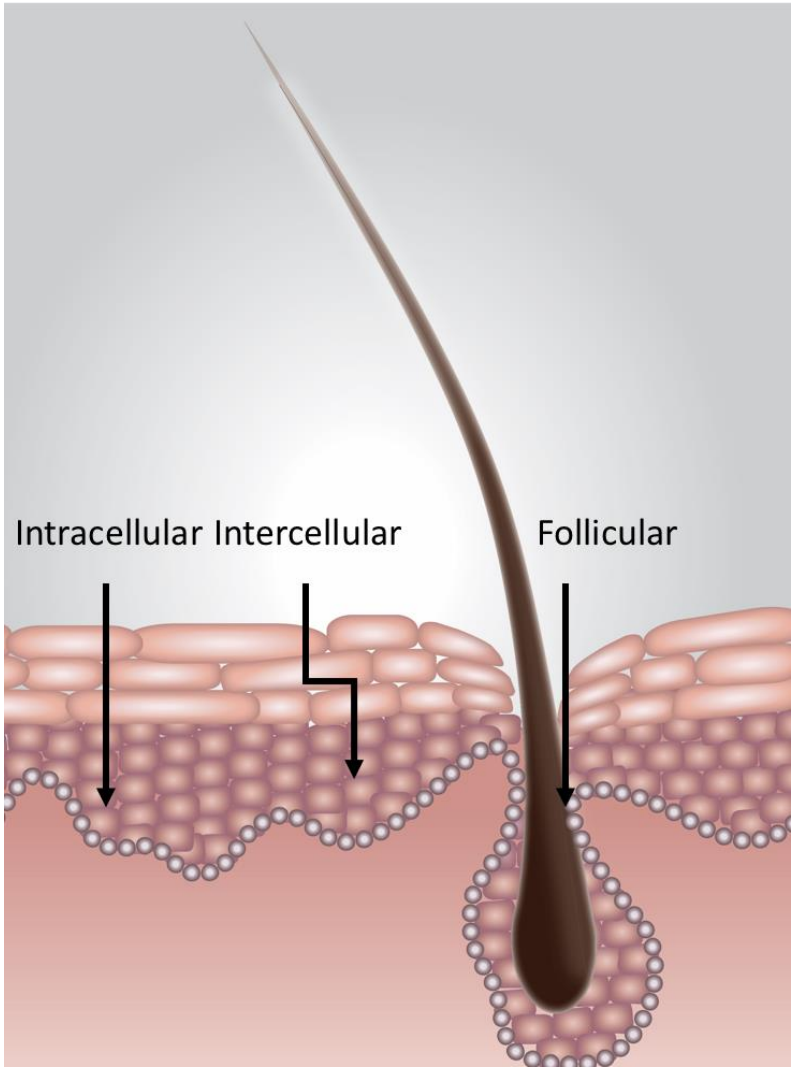

Figure 2: Schematic representation of the main three skin penetration routes.

1.3 Penetration Enhancers*

Penetration enhancers are compounds or methods which aid the intrusion of other molecules/therapeutics into the deepest layers of the skin, either by changing the solubility of the transported therapeutic or by disrupting the SC, and are mostly used in transdermal therapies.[16,17] Penetration enhancers can be categorized into two classes: physical or chemical penetration enhancers.[18]

1.3.1 Physical Penetration Enhancers

The physical disruption of the SC can be achieved by utilizing electroporation, ultrasound, jet injection or microneedles (**Figure 3**).[16]

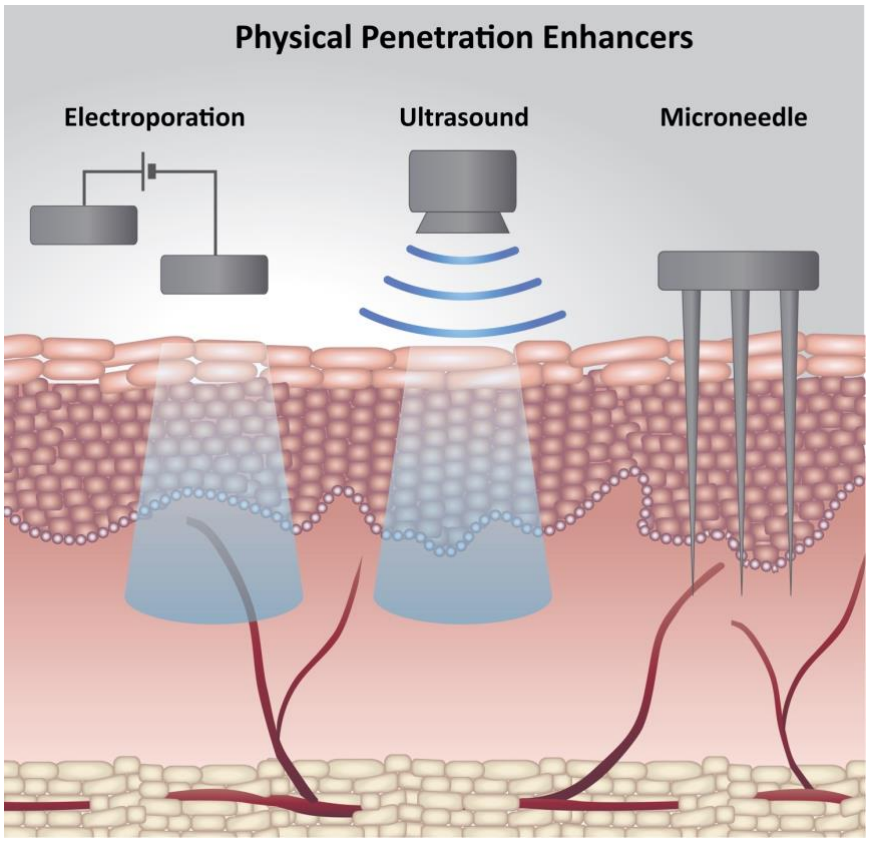

Figure 3: Examples of commonly used physical penetration enhancers.

**The following segments (Penetration Enhancers to Chemical Penetration Enhancers) are part or have been modified from the review entitled: Smart nanocarriers for skin applications: from basic studies to clinical development. In the mentioned publication, the author revised and summarized relevant literature. The author developed the outline and worked on the manuscript together with the other co-authors.*

Physical penetration enhancers can be further categorized into methods that do not puncture the skin (hence no pores are created e.g. electroporation, iontophoresis and sonophoresis), and methods that puncture the skin (e.g. microneedles).[18] Techniques that do not puncture the skin enhance the skin penetration by permeabilizing the lipid bilayers in the skin. These techniques are associated with the use of short duration and high intensity electric pulses (electroporation), continuous low intensity electric field at a constant current (iontophoresis)[19] and low frequency ultrasound (sonophoresis).[20] However, they are usually expensive, have a limited application area and rather limited penetration depths.[21] An attractive alternative is to use techniques which create channels (pores) within the skin (e.g. microporation and microneedles). In microporation, an electric current is pulsed through the array of resistive elements placed on the skin resulting in localized ablation of the corneocytes in the SC.[22,23] Intradermal injections using microneedles is another popular technique for the direct delivery of therapeutics (irrespective of their size) to the viable tissue layers of the skin using several micrometer sized needles.[24] This is the easiest and cheap technique for the transdermal delivery and with the advancement in the technology various kinds of microneedles are available including solid, coated, dissolving and hollow.[25] Recently microneedles have been attracting great interest as these can be used to create micron size pathways in the skin, helping the drug reaching the epidermis or upper dermis, from where they can enter the systemic circulation.[26] Microneedles can also be designed to degrade under specific conditions, helping to control the release of the transported cargo.[26-29] Prausnitz et al, reported the development of a reversible contraceptive microneedle patch to slowly release the contraceptive hormone, levonorgestrel. The slow release of levonorgestrel was achieved by the slow degradation of poly(lactic-co-glycolic) acid, which was used for encapsulating the drug, over the course of a month in rats.[30] Jung et al, investigated the delivery of a wide range of biomolecules (including vaccines, peptides and proteins) across the skin by employing hyaluronic acid backbone-based dissolving microneedles (DMNs). In this study, the authors optimized the shape of the microneedles to achieve tissue interlocking (TI) as well as enhance the penetration efficacy of various biomolecules into mouse skin.[31]

1.3.2 Chemical Penetration Enhancers

Another commonly used strategy to enhance the penetration of compounds into the skin is the co-formulation with chemical agents which disturb the SC. There is a great number of chemical compounds able to enhance skin penetration (**Figure 4** and Table 2). Their effect on the skin depends on the chemical class of the compound and its specific interaction with the skin.[28]

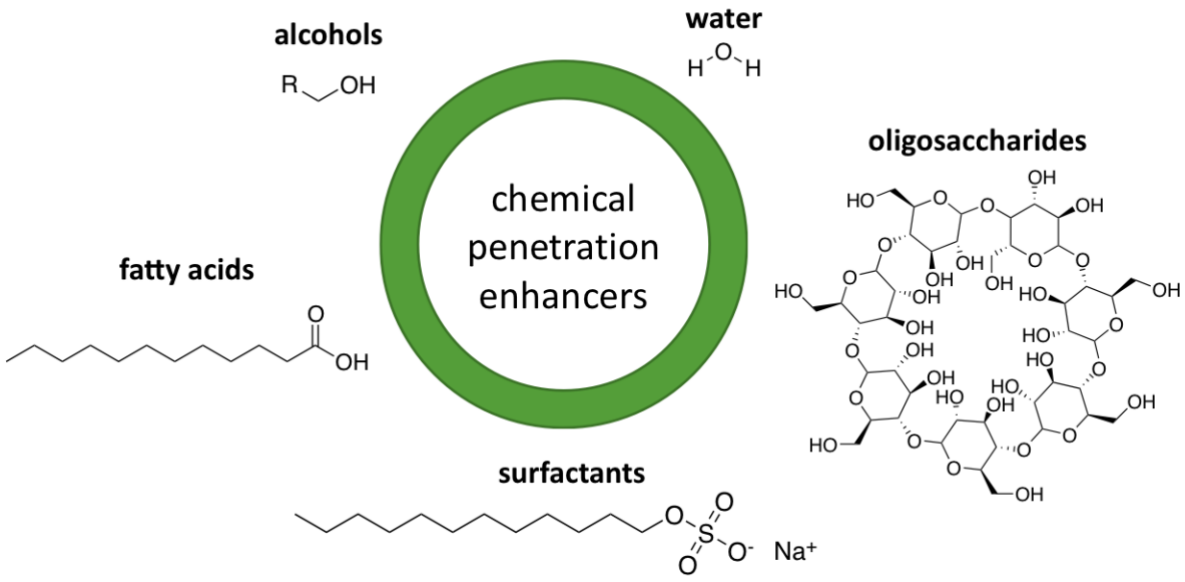

Figure 4: Examples and structures of commonly used chemical penetration enhancers.

Table 2: List of selected chemical penetration enhancers and their chemical class.

Chemical class	**Enhancer**
Alcohols	Ethanol, propanol, isopropyl alcohol, decanol, octanol, oleyl alcohol
Fatty acids	Lauric acid, linoleic acid, stearic acid
Surfactants	Sodium lauryl sulphate, Tween 80, alkyl trimethyl ammonium halides
Oligosaccharides	Cyclodextrin
Water	Water

Short chain alcohols like ethanol and isopropyl alcohol are known to have skin penetration features; however, their exact mode of action still needs to be clarified. In a comparative study by Fuji, Imai et al., the penetration enhancement of ethanol, propanol and iso-propanol were

investigated on Yucatan micropig skin using p-hydroxy benzoic acid methyl ester (HBM) as a model pro-drug.[32] This study showed that all three alcohols were able to enhance the penetration of HBM; however, the metabolism of HBM in the skin was found to be alcohol dependent. It was found that each alcohol induced different species and amount of metabolite which ended up modifying the skin permeation and retention of the drug. These results highlight the importance of understanding the effect of the alcohol metabolites on the drug metabolism within the skin before topical application. Esters of terpene alcohols were also found to induce skin penetration. Vávrová et al., synthesized hybrid terpene-amino acids from a great variety of natural terpenes (e.g. citronellol, nerol, linalool, menthol, etc.) and 6-(dimethylamino) hexanoic acid using ester linkage.[33] The skin penetration features of the obtained compounds was assessed *ex vivo* by studying their ability to enhance the delivery of theophylline and hydrocortisone in human skin. Especially citronellyl, bornyl and cinnamyl esters demonstrated great penetration enhancing properties as well as low cellular toxicity. Utilizing infrared spectroscopy, it was implied that the esters fluidized the SC; however, transepidermal water loss and electrical impedance investigations of the treated skin revealed full recovery after 24 h.

Other chemical classes that enjoy great representation in commercially available products are fatty acids and surfactants. Fatty acids are part of diverse plant oils such as jojoba oil, coconut oil or olive oil and have been found to be beneficial for the skin, hence, being part of many skin care products (e.g. lauric acid or linoleic acid).[34] Kim et al., studied the effects of chain length and unsaturation degree of various fatty acids on the penetration enhancement of diclofenac on rat skin.[35] Propylene glycol was used to solubilize the fatty acid and diclofenac, while Keshary-Chien diffusion cells were employed to investigate the permeation of the drug through rat skin. Utilizing saturated fatty acids, a correlation between their enhancement efficacy and the length of their carbon chain was reported. It was found that palmitic acid exhibited the greatest permeation rate among the tested saturated fatty acids. Interestingly, when investigating the permeation effect induced by unsaturated fatty acids, a combination effect between the fatty acid and propylene glycol was established. Oleic acid was found to exhibit the greatest penetration enhancement properties among the studied unsaturated fatty acids.

Most of the investigations regarding the penetration enhancement features of fatty acids are performed in presence of a co-solvent, hence the analysis of the individual properties of the

fatty acids in question are difficult to investigate. In an effort to address this issue, Li et al. studied the penetration enhancement properties of commonly used fatty acids to transport estradiol (E2ß) through human epidermal membrane (HEM) in presence of volatile solvents as co-solvents.[36] Furthermore, they investigated the permeation enhancement effect *Emax* of the fatty acids. *Emax* refers to the permeation enhancement achieved by a compound on the lipoidal pathway of HEM close to a thermodynamic equilibrium. It was claimed that saturating the SC lipid domain with high amounts of fatty acids induces comparable conditions to when *Emax* is reached. SC uptake studies hinted that the penetration enhancement mechanism induced by the fatty acids was induced by mostly enhancing the penetration partitioning into the SC intercellular lipid domain.

Surfactants are one of the most commercially used penetration enhancers, they are part of many formulations in various products ranging from cosmetics to pharmaceutics.[37] Surfactants disrupt the lipid and protein layers in the stratum corneum, therefore enhancing the penetration of formulated molecules. The chemical properties of surfactants to self-assemble into micelles increase the solubility of strong hydrophobic compounds leading to stable formulations. However, high amounts of surfactants often cause irritation. Sodium lauryl sulfate (SLS) is an anionic surfactant, widely used due to its ability to enhance skin penetration by increasing the fluidity of epidermal lipids.[38] Bergeron et al., investigated the influence of SLS on the efficiency of gel formulations containing foscarnet, an antiviral agent, against herpes simplex virus type 1 (HSV-1) infected mice. It was found that adding 5% of SLS to the gel formulation lead to a significant reduction of the lesion score, which was attributed to the enhanced penetration of foscarnet into the epidermis. Further studies revealed that SLS also inhibited cytopathic effects caused by the strain F of the HSV-1.[37]

An interesting strategy is the combination of surfactants. Mitragotri et al., reported on the effects of using sodium dodecyl sulfate (SDS) and dodecyl trimethylammonium bromide (C_{12}TAB) on the skin barrier. It was found that the addition of C_{12}TAB reduced the disruption of the skin barrier properties induced by SDS while C_{12}TAB decreased the concentration of monomers and sub-micellar aggregates. It could be shown that the concentration of monomers and sub-micellar aggregates directly correlate with the perturbation of the skin barrier properties. In contrast, the total surfactant concentration was not found to have a correlation with the surfactant induced skin barrier disruption.[39]

Another class of well-known chemical penetration enhancer are oligosaccharides, among these, especially cyclodextrins (CDs) have been extensively investigated. Cyclodextrins are natural cyclic oligosaccharides, comprised of D-glucopyranose units linked by α–(1,4) glycosidic bonds. A typical characteristic for CDs is their hydrophilic outer surface as well as hydrophobic core. This core is usually exploited to entrap small hydrophobic compounds.[40] Although, CD is known to be a penetration enhancer, the exact permeation mechanism has still not been revealed. Some authors claim that the drugs entrapped within CD are in a diffusive form, due to the solubilization in the CDs, at their exterior and hence separating from the CDs void into the lipophilic barrier.[41] In contrast, other reports suggest that the CDs could extract some of the lipophilic components of the SC, thus disrupting the otherwise highly ordered barrier.[42]

Jain et al., reported the use of cyclodextrin to solubilize curcumin as well as enhance its skin penetration through rat skin.[43] This work highlights the increased permeability of curcumin when complexed in CD. Furthermore, it could be demonstrated that the curcumin-CD complex caused less irritation as compared to curcumin alone. Using a paw edema model to test the anti-inflammatory efficacy of the curcumin-CD complex revealed significant enhanced biological activity in comparison to the curcumin gel alone.

Among the penetration enhancers, water is a special case, as it is inexpensive, and the skin can quickly recover from its exposure. Many clinical formulations and products (e.g. ointments, patches) utilize water to enhance the penetration of formulated drugs.[18] Generally, the skin hydration seems to increase the transdermal delivery of both hydrophilic and hydrophobic compounds, although in some cases hydrophobic compounds have been found to not penetrate and further induce skin irritation.[18,28]

Nanoparticles able to induce skin hydration have been found to be advantageous in skin delivery applications, as these can enhance the penetration of previously encapsulated cargos.

1.4 Nanoparticles and Nanomedicine

The development of nano-sized particles (typically ranging between 10 to 1000 nm) paved the way to designing new, exciting therapy and diagnostic strategies in medicine, leading to the creation of nanomedicine. Nanomedicine is a medical field in which nano agents are employed to diagnose, treat or prevent diseases or abnormal physiological conditions. One of the crucial aims of nanomedicine is to increase the efficacy of approved therapeutics as well as reduce or eliminate their side effects. For this purpose, many researchers have been inspired by the Nobel prize winning concept of Dr. Paul Ehrlich: The magic bullets (1900).[44] The idea is to be able to only kill the source of a disease (e.g. microbes), without damaging any other part of the human body. Advances in fields such as biology, molecular biology, genetics and chemistry have allowed the development of targeting strategies for specific diseases, enabling the creation of diverse nanotherapeutics.[45] The main goal is to develop personalized treatments for each patient, while exploiting the biological or molecular characteristics of their diseases. The use of nanoparticles to transport therapeutics within the human body has demonstrated great potential for treating different diseases such as cancer, brain diseases as well as inflammatory skin disorders. [46-48] Nanoparticles can be created out of inorganic as well as organic materials and can possess very defined architectures, all of which can be tailored depending on the desired application (**Figure 5**).[49-52] Several advantages of nanoparticles include protecting therapeutics from the biological environment as well as increasing the therapeutics solubility, biocompatibility, and prolong its circulation time in the bloodstream.[53-55] In addition, nanoparticles can be functionalized to recognize disease characteristic functional groups, allowing the disease's specific targeting.[56,57]

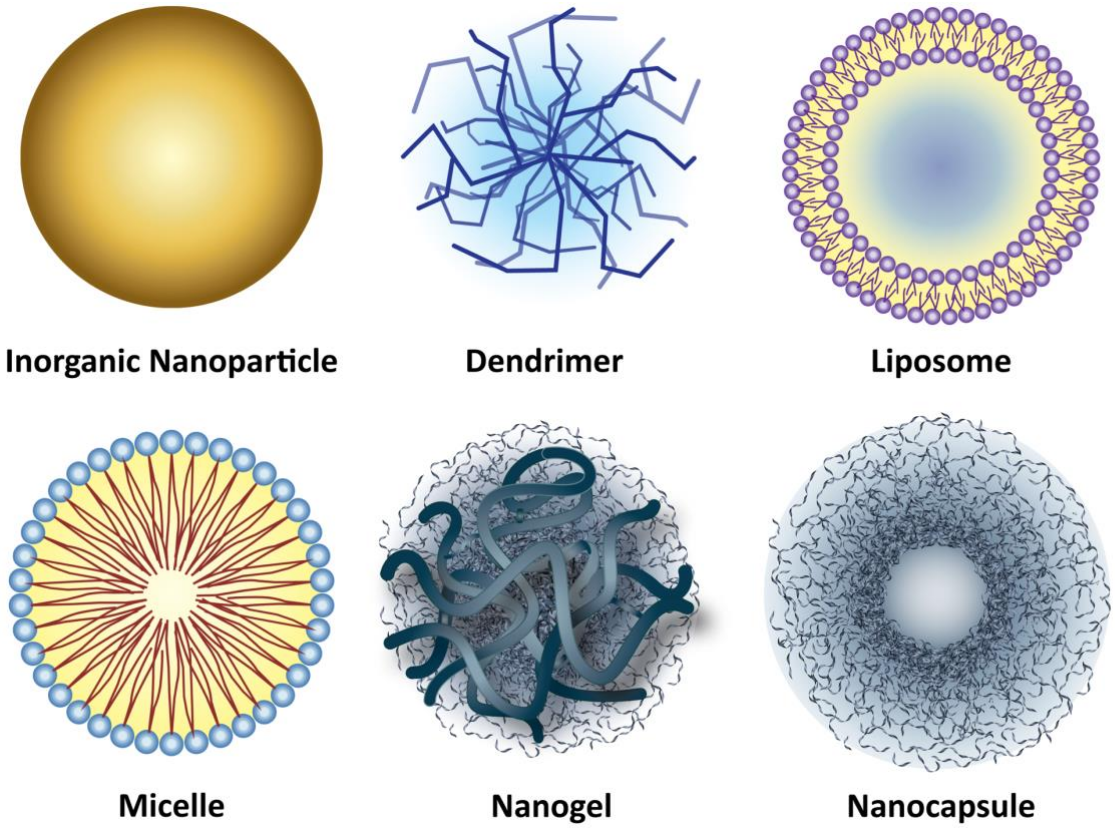

Figure 5: Illustration of some of the most used nanoparticles for biomedical applications.

1.4.1 Soft Nanoparticles and the Skin

Delivering therapeutics through the skin offers multiple benefits over other administration routes (e.g. oral and intravenous drug delivery), specifically when it comes to the treatment of skin diseases. It prevents the digestion or clearance of the therapeutic as well as possible digestion in the gastrointestinal tract. In addition, it allows the application of the therapeutic directly at the biological site of action, therefore decreasing undesired side effects. Soft nanoparticles have been found to be suitable strategies for delivering bioactives across the SC.[58,59] Among the most well-known nanoparticles systems, micelles, nanogels and nanocapsules deserve a special mention.

Micelles are defined by the type of intermolecular forces that form them. They can be classified as amphiphilic micelles, polyionic complex micelles (pic) and micelles built by metal complexation.[60] Micelles are self-assembled structures of surfactants, and form spontaneously when the concentration of the surfactant is high enough, above the so-called critical micellar concentration.[61] During the micelle formation, the hydrophobic tails of the

surfactants aggregate in water, while the hydrophilic parts are exposed; hence leading to particles with a hydrophobic core and a hydrophilic shell. This process is called micellization and is both thermodynamically as well as entropically favourable.[62] This has therefore been exploited to encapsulate hydrophobic therapeutics for biomedical applications. Polymeric micelles are not only interesting in research but have also made it to the market due to their easy scale-up, low cost and facile formulation.[63] However, micelles still present major drawbacks, such as the lack of cross-linking, which leads to micelles being very sensitive to environmental changes (salt concentrations, osmosis, pH, etc.).

Nanogels (NGs) are 3D cross-linked polymer networks, capable of absorbing great quantities of water. These versatile nanomaterials have been found to be an excellent nanocarrier, finding a wide range of applications.[64-67] Unlike micelles, NGs are physically entangled or chemically cross-linked, hence they are more robust and not that prone to mechanical failures (e.g. micelles can burst easily). In addition, if smart building blocks are employed, NGs can respond to internal and/or external stimuli (e.g. pH, temperature, light, magnetic fields, etc.).[68] Smart NGs undergo strong physico-chemical changes when exposed to such stimuli, which enables the controlled release of previously encapsulated therapeutics in a controlled manner.[69,70] Especially, thermoresponsive NGs (which can shrink or swell upon applying a thermal trigger) have been found to be suitable candidates to transport therapeutics across biological barriers such as the skin.[1]

Calderón et al., developed thermoresponsive NGs based on dendritic polyglycerol as a cross-linker as well as linear polyglycerol as thermoresponsive polymer (tPG). The NGs were synthesized using a nanoprecipitation approach which enabled their facile decoration with β-CD (7 D-glucopyranose). The β-CD decorated NGs could be used to encapsulate the corticosteroid dexamethasone (DXM) and could transport it to deeper layers of the skin.[71] Electron paramagnetic resonance investigations demonstrated that DXM was localized in the hydrophobic void of the β-CD units of the NGs. The studies revealed that the β-CD NGs transported DXM into the epidermis and dermis of human skin in *ex vivo* in a more efficient fashion than commercially available DXM-based cream. The therapeutic efficiency of the DXM loaded β-CD NGs system was assessed on inflammatory skin equivalents. It could be demonstrated that DXM loaded β-CD NGs could downregulate the expression of proinflammatory thymic stromal lymphopoietin (TSLP). Moreover, β-CD NGs showed better

results than a commercially available DXM formulation (LAW cream), as well as the non-decorated NGs, highlighting their potential as strategy for treating skin inflammatory diseases. Thermoresponsive soft systems (e.g. NGs or hydrogels) have been found to induce skin hydration and further enhance the penetration of hydrophilic compounds (ranging from dyes to proteins).[72,73] Recent studies by Calderón et al., highlight the skin hydration features of thermoresponsive nanogels (tNGs).[72] Employing dPG as macro-crosslinker and PNIPAM, poly(glycidyl methyl ether-co-ethyl glycidyl ether) (p(GME-co-EGE)) and p(di(ethylene glycol) methyl ether methacrylate - co - oligo ethylene glycol methacrylate) p(DEGMA - co - OEGMA475) as thermoresponsive polymers, three types of tNGs were synthesized. The NGs were labeled with indodicarbocyanine (IDCC) and loaded with fluorescein. The IDCC enabled to track the penetration of the tNGs across the skin, while the release of fluorescein could be independently studied using fluorescence microscopy. Combining electron microscopy with Raman spectromicroscopy it could be demonstrated that the SC of the treated skin samples exhibited a disruption in the structure of proteins and lipids. It was claimed that these findings arose from hydration effects induced by the tNGs.

Exploiting the thermoresponsive features of tPG, Calderón, Hedtrich et al. designed a novel water-in-water thermo nanoprecipitation for synthesizing tNGs.[74] This novel approach utilizes very mild conditions, thus allowing the *in-situ* encapsulation of etanercept (ETR), an anti-TNFα fusion protein. Studies on inflammatory skin models revealed that the NGs transported ETR into the viable epidermis. Moreover, the delivered ETR was able to reduce the inflammation, thus proving its therapeutic efficiency. Additional experiments corroborated that the encapsulation and release procedures did not cause structural changes in ETR.

One challenge with dealing with responsive nanogels is that the controlled release usually only works for larger, high molecular weight compounds (e.g. proteins), while small molecules can freely diffuse out of the nanogel.[57,75] Moreover, many therapeutic relevant drugs are hydrophobic and thus it is difficult to encapsulate them within the hydrophilic nanogel network.[59]

Nanocapsules (NCs) represent an interesting option for overcoming the issues presented with micelles and nanogels, while at the same time taking advantage of their features. Nanocapsules are water soluble/dispersible hollow core-shell nanoparticles.[76,77] Like NGs and micelles, NCs can be build out of any polymer material and are suitable nanocarriers for biomedical applications (e.g. skin applications).[78,79]

1.4.1.1 Nanocapsules

The core of NCs is often used as reservoir for hosting large amounts of diverse therapeutics, which highlights the potential of NCs as drug delivery systems.[80,81] Furthermore, the polymeric shell can enhance the circulation lifetime of the nanoparticles and the cargo. Additionally, the shell can shield the payload from the biological environment (e.g. protection from pH, enzymes, etc.), while at the same time diminish possible side effects by decreasing the leakage of the cargo.[82] Moreover, the empty void and thick shell of the NCs are very appealing for tuning their mechanical properties to better overcome diverse biological barriers. These features can be exploited for transporting delicate and not hydrophilic cargo through the skin, like quercetin. Quercetin is a flavonoid that exhibits great antioxidant and anti-inflammatory properties, therefore handled as a potential candidate in skin applications.[83] In addition, NCs have been found to efficiently deliver other flavonoids and antioxidants across the skin.[84] L. Marchiori et al. synthesized a gel formulation based on silibinin-loaded pomegranate oil NCs as an alternative for topically treating cutaneous UVB radiation-induced damages (sun burn caused by radiation from 280-320 nm).[85] The formulation exhibited a similar in vivo anti-inflammatory properties as compared to the commercially used formulation (hydrogel containing silver sulfadiazine).

In a follow-up work, L. Cruz et al., found that a Pemulen®TR2 gel based on NCs formed by the interfacial deposition of previously synthesized polymers showed good silibinin (a flavonoid) encapsulation and could significantly reduce the inflammation in contact dermatitis in mice without altering the properties of healthy skin.[86]

Furthermore, the use of NCs to transport larger cargos has been found advantageous. Studies revealed that NCs were able to encapsulate and transport collagen across the skin.[87] This was investigated in a murine model for local dermal fibrosis. It could be demonstrated that the NCs were able to induce a stronger reduction of the fibrosis compared to commercially available injections of the free enzyme.

Primarily, there are two options to form the shell of the nanocapsules. The first option is to produce the shell directly in a synthetic procedure, the other option is to use pre-formed polymers to embed the core utilizing deposition techniques. Over the years, many synthetic approaches have been developed for yielding NCs such as miniemulsion/ inverse miniemulsion polymerization and the template-based method.[88,89]

Miniemulsion based synthesis is based on mixing two immiscible phases forming an emulsion (water-in-oil or oil-in-water) in which one of the liquids is distributed in the other one in the form of droplets. Next, the size and polydispersity of the droplets is tailored by applying external forces, e.g. high shear forces through ultrasonication.[90] The droplets are stabilized throughout the whole process by surfactants, which among others, prevent the droplets from coalizing.[91] The final agent needed to form stable miniemulsions is an osmotic pressure agent, which helps against the Ostwald ripening. The osmotic pressure agent increases the osmotic pressure inside the droplets, thus counteracting the Laplace pressure and leading to a pressure equilibrium.[92] Depending on the miniemulsion, the osmotic pressure agent needs to be extremely hydrophobic (for oil-in-water) or hydrophilic (for water-in-oil).[77] The formation of the shell is also based on the immiscibility of the resulting polymer and the droplet. The first known nanocapsules synthesized via miniemulsion polymerization was reported by Landfester et al.[93] It was proven, that poly-styrene as well as poly(methyl methacrylate) NCs can be obtained depending on the surfactant and reaction conditions employed. The study also showed, that the NCs were formed as the growing polymer became insoluble in the droplet and phase separation occurred. Using emulsion polymerization it is possible to scale-up the synthesis, as well as *in-situ* encapsulate therapeutic agents; however, the high amounts of surfactant required to stabilize the reaction can often be problematic as it is difficult to purify the products.[82] In addition, it has been claimed, that NCs produced *via* miniemulsion polymerizations can often not be entirely hollow; thus, the advantages of the empty void cannot be used.[94] In contrast, NCs prepared by employing sacrificial cores, allow a precise control of the core void size, high reproducibility at the nano-scale and narrow polydispersity.[89,95]

Studies have shown that NCs prepared using sacrificial templates also allow the precise control of the structural features of the polymer shell of the NCs (e.g. shell thickness, surface charge, permeability and mechanical properties).[96] For this methodology, the choice of the template is crucial; it should be easy to synthesize and later to digest (Table 3).[97,98] Additionally, the template needs to be chemically inert during the formation of the shell, while allowing the grafting of the shell to its surface (the grafting can be charged based (often used in layer-by-layer approaches) or covalent).[99]

Table 3: Examples of commonly used core materials, their digestion conditions and information about their ability to encapsulate active substances prior to the NCs' synthesis.

Core material	Pre-synthetic loading of active substance	Digestion conditions
Poly(methyl methacrylate)	No	Organic solvent*
Polystyrene	No	Organic solvent*
Melamine formaldehyde	No	HCl
Nanogels based on calcium arginate	Yes	Ethylenediaminetetraacetic acid
Silica nanoparticles	Yes	NaOH or HF

*organic solvents like tetrahydrofuran, chloroform or dichlormethane.

Typical templates include colloidal particles formed from poly(methyl methacrylate), polystyrene and melamine formaldehyde. These templates have the advantage of being commercially available in a wide range of sizes (from 100 nm to several μm) and with narrow polydispersity indexes. However, none of the mentioned possible templates allows a pre-synthetic loading of active substances, which ultimately leads to low encapsulation efficiency as well as poor release reproducibility.[96] An attractive alternative is to use nanogels or hydrogels as sacrificial templates, these are able to entrap therapeutics within their network before building the shell of the NCs. Nanogels based on calcium alginate are quite popular as they can be digested by utilizing ethylenediaminetetraacetic acid (EDTA); however, the complete removal of the core is often challenging due to high cross-linking degrees within the polymeric network as well as high swelling pressure after the nanogels digestion which often leads to the rupture of the NCs' shell.[100] Furthermore, nanogels exhibit relatively higher polydispersity values when compared to some inorganic particles (e.g. silica nanoparticles) due to the poor size control during their synthesis.[100] Silica nanoparticles are commercially available in a vast variety of sizes and with different surface charges but can also be easily synthesized and functionalized in the laboratory.[101] Employing the well-known Stöber method it is possible to synthesize silica nanoparticles with narrow polydispersity and defined sizes (10 nm to several micrometer).[102] In addition, it is also possible to control the porosity of silica nanoparticles, thus allowing the loading of therapeutics before the synthesis of the NCs.[103]

Moreover, silica nanoparticles can be fully digested in presence of sodium hydroxide or hydrofluoric acid, thus fulfilling the template criteria for yielding NCs.[104,105]

One of the greatest limitations in the field of NCs is to control the permeability of the shell as this directly controls the release kinetics of therapeutics (**Figure 6**, **(I)**). For this purpose, the use of smart materials as building blocks has proven useful (**Figure 6, (II)** and **(III)**).

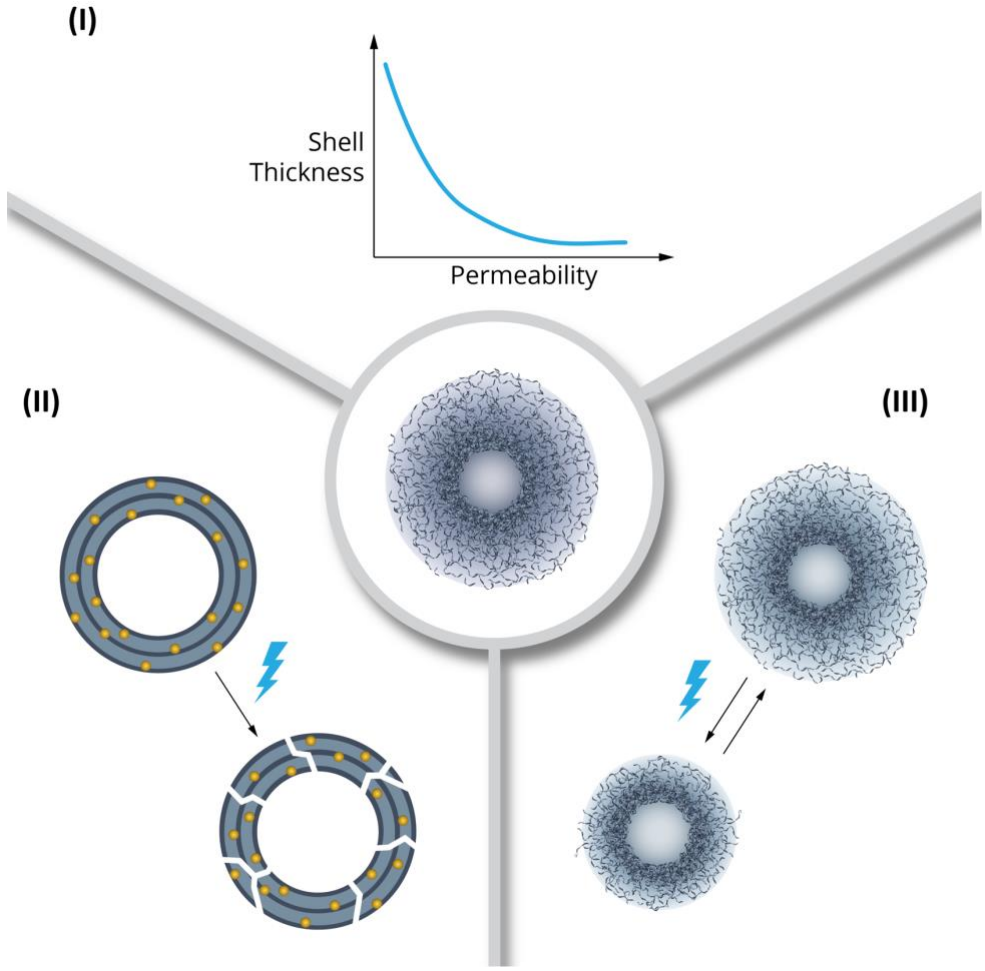

Figure 6: (I) Illustration of the importance of the control of the permeability of the NCs' shell. Control of the permeability of the shell by introducing responsive polymers to (II) degrade the shell (e.g. polymers responsive towards light, magnetic field or pH), or to (III) change the size of the shell (e.g. by using polymers responsive towards pH or temperature changes).

NCs build with thermoresponsive polymers are promising, as the volume phase transition temperature (VPTT) could be used to control the permeability of NCs' shell (**Figure 6 (III)**).[106] Depending on the type of thermoresponsive polymer employed, the NCs can exhibit either a lower critical solution temperature (LCST) or an upper critical solution temperature (UCST) behavior.[106] LCST-type polymers remain hydrated by hydrogen bonds with water molecules

below the LCST causing the NCs to swell; however, with increasing temperature (above the LCST) the polymers become hydrophobic therefore leading to the shrinkage of the NCs. This effect is caused due to the prevalence of the entropic contributions by the expelled water molecules from the polymeric network.[107] Ultimately, the NCs could aggregate if not sufficient hydrophilic components are present in the shell as strength between the thermoresponsive polymer chains becomes stronger than the polymer-water interactions.[106] After cooling, the NCs should regain their original shape and size, in a fully reversible manner. In contrast, UCST-type polymers exhibit a contrary behavior as LCST polymers. When in solution, UCST polymers transition from a shrunken state (below the UCST) to a swollen state (above the UCST) by increasing the temperature. However, the transition is often more delicate than the transition for LCST-polymers and can often be disturbed by diverse factors such as the polymer concentration, the salt content and the pH of the solution; thus, limiting its application. Regardless of the thermoresponsive polymer type employed, nanoparticles displaying thermoresponsive features are great drug delivery nanocarriers as the change from swollen to shrunken state can be precisely controlled.[75]

Despite of extensive studies on thermoresponsive polymers for building nanocarriers, only the following thermoresponsive NCs systems have been reported so far: poly(*N*-vinylcaprolactam), poly-(*N*-isopropylacrylamide)-*N,N´*-methylenebisacrylamide (PNIPAM-BIS) and poly-(*N*-isopropylmethacrylamide)-BIS (PNIPMAM-BIS).[49,76,77,108] Due to the excellent results obtained by using thermoresponsive NGs for skin applications, this thesis is devoted to exploring the synthesis of thermoresponsive NCs with suitable mechanical properties as a novel alternative for enhancing the penetration of, as well as transporting therapeutics inside the human skin.

1.5 Physico-mechanical Properties of Nanocarriers and How to Measure them

It was not until recently, that the importance of physico-mechanical properties of nanocarriers emerged as a new exciting field for targeting. This strategy is inspired by cells and viruses, which can alter their physico-mechanical properties in order to obtain specific biological functions.[109] This concept has been already proven to be a suitable strategy for targeting, otherwise difficult biological sites, such as caveolae for overcoming the sterically obscure (e.g. through plasma-lemma vesicle associated protein) endothelial barrier.[110] Additionally, it has

been reported, that the physico-mechanical properties of nanocarriers can often decide their drug delivery efficacy.[111] In particular, elastic nanocarriers have been found to penetrate biological barriers more efficiently than rigid nanocarriers.[112] In the case of the skin, elastic/deformable nanocarriers have been found to penetrate across the SC, into the deeper layers of the skin and even reach the blood circulation.[113] Transferosomes are an example for such nanocarrier, they are specially designed liposomes for transdermal and/or topical drug delivery purposes. It has been hypothesized that the efficacy of transferosomes resides in their high deformability, feature that can be exploited for changing their shape in order to pass through the natural pores within the SC.[114] Furthermore, many studies have highlighted the benefits of using elastic nanocarrier systems, and in some cases these have even outperformed commercially available or conventional treatments.[115,116]

One of the issues limiting this new exciting targeting field are the dimension of the particles and the reproducibility and quantification of their mechanical properties. Although there are many classical methods for investigating mechanical properties (e.g. rheology, tensile tests, etc), these are conceived for larger systems (e.g. films).[117-119] To study nanoparticles utilizing classical methods it is necessary to create films or hydrogels out of the nano-systems; however, this could alter their intrinsic mechanical properties; hence the measured properties could strongly differ from the mechanical properties of the nanoparticles. Therefore, it is imperative to use techniques to study the mechanical properties of nanoparticles which can detect changes at the single particle level (e.g. atomic force microscopy).

1.5.1 Atomic Force Microscopy (AFM)

In 1986 atomic force microscopy (AFM) was developed and marked a milestone in the history of diverse fields, such as physics, biology, chemistry and medicine.[120] AFM is used to study the structural features of samples immobilized on substrates, while being able to study quantitative physical and chemical properties, simultaneously. In general, the working principle of the AFM consists on 'sensing' the sample's surface using a precise control of the forces acting between a small probe and the material, generally via a feedback mechanism.

Nowadays, this technique is extremely sensible, allowing the observation of atomic-scale structures via high-resolution images, and controlling forces down two the pN scale.[121] The

AFM is considered to be one of the most versatile analytical methods in nanoscience, as it can image almost any surface under numerous environmental conditions.[122-124] One of these conditions enables the AFM to operate in liquids, at different temperatures, which allows the study of biomolecules in their native conditions, with nanometer lateral resolution.[125] For example, AFM has enabled the discovery of the nature of the rotary catalysis of F1- adenosine triphosphate driven motors, or unravel and quantify the biomolecular dynamic processes within natural and synthetic nuclear pore complexes.[126] In order to obtain high resolution images and additional quantitative information of highly complex biological samples (e.g. proteins, viruses, cells and tissues) various AFM specialized modes and probes have been developed over the years.[127] These advances take full advantage of the nature of the sample, as well as the great signal-to-noise ratio and high sensitivity of the AFM to obtain both high-resolution images with physico-mechanical quantitative information about the sample's properties, as elasticity, adhesion, hydrophilicity, deformability and magnetic properties among many others.[128-130]

From the technical point of view, the AFM is usually comprised of a probe, a photodiode, specialized electronics, and a piezoelectric element, which allows control of probe motion. The scanning process is driven by an (x,y,z) scanner that allows to move the sample and/or the stage with respect to the probe, or viceversa.[124,131,132] The AFM probe is composed by a sharp tip that is fixed to a cantilever. This latter element acts as a diving board, reacting under the interactions between the atoms at the apex of the tip and the samples' surface. The movement of the cantilever causes a change of its inclination and angle, which can be usually tracked by the variations of a laser beam reflecting from the cantilever into a 4-segmented photodiode.[133,134] In the final step, the vertical movement of the probe is quantified from the cantilever bending. An image is obtained by laterally mapping the surface of a sample, while the vertical movement of the tip is continuously corrected to obtain a constant setpoint, via a feedback mechanism.[132] Any difference in these forces as a function of the tip (x,y,z) position with respect to the atomic arrangements of the samples' surface is employed to build the image. The morphological information of the sample is usually displayed at each pixel of the image as a measurement of the samples' height.[133] This information is typically shown by a false color image, that uses a colour gradient varying from dark (low height) to bright (high height). From these sort of images, it is possible to measure peak-to-valley distances, calculate

histograms for the heights, as well as investigate fine details of the surface like helical pitch and chirality of polymer helixes (e.g. nanocellulose fibrils).[135]

Depending on the utilized mode, the way of action of the AFM changes. In contact mode the deflection of the cantilever as a result of the interatomic forces between tip and surface (up/down) is kept constant throughout imaging. In contrast, intermittent contact techniques, as the so-called tapping mode, monitor the amplitude at which the cantilever vibrates, near its resonant frequency, to obtain information about the samples' surface.[136] These two modii are perhaps the most widely used for investigating nano/microparticles and soft biological samples; however, these techniques still have decisive limitations.[137] Contact mode allows to generate high resolution images, yet soft samples can sustain great damage due to shear forces. Tapping mode is advantageous for very soft materials as the tip causes negligible friction and shear forces. However, the applied force is not easily monitored. Also, the phase signal generated during tapping mode imaging is difficult to interpret as it is the result of the convolution of various volume and surface parameters (e.g. adhesion forces, contact area, elasticity, dissipation and viscosity).

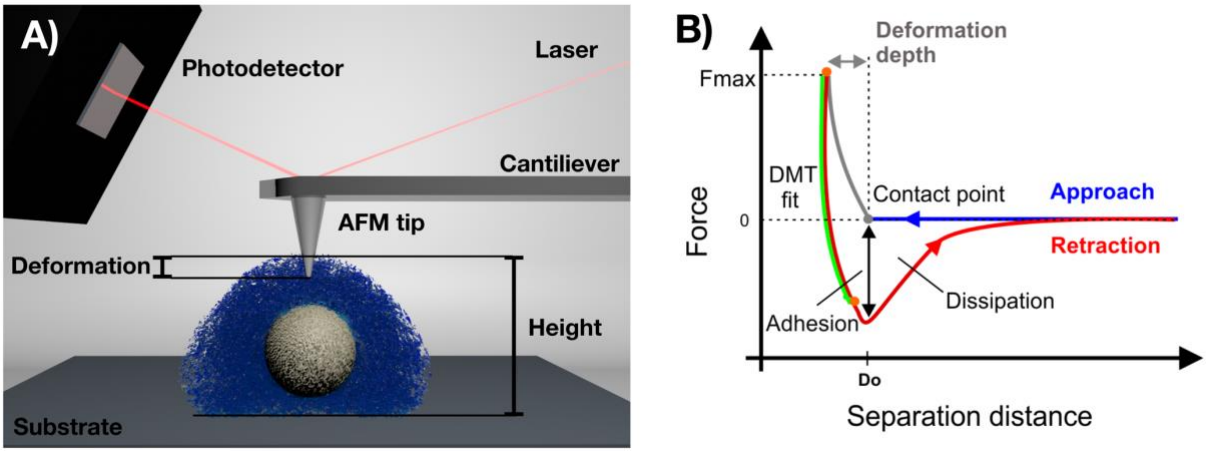

Figure 7: (A) Schematic representation of the mapping of a nanoparticle with an AFM, as well as the AFM components. (B) Typical force separation curve obtained by the AFM in PeakForce QNM mode. Reprinted with permission from reference 138. Copyright 2020 American Chemical Society.

In recent years there have been several developments focused on to overcoming these issues. JPK has developed the qi mode, Assylum Research the AM-FM viscoelastic mapping, and Bruker the PeakForce QNM (PF-QNM) mode. This latter scanning mode is among the most cited in recent literature since it allows to obtain high resolution images and mechanical

information through fast mapping and without exerting excessive damage to the sample while at the same time continuously monitoring the applied force.[122,139] Also, PF-QNM allows the study of the mechanical properties of materials in solution (**Figure 7A**).[122,128,140] Also, this operation mode has been used to investigate the morphology as well as quantify the mechanical deformation induced by the AFM tip on soft nanoparticles at the single particle level.[128,141,142] An importan advantage of PF-QNM ist that the system records the applied force on the sample during the scanning.[122] In brief, the probe is oscillated sinusoidally at a frequency much lower that the resonant frequency of the cantilever (typically 1 or 2 kHz). The interaction of the moving probe with the sample surface leads to the generation of force separation curves, produced at each contact between the tip and the samples' surface. During the scan process, each force separation curve is analyzed in real time, enabling the quantification of numerous nanomechanical properties, as deformation, adhesion and Young's modulus, among others.[128,140] The maximum value of the applied force, known as peak force, is used as feedback parameter. This complete analysis allows the visualization of the mechanical properties as 2D or 3D mechanical maps, while observing structural features via the height image.

The detailed analysis of the force separation curve is schematically shown in **Figure 7B** for a full approach-retraction cycle. Firstly, the tip is pulled down to the samples' surface due to attractive forces (e.g. van der Waals, electrostatic, capillary). Next, the attractive forces overcome the stiffness of the cantilever causing the tip to touch the samples' surface (contact point, D0 in **Figure 7B**). From this point on, the tip pushes the sample from the contact point until the force set point at F_{max} is reached. For soft materials, the distance between contact point and F_{max}, is the deformation depth reached by the tip. This information can be used to create a contrast in maps of surface topography or height and deformation. Further parameters like adhesion force and energy dissipation, can be obtained by investigating the withdrawal of the tip after reaching F_{max} (red curve in **Figure 7B**). Using PF-QNM it is possible to obtain information about the Young's modulus (elastic modulus) of the sample. This parameter is calculated by fitting the retraction curve to a proper model of contact mechanics.

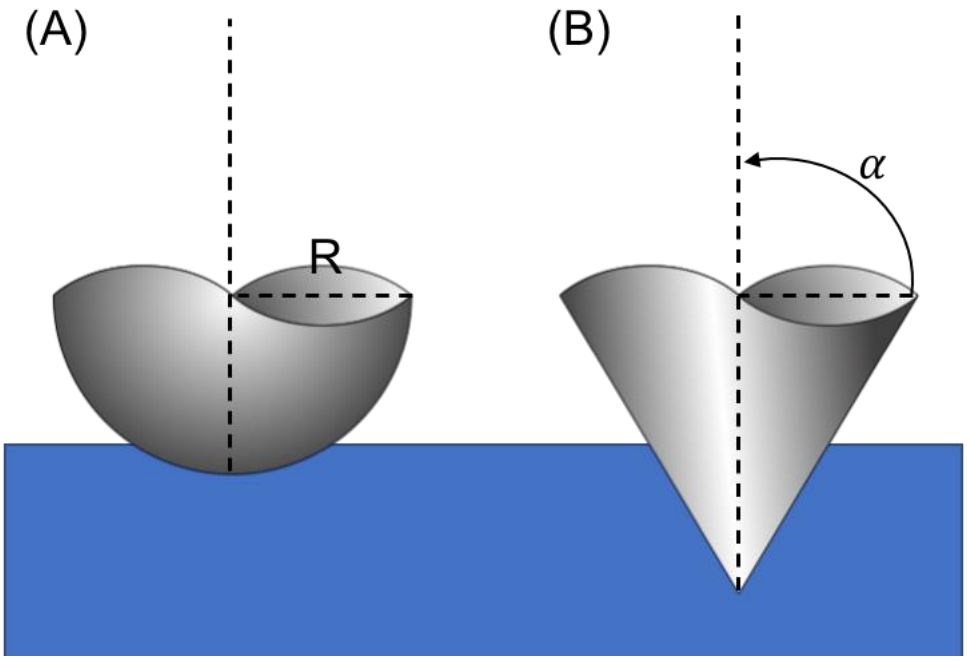

Figure 8: (A) Illustration of the contact between a sphere and a flat surface (Derjaguin-Müller-Toporov model). (B) Representation of the deformation of an elastic surface by a rigid conical indentor (Sneddon model).

The Derjaguin-Müller-Toporov (DMT) model refers to the contact between a sphere of defined radius and a flat surface (**Figure 8A**). In its simplest yet powerful form, the DMT model is an extension of the Hertz model of contact mechanics, comprising more parameters such as attractive interactions around the contact area (adhesive forces between the tip and the surface).[139] In the DMT model the Young's modulus (*E*) can be calculated from the force *F* as follows[139,143]:

$$F - F_{\mathrm{adh}} = \frac{4}{3}\frac{E}{(1-\nu_{\mathrm{s}})^2}\sqrt{R}\,d^{3/2} \qquad (1)$$

where *F* is the applied force, F_{adh} the adhesion force, *R* is the effective radius of the tip, v is the Poisson's ratio of the sample, and *d* is the separation distance. Generally, the DMT model is applicable to high-density polymers with poor deformability and should not be used for rather soft materials (Bruker Application Notes). For this reason, when performing PF-QNM mapping and nanoindentations (also known as force spectroscopy analysis) on soft materials, it is recommended to use other models in order to extract the Young's moduli.[144] Especially, the Sneddon model has proven to be suitable for calculating the elastic modulus of soft materials

such as cells.[145] This model describes the interaction between an elastic half space deformed by a rigid conical tip (**Figure 8B**; Eq. 2).[146]

Eq. 2 $$F = \frac{2}{\pi}\frac{E}{(1-\nu^2)} * \tan(\alpha) * d^2$$

In this model *F* represents the load force, *E* is the Young's modulus, *d* is the indentation depth, α is the half-angle of the tip and *v* is the Poisson's ratio.

Nanoparticles that induce skin hydration, hence enhancing the skin penetration of other compounds across the skin, need to hydrate the SC. It is known that nanoparticles need to penetrate within the SC layers and release there the encapsulated water.[147] In order to penetrate the SC, the right balance between flexibility and robustness of the NCs' shell needs to be found. Therefore, it is imperative to analyze the mechanical properties of the NCs below and above their VPTT, which can be achieved by employing AFM in PeakForce mode.

2 Scientific Goals

Transporting therapeutics through the skin is a challenging task, as the skin is one of the most complex and efficient biological barriers of the human body. The barrier function of the skin is crucial and is mostly attributed to the stratum corneum (SC), which restricts the intrusion of foreign substances. Thus, resulting in low penetration of therapeutics and therefore low therapeutic efficacy. Methods to enhance the penetration of therapeutics into the skin are well-known, nevertheless these often can cause strong side effects such as irritation or even irreversible damage to the skin. An alternative for skin penetration is to induce the hydration of the skin, which has been found to disturb the lipids and proteins structure of the SC; therefore, enabling the penetration of therapeutics. However, to induce skin hydration, exposure to water is insufficient, as the skin requires a long time to hydrate. Over the years, the use of nanocarriers to deliver sensitive therapeutics into the deeper layers of the skin, has shown great potential. Especially the use of nanocarriers which can react to the biological changes within the skin, have demonstrated fascinating results. Thermoresponsive nanocapsules (**NCs**) are great candidates for topical applications as they allow the release of therapeutics in a controlled manner with interesting mechanical properties (e.g. flexibility) for overcoming the SC.

The main objective of this thesis is to synthesize novel thermoresponsive **NCs** for skin applications and study the effects of the thermoresponsive features and core structure on the nanocarrier as well as on the skin (**Figure 9**). The obtained information will be better analyzed by comparing the results of the **NCs** to well-known thermoresponsive core-shell nanoparticles (nanogels and nanogels with an inorganic core). The network of **NCs** and nanoparticles will contain the same building blocks (thermoresponsive polymers and cross-linker) but their core will differ, which should suffice to generate great differences regarding the nanocarriers' mechanical properties, hydrophilicity and interaction with the skin.

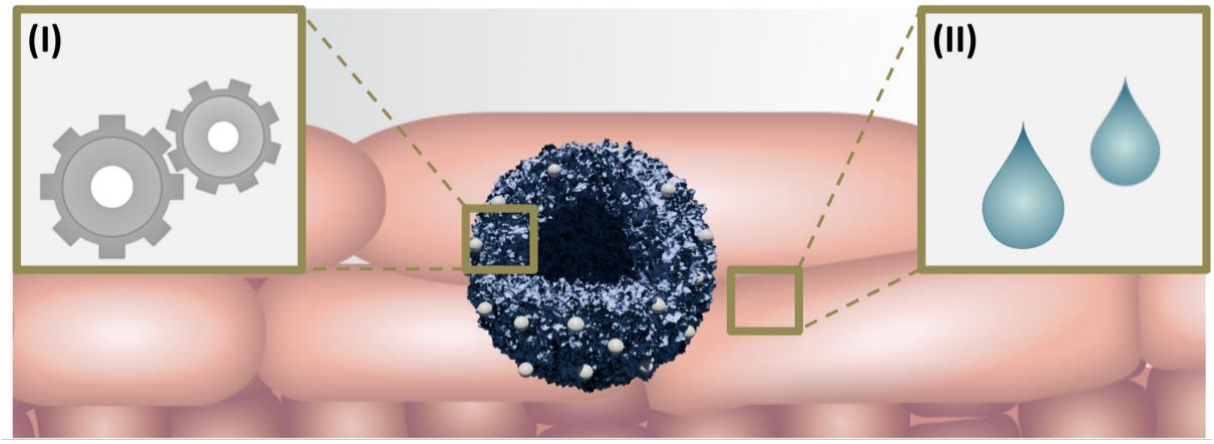

Figure 9: Illustration of the goals of the thesis. (I) Investigation of the effect of the core on the thermomechanical properties of nanocapsules. (II) Effect induced by the thermoresponsive features of nanocapsules on the skin (hydration).

The choice of thermoresponsive polymer and cross-linkers is crucial for tailoring the volume phase transition temperature (VPTT) of the nanocarriers as well as to control their mechanical properties to address specific biomedical applications. **Section 3** of this doctoral thesis consists of two chapters that describe the development and evaluation of thermoresponsive **NCs** with regard to their mechanical properties and interaction with excised human skin (hydration).

In **section 3.1**, the temperature driven changes in the mechanical properties of three different thermoresponsive nanocarriers shall be investigated i.e., **NCs**, nanogels and nanogels with a silica core. To validate the findings, only well-known thermoresponsive nanoparticles shall be utilized. Functionalized silica nanoparticles shall be used as sacrificial templates for synthesizing the **NCs** and the same quantities of *N*-isopropylacrylamide (NIPAM) and *N,N'*-methylenebisacrylamide (BIS) shall be used to build the network of the three nanocarriers. State-of-the-art techniques such as atomic force microscopy in PeakForce mode in liquid, nanoindentations, cryogenic electron microscopy (cryo-EM) and computational simulations (finite element method) shall be utilized to understand how the nanoparticle's core and inner structure affect the thermomechanical properties of thermoresponsive, soft nanoparticles.
The obtained findings shall serve as platform for the rational design of novel, soft thermoresponsive **NCs**. In **section 3.2**, the aim is to develop novel thermoresponsive **NCs** with a large core-void and thick polymeric shells that can induce skin hydration. These **NCs** are cross-linked by dendritic polyglycerol (dPG) as well as NIPAM and *N*-isopropylmethacrylamide

(NIPMAM) as thermoresponsive moieties that are inspired by dPG-PNIPAM nanogels. Thus, they should be able to induce skin hydration, which shall be studied by investigating the SC with label-based as well as label-free microscopy methods. In addition, the combination of specific ratios of NIPAM and NIPMAM shall be investigated to allow control over the VPTT of the **NCs**. The aim is to obtain **NCs** with a VPTT higher than the normal body temperature (37 °C) to be able to investigate the effect of the thermoresponsive features of the **NCs** upon hydration of the skin. Moreover, the penetration enhancement properties of the **NCs** shall be proven, utilizing Atto Oxa12 NHS ester as a model dye for high molecular weight compounds.

3 Publications & Manuscripts

3.1 Effect of Core Structure on the Mechanical Properties of Soft Nanoparticles

E. R. Osorio-Blanco, J. Bergueiro, B. E. Abali, S. Ehrmann, C. Böttcher, A. J. Müller, J. L. Cuéllar-Camacho, M. Calderón, *Chemistry of Materials* **2020**, *32*, 518-528.

The article is electronically available: https://doi.org/10.1021/acs.chemmater.9b04258

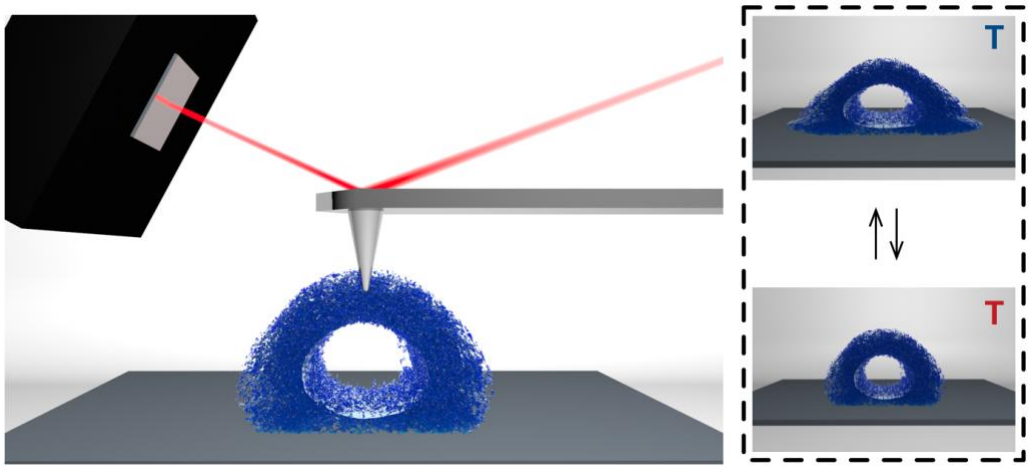

Figure 10: Illustration of the investigation of the mechanical properties of thermoresponsive, polymeric nanocapsules via AFM. Reprinted with permission from reference 138. Copyright 2020 American Chemical Society.

Abstract:

The mechanical properties of nanoparticles, especially those designed for biomedical purposes, have a large impact on their performance and have been scarcely studied. Thermoresponsive polymer-based nanoparticles are increasingly being used in biomedical applications; therefore, it is crucial to determine their thermo-mechanical response in the regime beyond their volume phase transition temperature (VPTT). The morphological characterization and comparison of thermoresponsive nanogels (NGs), silica core nanogels (SiO_2@NGs), and nanocapsules (NCs) in liquids, both below and above the VPTT, are explored in this study. We employed atomic force microscopy in Peak Force QNM mode as well as by dynamic light scattering, nanoparticle tracking analysis and cryogenic electron microscopy

(cryo-TEM). Surprisingly, nanocapsules presented increased resistance to deformation, when compared to nanogels, above the VPTT. This was attributed to differences in the cross-link density radial distribution between nanogels and nanocapsules derived from the synthetic approach employed. In addition, the Young's modulus was calculated from nanoindentations and by computer simulations, showing a significant change in NCs upon crossing the VPTT from MPa to GPa. Conversely, NGs displayed a Young's modulus in the kPa range, both below and above the VPTT. The findings of this study show that structural design and thermoresponsivity strongly influence the thermomechanical properties of nanoparticles. This in turn needs to be taken into consideration in the design of future nanocarriers.

Author's contribution:

In this publication, the author contributed with the concept and the experimental design of the study. The synthesis and characterization of the three types of nanoparticles were conducted by the author including the synthesis and functionalization of the silica nanoparticles employed during the study. Analytical characterization of the polymeric nanoparticles using NMR, DLS, NTA, and part of the AFM and TEM measurements were carried out by the author. Furthermore, the author developed the outline and wrote the article with collaboration of the co- and corresponding authors.

Cover art proposal:

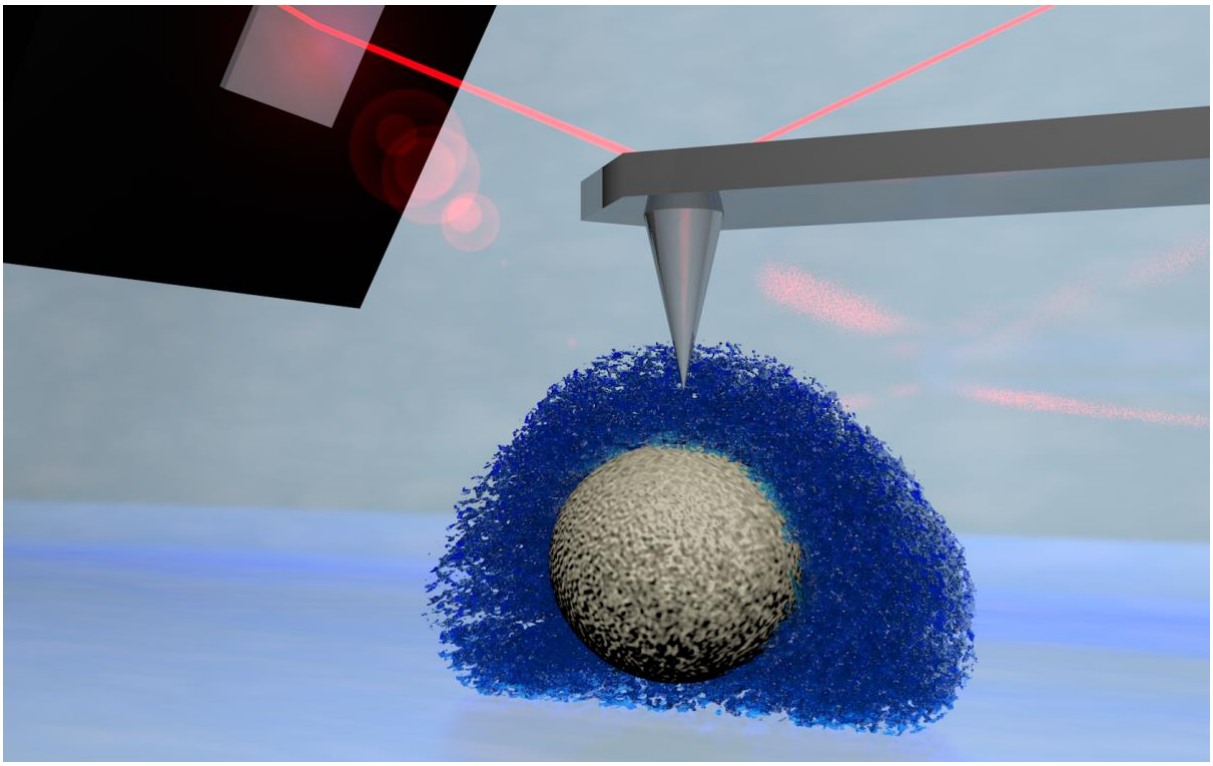

Figure 11: The mechanical properties of nanoparticles, in particular those designed for biomedical purposes, can have a tremendous effect on their performance. Atomic force microscopy in PeakForce mode, together with nanoindentations can be used to examine the thermo-mechanical properties of soft, thermoresponsive nanocarriers with different core-architecture. The cover art proposal was not selected.

3.2 Polyglycerol-based Thermoresponsive Nanocapsules Induce Skin Hydration and Serve as Skin Penetration Enhancer

E. R. Osorio-Blanco, F. Rancan, A. Klossek, L. Hoffmann, J. H. Nissen, J. Bergueiro, S. Hasenstab-Riedel, A. Vogt, E. Rühl, M. Calderón, *ACS Appl Mater Interfaces* **2020**.

The article is electronically available: https://doi.org/10.1021/acsami.0c06874

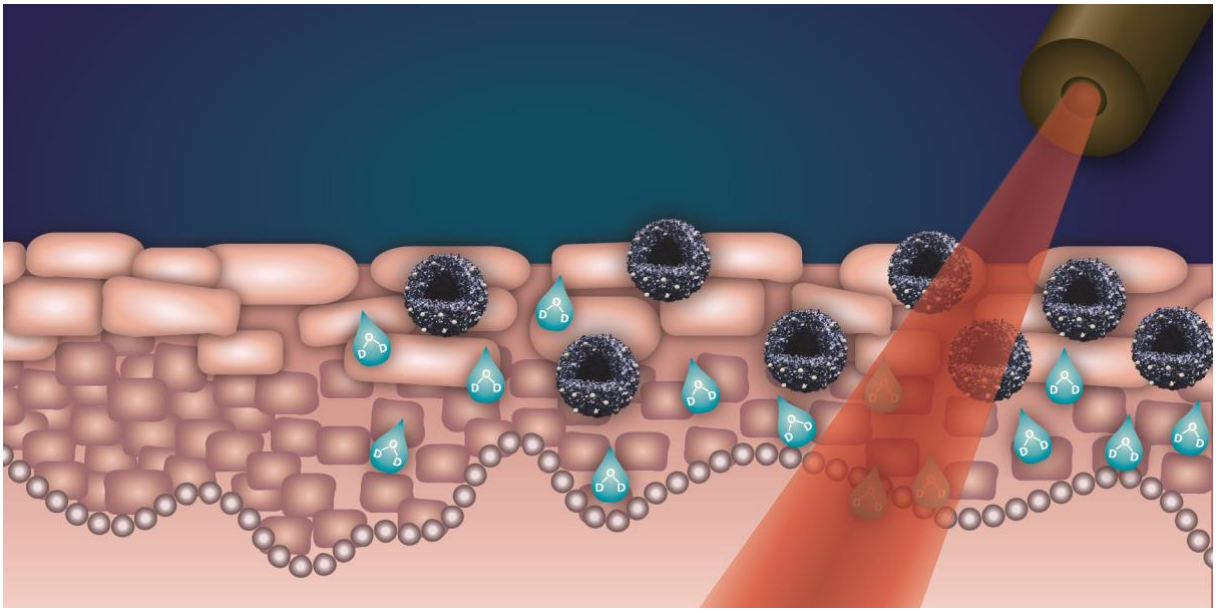

Figure 12: Graphic representation of how thermoresponsive nanocapsules induce skin hydration. Reprinted with permission from reference 147. Copyright 2020 American Chemical Society.

Abstract:

The use of penetration enhancers (chemical or physical) has been proven to dramatically improve the penetration of therapeutics. Nevertheless, their use poses great risks, as they can lead to permanent damage on the skin, reducing its barrier efficiency and resulting in the intrusion of harmful substances. Among the most used skin penetration enhancers, water is greatly accepted since skin quickly recovers from its exposure. Nanocapsules (NCs) represent a promising combination of carrier system and penetration enhancer becasue their water containing void combined with their polymer-based shell can be used to induce high local skin hydration and simultaneously to transport drugs across the skin barrier. In this study,

nanocapsules were synthesized with a void of 100 nm size, a thermoresponsive shell based on different ratios of poly(*N*-isopropylacrylamide) (PNIPAM) and poly(*N*-isopropylmethacrylamide) (PNIPMAM) as thermoresponsive polymers, and dendritic polyglycerol (dPG) as macro cross-linker. These NCs can shrink or swell upon a thermal trigger, which was used to induce the release of the entrapped water in a controlled fashion. The interactions and effects of thermoresponsive NCs on the stratum corneum of excised human skin were investigated using fluorescence microscopy, high resolution microscopy, and stimulated Raman spectromicroscopy. It could be shown that the thermoresponsive NCs could increase the amount of deuterated water penetrated in the viable epidermis (VE). Moreover, NCs increased the skin penetration of a high molecular weight dye (Atto Oxa12 NHS ester, MW = 835 g/mol) with respect to formulations in water or 30% dimethylsulfoxide (DMSO), emphasizing the features of the NCs as a skin penetration enhancer.

Author's contribution

In this publication, the author contributed to the concept of dPG-based thermoresponsive nanocapsules (NCs). The author developed new synthetic methodologies for the dPG NCs as well as their characterization. Together with Dr. Fiorenza Rancan, the author designed the experimental outline to study the interaction between the NCs and excised human skin, especially regarding skin hydration. The author developed the outline and wrote the manuscript in close collaboration with Dr. Fiorenza Rancan. The co- and corresponding authors contributed throughout the experimental and write processes.

Cover art proposal:

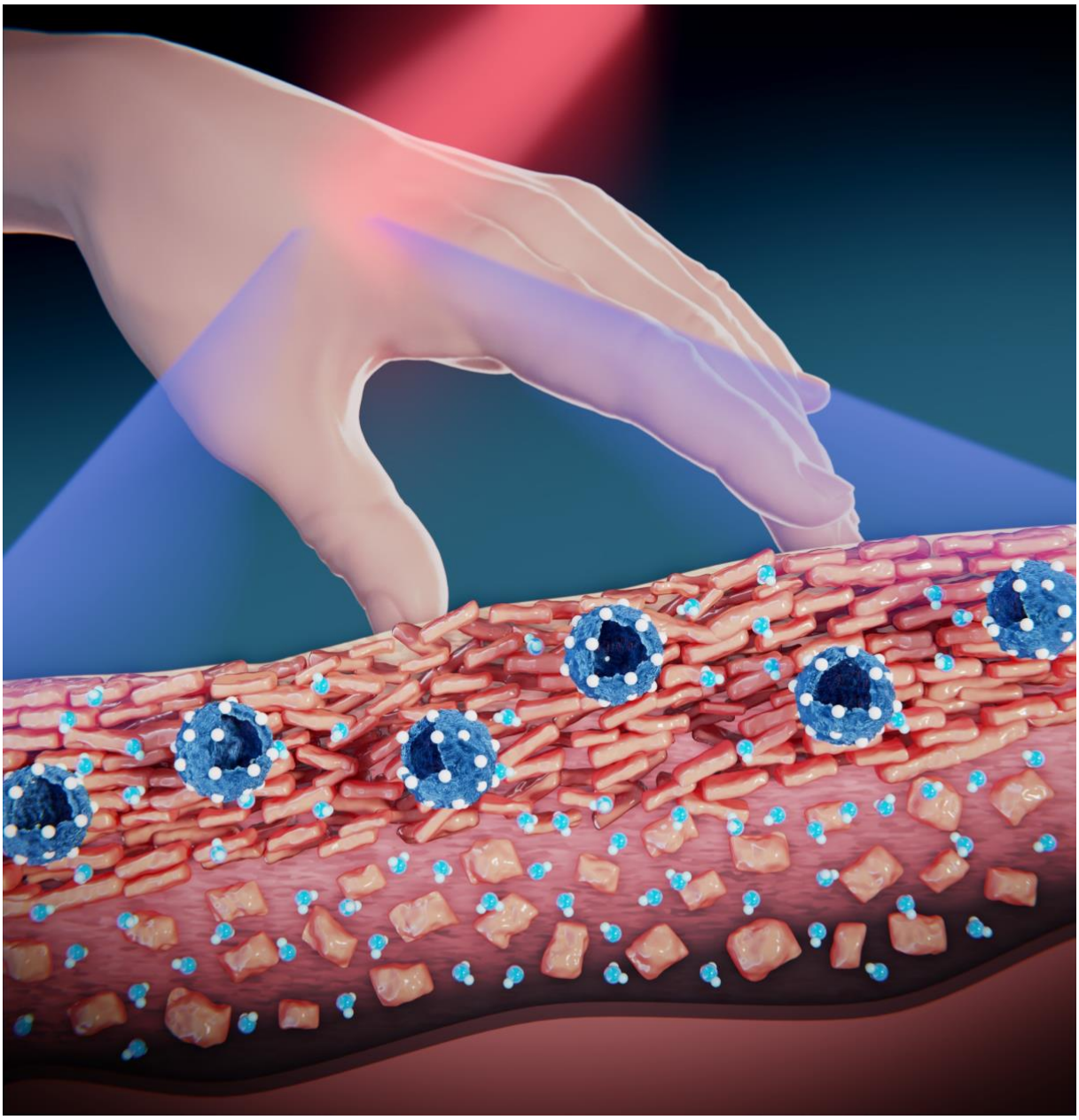

Figure 13: Skin hydration can be induced by soft thermoresponsive nanocapsules and can be further enhanced by increasing the temperature. This effect can be used to enhance the penetration of high molecular weight compounds into the deeper layers of the skin and is therefore an attractive technology for topical drug delivery. Cover art proposal was not accepted.

4 Conclusions & Outlook

The design of nanocarriers for delivering therapeutics across the skin was incited by the aim of improving the local treatment of inflammatory skin diseases or the systemic delivery of therapeutics by increasing patient compliance, reducing treatment derived pain and side effects, as well as increasing the therapy efficacy. It is undeniable that, as a result of multiple studies, a great understanding about the biological and physico-chemical properties of healthy and diseased skin has led to the development of multiple nanocarrier systems that could improve already existing therapies. Nonetheless, most nanocarrier systems still remain in preclinical studies, as their synthesis is highly demanding, and more efforts are needed towards their clinical translation and upscaling. Another limiting factor is the complexity of the skin barrier that represents a major obstacle for nanocarriers and other penetration enhancement technologies. Therefore, it is crucial to find the right balance between enhancing the penetration of therapeutics across the skin, while ensuring no irreversible or long-term damage to the protective barrier.

This thesis consists of two main projects that aim to develop novel thermoresponsive nanocapsules, with a large void core size and thick polymeric shells to facilitate the transport of therapeutics into the skin. The nanocapsules were synthesized using modified silica nanoparticles as sacrificial templates. This synthetic approach was chosen due to the facile digestion of silica nanoparticles (by incubation either in sodium hydroxide or in hydrofluoric acid) as well as to ensure reproducible void core sizes and narrow polydispersity. Hence, the well-known Stöber method was adapted to yield silica nanoparticles with diameters of around 100 nm and their surface was modified with the ligand 3-(trimethoxysilyl) propyl methacrylate (TPM).[101,148] The silica nanoparticles were then used as seeds during a seeded precipitation polymerization, wherein the newly introduced methacrylic functionalities served as anchor points to grow a polymeric network around the silica nanoparticles. Poly(*N*-isopropylacrylamide) (PNIPAM) and poly(*N*-isopropylmethacrylamide) (PNIPMAM) were chosen to build the thermoresponsive shell of the nanocapsules with the goal to control the temperature at which the nanocapsules undergo a transition from swollen to shrunken state (volume phase transition temperature; VPTT).

For the rational design of thermoresponsive nanocapsules for skin applications, it is imperative to understand the physicochemical properties defined by the material chemistry of the nanocapsules and their interaction with the skin as these could affect their biomedical performance. In the first project, the goal was to study the effect of the chosen synthetic pathway on the mechanical properties of the nanocapsules. As the investigation of the mechanical properties of soft nanoparticles is very challenging at the nanoscale, it was crucial to perform an unprecedented, comparative study utilizing different characterization techniques on well-known nanoparticle systems. For this purpose *N,N'*-Methylenebisacrylamide (BIS) was chosen as cross-linker and PNIPAM as the thermoresponsive motif to synthesize three different thermoresponsive nanoparticles with morphological differences in their core: nanogels (**NGs**), nanogels with a silica core (**SiO_2@NGs)** and nanocapsules (**NCs**). By employing the same synthetic approach, as well as maintaining the same amounts of cross-linker (5 mol%) (BIS), sodiumdodecylsulfate (SDS) as surfactant, potassium peroxodisulfate (KPS) as initiator and monomer (NIPAM) it was intended to ensure a similar crosslinking density, pore size and thermoresponsive behavior for the three types of nanoparticles. The three nanoparticle systems exhibited similar thermoresponsive tendencies and similar VPTT (between 33 °C and 34 °C), as confirmed from dynamic light scattering and nanoparticle tracking analysis. These findings suggested that the synthesis does not influence the thermal transition of PNIPAM based nanoparticles. However, cryogenic electron microscopy investigations (below and above the VPTT) revealed surprising differences regarding the polymer density distribution within the nanoparticles. It was found, that **NGs** presented a dense, uniform polymeric network in comparison to **SiO_2@NGs** and **NCs**, which displayed a polymer gradient with increasing density towards the core, suggesting different mechanical properties for the nanoparticles. This was further investigated by AFM in PeakForce QNM mode both below and above the VPTT of the nanoparticles in solution. AFM in PeakForce QNM allows to obtain not only morphological information and high-resolution images of the particles, but also, several mechanical parameters. This technique allowed the discovery of local differences in the internal material properties of the investigated nanoparticles. During this study it could be shown, that the different nanoarchitecture of the nanoparticles resulted in different structural responses towards the external applied deformation, although the same synthetic procedure, as well as same ratios of the monomers were employed. These results were attributed to the internal cross-linking

distribution within the nanoparticles, wherein **NCs** and **SiO_2@NGs** exhibited similar results but different tendencies were found for the **NGs**. Due to these pioneer findings, point nanoindentations were performed in order to corroborate the results of the PeakForce studies. By controlling the force and speed of the indentation it was possible to evaluate intrinsic changes in the mechanical properties of the nanoparticles. Notably, **NCs** exhibited a significant increase in their Young's modulus from low MPa to GPa range by increasing the temperature from 20 °C to 37 °C. Contrary to the **NCs**, the **NGs** showed a Young's modulus in the kPa range both below and above the VPTT. The marked differences between both nanoparticle systems was attributed to the presence or absence of silica nanoparticles during the synthesis. Owing to the high reactivity of BIS and the functionalized surface of the silica nanoparticles (in comparison to NIPAM) it is probable, that more BIS was consumed at the beginning of the reaction, resulting in a highly cross-linked, continuous, polymeric network (ring) present around the void of the **NCs**. This strongly cross-linked area within the NCs, together with their thermoresponsivity were found to be responsible for the tremendous increase of the **NCs**' Young's modulus above the VPTT. Conversely, no continuous highly cross-linked area was observed for the thermoresponsive network of the **NGs**. Instead, the force-separation curve course indicated possible non-thermoresponsive localized areas in the core of the **NGs**. Thus, the **NGs** still remained highly flexible upon crossing the VPTT, hence resulting in no significant change in their Young's modulus. These results are endorsed by the findings of Suzuki et al., wherein temperature controlled high speed AFM studies on PNIPAM-BIS **NGs**, synthesized using precipitation polymerization, exhibited non-thermoresponsive deca-nanometer sized domains within the **NGs**' core.[149] Computer simulations (finite element method) were performed using the parameters of the experiments to corroborate our findings. This not only confirmed the results of our study, but also proved that the Sneddon model (usually only used for macroscopic systems) can also be applied on soft nanoparticles. Altogether, this study highlighted the interplay between core architecture and material properties and their effect on the mechanical properties of soft nanoparticles.

These findings were taken into consideration while designing the novel **NCs** for inducing skin hydration in the second project. It was hypothesized that due to their polymeric network and large void core size, **NCs** should be able to induce high local skin hydration, which should serve to enhance the penetration of compounds into the skin. Like in the first study, thermoresponsive **NCs** were synthesized using modified silica nanoparticles as sacrificial

templates. Dendritic polyglycerol (dPG) was chosen as macrocross-linker, as it is highly hydrophilic, biocompatible and can be easily synthesized and functionalized.[150-152] Additionally, it has been shown, that dPG-based thermoresponsive nanocarriers can transport therapeutics across the skin by inducing skin hydration.[59,72,153] Moreover, by introducing dPG into the **NCs** shell we aimed to create a more flexible shell than in our previous studies with NIPAM-BIS **NCs**. The hypothesis was that dPG should serve as non-thermoresponsive defects within the polymeric network of the shell (similar to the highly cross-linked non-thermoresponsive parts in the core of the **NGs** from the first project), hence resulting in a flexible system both below and above the VPTT. NIPAM and NIPMAM were chosen to tailor the VPTT of the **NCs**. Interestingly, varying the ratio between both monomers did not only result in different VPTTs (34 °C to 47 °C) but also allowed a control over the thickness of the **NCs**' shell. Upon dissolving the silica core, the elasticity of the **NCs** were found to be increased. This was indirectly proven by examining the **NCs** with the AFM in soft tapping in air as well as in PeakForce mode in liquid. The **NCs** showed higher spreading on the substrate's surface as compared to before the digestion of the silica core. Unfortunately, no direct quantification of the elasticity properties could be obtained as imaging of the **NCs** with minimal forces (less than 200 pN) resulted in significant damage of their structure (puncturing and smearing of the **NCs**). To evaluate the skin hydration properties of the **NCs** as well as the effect induced by their thermoresponsive features, stimulated Raman spectromicroscopy (SRS) was employed. SRS is a state-of-the-art, label-free technique, which allows to track deuterated water within the different skin layers.[154] The **NCs** were lyophilized, re-dispersed in D_2O and subsequently apply them on excised human skin. SRS served to investigate the D_2O in the skin, therefore directly evaluating the skin hydration induced by the **NCs**. For this study, **NCs** with a high VPTT were chosen to investigate the effect of thermoresponsive feature of the **NCs** on skin hydration. By labeling the **NCs** with rhodamine B, it was possible to track the nanocarriers through the skin using fluorescence microscopy imaging. It was found, that **NCs** were able to penetrate deeper into the SC after digestion of their silica core, a result probably owed to an increase in the nanoparticles' flexibility. The SRS results showed, that the **NCs** indeed induced skin hydration, and that skin hydration increased after digesting the **NCs**' core. More importantly, it was demonstrated that the thermoresponsiveness further enhanced the D_2O concentration in different skin layers, hence the skin hydration. Especially the concentration in the viable epidermis drastically increased after applying a thermal trigger. In order to

evaluate if the skin hydration induced by the **NCs** sufficed to enhance the skin penetration of high molecular weight compounds, Atto Oxa12 (a high molecular weight dye) was employed as model drug. Studies showed that formulating the dye together with the **NCs** enhanced the skin penetration of Atto Oxa12 as compared to an aqueous formulation as well as a solution of the dye in 30% DMSO.

In conclusion, it could be shown that the interplay between the structure of the nanoparticles' core and material properties of the shell can dramatically affect the thermomechanical properties of nanoparticles. Additionally, the tremendous potential of thermoresponsive, soft, **NCs** to facilitate the delivery of high molecular weight compounds across the skin barrier was highlighted. Additionally, unprecedented findings about the effect of thermoresponsive properties on the skin could be unraveled.

As a future perspective, **NCs** with different Young's modulus should be studied in order to find the right balance between flexibility, deformability, structural integrity and skin penetration of the nanoparticles. Moreover, different sacrificial cores could be investigated as an alternative to silica nanoparticles. Especially the use of soft, hydrophobic beads could be interesting, as these could be loaded with hydrophobic drugs before performing the seeded precipitation polymerization. In light of the fascinating potential of thermoresponsive **NCs** for skin applications, it would be important to put more efforts in protocols for working under good manufacturing practice regulations, as well as reduce cost production to ease a possible transition from research to market. Additionally, it would be important to upscale the synthesis. For this purpose, the semi-batch methodology could be further explored. The semi-batch procedure, which allows the precise control over the monomer addition, could prove beneficial for improving the reactions yield. In addition, this process can be performed in reactors in a semi-automatic way, enabling the scale-up of the reaction.

5 References

(1) Tiwari, N.; Sonzogni, A. S.; Calderón, M. Can dermal delivery of therapeutics be improved using thermoresponsive nanogels? *Nanomedicine* **2019**, DOI:10.2217/nnm-2019-0345.

(2) Naolou, T.; Rühl, E.; Lendlein, A. Nanocarriers: Architecture, transport, and topical application of drugs for therapeutic use. *Eur J Pharm Biopharm* **2017**, DOI:10.1016/j.ejpb.2017.03.004.

(3) Schulz, R.; Yamamoto, K.; Klossek, A.; Flesch, R.; Honzke, S.; Rancan, F.; Vogt, A.; Blume-Peytavi, U.; Hedtrich, S.; Schäfer-Korting, M.et al. Data-based modeling of drug penetration relates human skin barrier function to the interplay of diffusivity and free-energy profiles. *Proc Natl Acad Sci U S A* **2017,** *114* (14), 3631.

(4) Craiglow, B. G. Ichthyosis in the newborn. *Semin Perinatol* **2013,** *37* (1), 26.

(5) Marukian, N. V.; Choate, K. A. Recent advances in understanding ichthyosis pathogenesis. *F1000Res* **2016,** *5*.

(6) Simpson, C. L.; Patel, D. M.; Green, K. J. Deconstructing the skin: cytoarchitectural determinants of epidermal morphogenesis. *Nat Rev Mol Cell Biol* **2011,** *12* (9), 565.

(7) Wickett, R. R.; Visscher, M. O. Structure and function of the epidermal barrier. *American Journal of Infection Control* **2006,** *34* (10, Supplement), S98.

(8) Vapniarsky, N.; Arzi, B.; Hu, J. C.; Nolta, J. A.; Athanasiou, K. A. Concise Review: Human Dermis as an Autologous Source of Stem Cells for Tissue Engineering and Regenerative Medicine. *Stem Cells Transl Med* **2015,** *4* (10), 1187.

(9) Kabashima, K.; Honda, T.; Ginhoux, F.; Egawa, G. The immunological anatomy of the skin. *Nat Rev Immunol* **2019,** *19* (1), 19.

(10) Bolzinger, M.-A.; Briançon, S.; Pelletier, J.; Chevalier, Y. Penetration of drugs through skin, a complex rate-controlling membrane. *Current Opinion in Colloid & Interface Science* **2012,** *17* (3), 156.

(11) Schneider, M.; Stracke, F.; Hansen, S.; Schäfer, U. F. Nanoparticles and their interactions with the dermal barrier. *Dermatoendocrinol* **2009,** *1* (4), 197.

(12) Hung, C.-F.; Chen, W.-Y.; Hsu, C.-Y.; Aljuffali, I. A.; Shih, H.-C.; Fang, J.-Y. Cutaneous penetration of soft nanoparticles via photodamaged skin: Lipid-based and polymer-based nanocarriers for drug delivery. *European Journal of Pharmaceutics and Biopharmaceutics* **2015,** *94*, 94.

(13) Baroli, B.; Ennas, M. G.; Loffredo, F.; Isola, M.; Pinna, R.; Arturo López-Quintela, M. Penetration of Metallic Nanoparticles in Human Full-Thickness Skin. *Journal of Investigative Dermatology* **2007,** *127* (7), 1701.

(14) Desai, P. R.; Shah, P. P.; Hayden, P.; Singh, M. Investigation of follicular and non-follicular pathways for polyarginine and oleic acid-modified nanoparticles. *Pharmaceutical research* **2013,** *30* (4), 1037.

(15) Sahle, F. F.; Giulbudagian, M.; Bergueiro, J.; Lademann, J.; Calderon, M. Dendritic polyglycerol and N-isopropylacrylamide based thermoresponsive nanogels as smart carriers for controlled delivery of drugs through the hair follicle. *Nanoscale* **2017,** *9* (1), 172.

(16) Ting, W. W.; Vest, C. D.; Sontheimer, R. D. Review of traditional and novel modalities that enhance the permeability of local therapeutics across the stratum corneum. *International Journal of Dermatology* **2004,** *43* (7), 538.

(17) Williams, A. C.; Barry, B. W. Penetration enhancers. *Adv Drug Deliv Rev* **2004,** *56* (5), 603.
(18) Lane, M. E. Skin penetration enhancers. *Int J Pharm* **2013,** *447* (1-2), 12.
(19) Banga, A. K.; Bose, S.; Ghosh, T. K. Iontophoresis and electroporation: comparisons and contrasts. *International Journal of Pharmaceutics* **1999,** *179* (1), 1.
(20) Tezel, A.; Dokka, S.; Kelly, S.; Hardee, G. E.; Mitragotri, S. Topical delivery of anti-sense oligonucleotides using low frequency sonophoresis. *Pharmaceutical Research* **2004,** *21* (12), 2219.
(21) Ting, W. W.; Vest, C. D.; Sontheimer, R. D. Review of traditional and novel modalities that enhance the permeability of local therapeutics across the stratum corneum. *Pharmacology and therapeutics: Review* **2004,** *43* (7), 538.
(22) Bramson, J.; Dayball, K.; Evelegh, C.; Wan, Y. H.; Page, D.; Smith, A. Enabling topical immunization via microporation: a novel method for pain-free and needle-free delivery of adenovirus-based vaccines. *Gene Ther* **2003,** *10* (3), 251.
(23) Lin, C. H.; Aljuffali, I. A.; Fang, J. Y. Lasers as an approach for promoting drug delivery via skin. *Expert Opin Drug Deliv.* **2014,** *11* (4), 599.
(24) Ye, Y.; Yu, J.; Wang, C.; Nguyen, N. Y.; Walker, G. M.; Buse, J. B.; Gu, Z. Microneedles Integrated with Pancreatic Cells and Synthetic Glucose-Signal Amplifiers for Smart Insulin Delivery. *Adv Mater* **2016,** *28* (16), 3115.
(25) Kim, Y. C.; Park, J. H.; Prausnitz, M. R. Microneedles for drug and vaccine delivery. *Adv Drug Deliv Rev* **2012,** *64* (14), 1547.
(26) Waghule, T.; Singhvi, G.; Dubey, S. K.; Pandey, M. M.; Gupta, G.; Singh, M.; Dua, K. Microneedles: A smart approach and increasing potential for transdermal drug delivery system. *Biomed Pharmacother* **2019,** *109*, 1249.
(27) Babity, S.; Roohnikan, M.; Brambilla, D. Advances in the Design of Transdermal Microneedles for Diagnostic and Monitoring Applications. *Small* **2018,** *14* (49), e1803186.
(28) Gupta, R.; Dwadasi, B. S.; Rai, B.; Mitragotri, S. Effect of Chemical Permeation Enhancers on Skin Permeability: In silico screening using Molecular Dynamics simulations. *Sci Rep* **2019,** *9* (1), 1456.
(29) Li, W.; Tang, J.; Terry, R. N.; Li, S.; Brunie, A.; Callahan, R. L.; Noel, R. K.; Rodríguez, C. A.; Schwendeman, S. P.; Prausnitz, M. R. Long-acting reversible contraception by effervescent microneedle patch. *Science Advances* **2019,** *5* (11), eaaw8145.
(30) Li;, W.; Tang;, J.; Li;, R. N. T. S.; Callahan;, A. B. R. L.; Rodríguez;, R. K. N. C. A.; Prausnitz, S. P. S. M. R. Long-acting reversible contraception by effervescent microneedle patch. *Science Advances* **2019,** *5*.
(31) Fakhraei Lahiji, S.; Kim, Y.; Kang, G.; Kim, S.; Lee, S.; Jung, H. Tissue Interlocking Dissolving Microneedles for Accurate and Efficient Transdermal Delivery of Biomolecules. *Sci Rep* **2019,** *9* (1), 7886.
(32) Fujii, M.; Ohara, R.; Matsumi, A.; Ohura, K.; Koizumi, N.; Imai, T.; Watanabe, Y. Effect of alcohol on skin permeation and metabolism of an ester-type prodrug in Yucatan micropig skin. *Eur J Pharm Sci* **2017,** *109*, 280.
(33) Kopecna, M.; Machacek, M.; Novackova, A.; Paraskevopoulos, G.; Roh, J.; Vavrova, K. Esters of terpene alcohols as highly potent, reversible, and low toxic skin penetration enhancers. *Sci Rep* **2019,** *9* (1), 14617.
(34) Lin, T. K.; Zhong, L.; Santiago, J. L. Anti-Inflammatory and Skin Barrier Repair Effects of Topical Application of Some Plant Oils. *Int J Mol Sci* **2017,** *19* (1).

(35) Kim, M. J.; Doh, H. J.; Choi, M. K.; Chung, S. J.; Shim, C. K.; Kim, D. D.; Kim, J. S.; Yong, C. S.; Choi, H. G. Skin permeation enhancement of diclofenac by fatty acids. *Drug Deliv* **2008,** *15* (6), 373.
(36) Ibrahim, S. A.; Li, S. K. Efficiency of fatty acids as chemical penetration enhancers: mechanisms and structure enhancement relationship. *Pharm Res* **2010,** *27* (1), 115.
(37) J. Piret; A. Désormeaux; H. Cormier, J. L. P. G. J. J. M. G. B. Sodium Lauryl Sulfate increases the Efficacy of a Topical Formulation of Foscarnet against Herpes Simplex Virus TAype 1 Cutaneous lesions in Mice. *Antimicrobial Agents and Chemotherapy* **2000**, 2263.
(38) Froebe, C. L.; Simion, F. A.; Rhein, L. D.; Cagan, R. H.; Kligman, A. Stratum corneum Lipid Removal by Surfactants: Relation to in vivo Irritation. *Dermatology* **1990,** *181* (4), 277.
(39) James-Smith, M. A.; Hellner, B.; Annunziato, N.; Mitragotri, S. Effect of surfactant mixtures on skin structure and barrier properties. *Ann Biomed Eng* **2011,** *39* (4), 1215.
(40) Muankaew, C.; Loftsson, T. Cyclodextrin-Based Formulations: A Non-Invasive Platform for Targeted Drug Delivery. *Basic Clin Pharmacol Toxicol* **2018,** *122* (1), 46.
(41) Felton, L. A.; Wiley, C. J.; Godwin, D. A. Influence of hydroxypropyl-beta-cyclodextrin on the transdermal permeation and skin accumulation of oxybenzone. *Drug Dev Ind Pharm* **2002,** *28* (9), 1117.
(42) Bentley, M. V. L. B.; Vianna, R. F.; Wilson, S.; Collett, J. H. Characterization of the Influence of some Cyclodextrins on the Stratum Corneum from the Hairless Mouse. *Journal of Pharmacy and Pharmacology* **1997,** *49* (4), 397.
(43) Ghanghoria, R.; Kesharwani, P.; Agashe, H. B.; Jain, N. K. Transdermal delivery of cyclodextrin-solubilized curcumin. *Drug Deliv Transl Res* **2013,** *3* (3), 272.
(44) Strebhardt, K.; Ullrich, A. Paul Ehrlich's magic bullet concept: 100 years of progress. *Nature Reviews Cancer* **2008,** *8* (6), 473.
(45) Martin, J. D.; Cabral, H.; Stylianopoulos, T.; Jain, R. K. Improving cancer immunotherapy using nanomedicines: progress, opportunities and challenges. *Nature Reviews Clinical Oncology* **2020,** *17* (4), 251.
(46) Cuggino, J. C.; Blanco, E. R. O.; Gugliotta, L. M.; Alvarez Igarzabal, C. I.; Calderon, M. Crossing biological barriers with nanogels to improve drug delivery performance. *J Control Release* **2019,** *307*, 221.
(47) Ensign, L. M.; Cone, R.; Hanes, J. Oral drug delivery with polymeric nanoparticles: the gastrointestinal mucus barriers. *Adv Drug Deliv Rev* **2012,** *64* (6), 557.
(48) Goyal, R.; Macri, L. K.; Kaplan, H. M.; Kohn, J. Nanoparticles and nanofibers for topical drug delivery. *J Control Release* **2016,** *240*, 77.
(49) Dubbert, J.; Nothdurft, K.; Karg, M.; Richtering, W. Core-shell-shell and hollow double-shell microgels with advanced temperature responsiveness. *Macromol Rapid Commun* **2015,** *36* (2), 159.
(50) Fleige, E.; Quadir, M. A.; Haag, R. Stimuli-responsive polymeric nanocarriers for the controlled transport of active compounds: concepts and applications. *Adv Drug Deliv Rev* **2012,** *64* (9), 866.
(51) Gao, L.; Zabihi, F.; Ehrmann, S.; Hedtrich, S.; Haag, R. Supramolecular nanogels fabricated via host-guest molecular recognition as penetration enhancer for dermal drug delivery. *J Control Release* **2019,** *300*, 64.
(52) Molina, M.; Asadian-Birjand, M.; Balach, J.; Bergueiro, J.; Miceli, E.; Calderon, M. Stimuli-responsive nanogel composites and their application in nanomedicine. *Chemical Society Reviews* **2015,** *44* (17), 6161.

(53) Mosquera, J.; Zhao, Y.; Jang, H. J.; Xie, N.; Xu, C.; Kotov, N. A.; Liz-Marzán, L. M. Plasmonic Nanoparticles with Supramolecular Recognition. *Advanced Functional Materials* **2019**, DOI:10.1002/adfm.201902082.
(54) Netsomboon, K.; Bernkop-Schnurch, A. Mucoadhesive vs. mucopenetrating particulate drug delivery. *Eur J Pharm Biopharm* **2016,** *98*, 76.
(55) Purbia, R.; Paria, S. Yolk/shell nanoparticles: classifications, synthesis, properties, and applications. *Nanoscale* **2015,** *7* (47), 19789.
(56) Ferber, S.; Tiram, G.; Sousa-Herves, A.; Eldar-Boock, A.; Krivitsky, A.; Scomparin, A.; Yeini, E.; Ofek, P.; Ben-Shushan, D.; Vossen, L. I.et al. Co-targeting the tumor endothelium and P-selectin-expressing glioblastoma cells leads to a remarkable therapeutic outcome. *Elife* **2017,** *6*.
(57) Miceli, E.; Wedepohl, S.; Osorio Blanco, E. R.; Rimondino, G. N.; Martinelli, M.; Strumia, M.; Molina, M.; Kar, M.; Calderon, M. Semi-interpenetrated, dendritic, dual-responsive nanogels with cytochrome c corona induce controlled apoptosis in HeLa cells. *Eur J Pharm Biopharm* **2018,** *130*, 115.
(58) Rancan, F.; Asadian-Birjand, M.; Dogan, S.; Graf, C.; Cuellar, L.; Lommatzsch, S.; Blume-Peytavi, U.; Calderon, M.; Vogt, A. Effects of thermoresponsivity and softness on skin penetration and cellular uptake of polyglycerol-based nanogels. *J Control Release* **2016,** *228*, 159.
(59) Rancan, F.; Volkmann, H.; Giulbudagian, M.; Schumacher, F.; Stanko, J. I.; Kleuser, B.; Blume-Peytavi, U.; Calderon, M.; Vogt, A. Dermal Delivery of the High-Molecular-Weight Drug Tacrolimus by Means of Polyglycerol-Based Nanogels. *Pharmaceutics* **2019,** *11* (8).
(60) Tanbour, R.; Martins, A. M.; Pitt, W. G.; Husseini, G. A. Drug Delivery Systems Based on Polymeric Micelles and Ultrasound: A Review. *Curr Pharm Des* **2016,** *22* (19), 2796.
(61) Oerlemans, C.; Bult, W.; Bos, M.; Storm, G.; Nijsen, J. F. W.; Hennink, W. E. Polymeric Micelles in Anticancer Therapy: Targeting, Imaging and Triggered Release. *Pharmaceutical Research* **2010,** *27* (12), 2569.
(62) Hill, J. P.; Shrestha, L. K.; Ishihara, S.; Ji, Q.; Ariga, K. Self-assembly: from amphiphiles to chromophores and beyond. *Molecules* **2014,** *19* (6), 8589.
(63) Yang, Y.; Bugno, J.; Hong, S. Nanoscale polymeric penetration enhancers in topical drug delivery. *Polymer Chemistry* **2013,** *4* (9).
(64) Aderibigbe, B. A.; Naki, T. Design and Efficacy of Nanogels Formulations for Intranasal Administration. *Molecules* **2018,** *23* (6).
(65) De Leon, A. S.; Molina, M.; Wedepohl, S.; Munoz-Bonilla, A.; Rodriguez-Hernandez, J.; Calderon, M. Immobilization of Stimuli-Responsive Nanogels onto Honeycomb Porous Surfaces and Controlled Release of Proteins. *Langmuir* **2016,** *32* (7), 1854.
(66) Nan, J.; Chen, Y.; Li, R.; Wang, J.; Liu, M.; Wang, C.; Chu, F. Polymeric Hydrogel Nanocapsules: A Thermo and pH Dual-responsive Carrier for Sustained Drug Release. *Nano-Micro Letters* **2014,** *6* (3).
(67) Soni, K. S.; Desale, S. S.; Bronich, T. K. Nanogels: An overview of properties, biomedical applications and obstacles to clinical translation. *J Control Release* **2016,** *240*, 109.
(68) Ramos, J.; Imaz, A.; Forcada, J. Temperature-sensitive nanogels: poly(N-vinylcaprolactam) versus poly(N-isopropylacrylamide). *Polym. Chem.* **2012,** *3* (4), 852.
(69) Duracher, D.; Elaissari, A.; Pichot, C. Preparation of poly(N-isopropylmethacrylamide) latexes kinetic studies and characterization. *Journal of Polymer Science Part a-Polymer Chemistry* **1999,** *37* (12), 1823.

(70) F. Meunier, A. E., C. Pichot. Preparation and Characterization of Cationic Poly(n)-Isopropylacrylamide) Copolymer Latexes. *Polymers for Advanced Technology* **1995,** *6*, 489.
(71) Giulbudagian, M.; Honzke, S.; Bergueiro, J.; Isik, D.; Schumacher, F.; Saeidpour, S.; Lohan, S. B.; Meinke, M. C.; Teutloff, C.; Schäfer-Korting, M.et al. Enhanced topical delivery of dexamethasone by beta-cyclodextrin decorated thermoresponsive nanogels. *Nanoscale* **2017,** *10* (1), 469.
(72) Giulbudagian, M.; Rancan, F.; Klossek, A.; Yamamoto, K.; Jurisch, J.; Neto, V. C.; Schrade, P.; Bachmann, S.; Rühl, E.; Blume-Peytavi, U.et al. Correlation between the chemical composition of thermoresponsive nanogels and their interaction with the skin barrier. *J Control Release* **2016,** *243*, 323.
(73) Sonzogni, A. S.; Yealland, G.; Kar, M.; Wedepohl, S.; Gugliotta, L. M.; Gonzalez, V. D. G.; Hedtrich, S.; Calderon, M.; Minari, R. J. Effect of Delivery Platforms Structure on the Epidermal Antigen Transport for Topical Vaccination. *Biomacromolecules* **2018,** *19* (12), 4607.
(74) Giulbudagian, M.; Yealland, G.; Honzke, S.; Edlich, A.; Geisendorfer, B.; Kleuser, B.; Hedtrich, S.; Calderon, M. Breaking the Barrier - Potent Anti-Inflammatory Activity following Efficient Topical Delivery of Etanercept using Thermoresponsive Nanogels. *Theranostics* **2018,** *8* (2), 450.
(75) Theune, L. E.; Charbaji, R.; Kar, M.; Wedepohl, S.; Hedtrich, S.; Calderon, M. Critical parameters for the controlled synthesis of nanogels suitable for temperature-triggered protein delivery. *Mater Sci Eng C Mater Biol Appl* **2019,** *100*, 141.
(76) Cao, Z.; Landfester, K.; Ziener, U. Preparation of dually, pH- and thermo-responsive nanocapsules in inverse miniemulsion. *Langmuir* **2012,** *28* (2), 1163.
(77) Cao, Z.; Ziener, U.; Landfester, K. Synthesis of Narrowly Size-Distributed Thermosensitive Poly(N-isopropylacrylamide) Nanocapsules in Inverse Miniemulsion. *Macromolecules* **2010,** *43* (15), 6353.
(78) Cong, Y.; Li, Q.; Chen, M.; Wu, L. Synthesis of Dual-Stimuli-Responsive Microcontainers with Two Payloads in Different Storage Spaces for Preprogrammable Release. *Angew Chem Int Ed Engl* **2017,** *56* (13), 3552.
(79) Fickert, J.; Wohnhaas, C.; Turshatov, A.; Landfester, K.; Crespy, D. Copolymers Structures Tailored for the Preparation of Nanocapsules. *Macromolecules* **2013,** *46* (3), 573.
(80) Marto, J.; Ribeiro, H. M.; Almeida, A. J. In *Smart Nanocontainers*, 2020, DOI:10.1016/b978-0-12-816770-0.00017-4.
(81) Pastorino, L.; Dellacasa, E.; Dabiri, M. H.; Fabiano, B.; Erokhina, S. Towards the Fabrication of Polyelectrolyte-Based Nanocapsules for Bio-Medical Applications. *BioNanoScience* **2016,** *6* (4), 496.
(82) Iyisan, B.; Landfester, K. Modular Approach for the Design of Smart Polymeric Nanocapsules. *Macromol Rapid Commun* **2019,** *40* (1), e1800577.
(83) Hatahet, T.; Morille, M.; Hommoss, A.; Devoisselle, J. M.; Muller, R. H.; Begu, S. Liposomes, lipid nanocapsules and smartCrystals(R): A comparative study for an effective quercetin delivery to the skin. *Int J Pharm* **2018,** *542* (1-2), 176.
(84) Simon, L.; Lapinte, V.; Lionnard, L.; Marcotte, N.; Morille, M.; Aouacheria, A.; Kissa, K.; Devoisselle, J. M.; Begu, S. Polyoxazolines based lipid nanocapsules for topical delivery of antioxidants. *Int J Pharm* **2020,** *579*, 119126.
(85) Marchiori, M. C. L.; Rigon, C.; Camponogara, C.; Oliveira, S. M.; Cruz, L. Hydrogel containing silibinin-loaded pomegranate oil based nanocapsules exhibits anti-

inflammatory effects on skin damage UVB radiation-induced in mice. *J Photochem Photobiol B* **2017,** *170*, 25.

(86) Rigon, C.; Marchiori, M. C. L.; da Silva Jardim, F.; Pegoraro, N. S.; Chaves, P. D. S.; Velho, M. C.; Beck, R. C. R.; Ourique, A. F.; Sari, M. H. M.; Oliveira, S. M.et al. Hydrogel containing silibinin nanocapsules presents effective anti-inflammatory action in a model of irritant contact dermatitis in mice. *Eur J Pharm Sci* **2019,** *137*, 104969.

(87) Villegas, M. R.; Baeza, A.; Usategui, A.; Ortiz-Romero, P. L.; Pablos, J. L.; Vallet-Regi, M. Collagenase nanocapsules: An approach to fibrosis treatment. *Acta Biomater* **2018,** *74*, 430.

(88) Lademann, J.; Patzelt, A.; Richter, H.; Lademann, O.; Baier, G.; Breucker, L.; Landfester, K. Nanocapsules for drug delivery through the skin barrier by tissue-tolerable plasma. *Laser Physics Letters* **2013,** *10* (8), 083001.

(89) Schmid, A. J.; Dubbert, J.; Rudov, A. A.; Pedersen, J. S.; Lindner, P.; Karg, M.; Potemkin, II; Richtering, W. Multi-Shell Hollow Nanogels with Responsive Shell Permeability. *Sci Rep* **2016,** *6*, 22736.

(90) Bentz, K. C.; Savin, D. A. Hollow polymer nanocapsules: synthesis, properties, and applications. *Polymer Chemistry* **2018,** *9* (16), 2059.

(91) Landfester, K.; Bechthold, N.; Tiarks, F.; Antonietti, M. Formulation and Stability Mechanisms of Polymerizable Miniemulsions. *Macromolecules* **1999,** *32* (16), 5222.

(92) Landfester, K.; Musyanovych, A. *Hydrogels in Miniemulsions*; Springer Berlin Heidelberg: Berlin, Heidelberg, 2010.

(93) Tiarks, F.; Landfester, K.; Antonietti, M. Silica Nanoparticles as Surfactants and Fillers for Latexes Made by Miniemulsion Polymerization. *Langmuir* **2001,** *17* (19), 5775.

(94) Dubbert, J.; Honold, T.; Pedersen, J. S.; Radulescu, A.; Drechsler, M.; Karg, M.; Richtering, W. How Hollow Are Thermoresponsive Hollow Nanogels? *Macromolecules* **2014,** *47* (24), 8700.

(95) Song, X.; Bao, B.; Tao, J.; Zhao, S.; Han, X.; Liu, H. Deswelling Dynamics of Thermoresponsive Microgel Capsules and Their Ultrasensitive Sensing Applications: A Mesoscopic Simulation Study. *The Journal of Physical Chemistry C* **2018,** *123* (3), 1828.

(96) Larrañaga, A.; Lomora, M.; Sarasua, J. R.; Palivan, C. G.; Pandit, A. Polymer capsules as micro-/nanoreactors for therapeutic applications: Current strategies to control membrane permeability. *Progress in Materials Science* **2017,** *90*, 325.

(97) Shchepelina, O.; Kozlovskaya, V.; Kharlampieva, E.; Mao, W.; Alexeev, A.; Tsukruk, V. V. Anisotropic Micro- and Nano-Capsules. *Macromolecular Rapid Communications* **2010,** *31* (23), 2041.

(98) Zhu, H.; Stein, E. W.; Lu, Z.; Lvov, Y. M.; McShane, M. J. Synthesis of Size-Controlled Monodisperse Manganese Carbonate Microparticles as Templates for Uniform Polyelectrolyte Microcapsule Formation. *Chemistry of Materials* **2005,** *17* (9), 2323.

(99) Mora-Huertas, C. E.; Fessi, H.; Elaissari, A. Polymer-based nanocapsules for drug delivery. *Int J Pharm* **2010,** *385* (1-2), 113.

(100) De Geest, B. G.; Déjugnat, C.; Prevot, M.; Sukhorukov, G. B.; Demeester, J.; De Smedt, S. C. Self-Rupturing and Hollow Microcapsules Prepared from Bio-polyelectrolyte-Coated Microgels. *Advanced Functional Materials* **2007,** *17* (4), 531.

(101) Li, S.; Wang, J.; Zhao, S.; Cai, W.; Wang, Z.; Wang, S. Effect of surface modification and medium on the rheological properties of silica nanoparticle suspensions. *Ceramics International* **2016,** *42* (6), 7767.

(102) Han, Y.; Lu, Z.; Teng, Z.; Liang, J.; Guo, Z.; Wang, D.; Han, M.-Y.; Yang, W. Unraveling the Growth Mechanism of Silica Particles in the Stöber Method: In Situ Seeded Growth Model. *Langmuir* **2017,** *33* (23), 5879.
(103) Esim, O.; Kurbanoglu, S.; Savaser, A.; Ozkan, S. A.; Ozkan, Y. In *New Developments in Nanosensors for Pharmaceutical Analysis*; Ozkan, S. A.;Shah, A., Eds.; Academic Press, **2019**, DOI:https://doi.org/10.1016/B978-0-12-816144-9.00009-2.
(104) Greenberg, S. A. The Depolymerization of Silica in Sodium Hydroxide Solutions. *The Journal of Physical Chemistry* **1957,** *61* (7), 960.
(105) Zhong, C.; He, M.; Lou, K.; Gao, F. In *Neurotoxicity of Nanomaterials and Nanomedicine*; Jiang, X.;Gao, H., Eds.; Academic Press, **2017**, DOI:https://doi.org/10.1016/B978-0-12-804598-5.00010-6.
(106) Roy, D.; Brooks, W. L.; Sumerlin, B. S. New directions in thermoresponsive polymers. *Chem Soc Rev* **2013,** *42* (17), 7214.
(107) Li, C.; Ma, Y.; Tian, Z. Thermal Switching of Thermoresponsive Polymer Aqueous Solutions. *ACS Macro Letters* **2017,** *7* (1), 53.
(108) Aguirre, G.; Ramos, J.; Heuts, J. P. A.; Forcada, J. Biocompatible and thermo-responsive nanocapsule synthesis through vesicle templating. *Polymer Chemistry* **2014,** *5* (15), 4569.
(109) G. J. L. Wuite, C. F. S. PNAS, **2006**.
(110) Myerson, J. W.; Braender, B.; McPherson, O.; Glassman, P. M.; Kiseleva, R. Y.; Shuvaev, V. V.; Marcos-Contreras, O.; Grady, M. E.; Lee, H. S.; Greineder, C. F.et al. Flexible Nanoparticles Reach Sterically Obscured Endothelial Targets Inaccessible to Rigid Nanoparticles. *Adv Mater* **2018,** *30* (32), e1802373.
(111) Hui, Y.; Yi, X.; Hou, F.; Wibowo, D.; Zhang, F.; Zhao, D.; Gao, H.; Zhao, C. X. Role of Nanoparticle Mechanical Properties in Cancer Drug Delivery. *ACS Nano* **2019,** *13* (7), 7410.
(112) Liang, Q.; Bie, N.; Yong, T.; Tang, K.; Shi, X.; Wei, Z.; Jia, H.; Zhang, X.; Zhao, H.; Huang, W.et al. The softness of tumour-cell-derived microparticles regulates their drug-delivery efficiency. *Nature Biomedical Engineering* **2019**, DOI:10.1038/s41551-019-0405-4.
(113) Bal, S. M.; Ding, Z.; van Riet, E.; Jiskoot, W.; Bouwstra, J. A. Advances in transcutaneous vaccine delivery: do all ways lead to Rome? *J Control Release* **2010,** *148* (3), 266.
(114) Leimann, F. V.; Costa, C.; Gonçalves, O. H.; Musyanovych, A.; Landfester, K.; Sayer, C.; de Araújo, P. H. H. Poly(3-hydroxybutirate-co-3-hydroxyvalerate)-Polystyrene Hybrid Nanoparticles via Miniemulsion Polymerization. *Macromolecular Reaction Engineering* **2016,** *10* (1), 39.
(115) Wang, J.; Hu, J. H.; Li, F. Q.; Liu, G. Z.; Zhu, Q. G.; Liu, J. Y.; Ma, H. J.; Peng, C.; Si, F. G. Strong cellular and humoral immune responses induced by transcutaneous immunization with HBsAg DNA-cationic deformable liposome complex. *Exp Dermatol* **2007,** *16* (9), 724.
(116) Vij, M.; Natarajan, P.; Pattnaik, B. R.; Alam, S.; Gupta, N.; Santhiya, D.; Sharma, R.; Singh, A.; Ansari, K. M.; Gokhale, R. S.et al. Non-invasive topical delivery of plasmid DNA to the skin using a peptide carrier. *J Control Release* **2016,** *222*, 159.
(117) Mehravar, E.; Agirre, A.; Ballard, N.; van Es, S.; Arbe, A.; Leiza, J. R.; Asua, J. M. Insights into the Network Structure of Cross-Linked Polymers Synthesized via Miniemulsion Nitroxide-Mediated Radical Polymerization. *Macromolecules* **2018,** *51* (23), 9740.

(118) Seuss, M.; Schmolke, W.; Drechsler, A.; Fery, A.; Seiffert, S. Core-Shell Microgels with Switchable Elasticity at Constant Interfacial Interaction. *ACS Appl Mater Interfaces* **2016,** *8* (25), 16317.
(119) Yu, M.; Xu, L.; Tian, F.; Su, Q.; Zheng, N.; Yang, Y.; Wang, J.; Wang, A.; Zhu, C.; Guo, S.et al. Rapid transport of deformation-tuned nanoparticles across biological hydrogels and cellular barriers. *Nat Commun* **2018,** *9* (1), 2607.
(120) Guz, N.; Dokukin, M.; Kalaparthi, V.; Sokolov, I. If cell mechanics can be described by elastic modulus: study of different models and probes used in indentation experiments. *Biophys J* **2014,** *107* (3), 564.
(121) Dunér, G.; Thormann, E.; Dėdinaitė, A.; Claesson, P. M.; Matyjaszewski, K.; Tilton, R. D. Nanomechanical mapping of a high curvature polymer brush grafted from a rigid nanoparticle. *Soft Matter* **2012,** *8* (32).
(122) Fischer, H.; Stadler, H.; Erina, N. Quantitative temperature-depending mapping of mechanical properties of bitumen at the nanoscale using the AFM operated with PeakForce Tapping mode. *J Microsc* **2013,** *250* (3), 210.
(123) Guerrero, C. R.; Garcia, P. D.; Garcia, R. Subsurface Imaging of Cell Organelles by Force Microscopy. *ACS Nano* **2019**, DOI:10.1021/acsnano.9b04808.
(124) Guo, D.; Li, J.; Xie, G.; Wang, Y.; Luo, J. Elastic properties of polystyrene nanospheres evaluated with atomic force microscopy: size effect and error analysis. *Langmuir* **2014,** *30* (24), 7206.
(125) Takayuki Uchihashi, R. L., Toshio Ando, Hiroyuki Noji. High-Speed Atomic Force Microscopy Reveals Rotary Catalysis of Rotorless F1-ATPase. *Science* **2011,** *333* (6043), 755.
(126) Stanley, G. J.; Akpinar, B.; Shen, Q.; Fisher, P. D. E.; Lusk, C. P.; Lin, C.; Hoogenboom, B. W. Quantification of Biomolecular Dynamics Inside Real and Synthetic Nuclear Pore Complexes Using Time-Resolved Atomic Force Microscopy. *ACS Nano* **2019,** *13* (7), 7949.
(127) Dufrene, Y. F.; Ando, T.; Garcia, R.; Alsteens, D.; Martinez-Martin, D.; Engel, A.; Gerber, C.; Muller, D. J. Imaging modes of atomic force microscopy for application in molecular and cell biology. *Nat Nanotechnol* **2017,** *12* (4), 295.
(128) Cuellar, J. L.; Llarena, I.; Iturri, J. J.; Donath, E.; Moya, S. E. A novel approach for measuring the intrinsic nanoscale thickness of polymer brushes by means of atomic force microscopy: application of a compressible fluid model. *Nanoscale* **2013,** *5* (23), 11679.
(129) Cuellar, J. L.; Meinhoevel, F.; Hoehne, M.; Donath, E. Size and mechanical stability of norovirus capsids depend on pH: a nanoindentation study. *J Gen Virol* **2010,** *91* (Pt 10), 2449.
(130) Ivanovska, I. L.; de Pablo, P. J.; Ibarra, B.; Sgalari, G.; MacKintosh, F. C.; Carrascosa, J. L.; Schmidt, C. F.; Wuite, G. J. Bacteriophage capsids: tough nanoshells with complex elastic properties. *Proc Natl Acad Sci U S A* **2004,** *101* (20), 7600.
(131) Morales-Rivas, L.; Gonzalez-Orive, A.; Garcia-Mateo, C.; Hernandez-Creus, A.; Caballero, F. G.; Vazquez, L. Nanomechanical characterization of nanostructured bainitic steel: Peak Force Microscopy and Nanoindentation with AFM. *Sci Rep* **2015,** *5*, 17164.
(132) Passeri, D.; Rossi, M.; Tamburri, E.; Terranova, M. L. Mechanical characterization of polymeric thin films by atomic force microscopy based techniques. *Anal Bioanal Chem* **2013,** *405* (5), 1463.

(133) Sader, J. E.; Chon, J. W. M.; Mulvaney, P. Calibration of rectangular atomic force microscope cantilevers. *Review of Scientific Instruments* **1999,** *70* (10), 3967.
(134) Sader, J. E.; Sanelli, J. A.; Adamson, B. D.; Monty, J. P.; Wei, X.; Crawford, S. A.; Friend, J. R.; Marusic, I.; Mulvaney, P.; Bieske, E. J. Spring constant calibration of atomic force microscope cantilevers of arbitrary shape. *Rev Sci Instrum* **2012,** *83* (10), 103705.
(135) Usov, I.; Nystrom, G.; Adamcik, J.; Handschin, S.; Schutz, C.; Fall, A.; Bergstrom, L.; Mezzenga, R. Understanding nanocellulose chirality and structure-properties relationship at the single fibril level. *Nat Commun* **2015,** *6*, 7564.
(136) Haugstad, G. Overview of AFM. *Atomic Force Microscopy* **2012**, DOI:doi:10.1002/9781118360668.ch1.
(137) Vahabi, S.; Nazemi Salman, B.; Javanmard, A. Atomic force microscopy application in biological research: a review study. *Iran J Med Sci* **2013,** *38* (2), 76.
(138) Osorio-Blanco, E. R.; Bergueiro, J.; Abali, B. E.; Ehrmann, S.; Böttcher, C.; Müller, A. J.; Cuéllar-Camacho, J. L.; Calderón, M. Effect of Core Nanostructure on the Thermomechanical Properties of Soft Nanoparticles. *Chemistry of Materials* **2020,** *32* (1), 518.
(139) Young, T. J.; Monclus, M. A.; Burnett, T. L.; Broughton, W. R.; Ogin, S. L.; Smith, P. A. The use of the PeakForceTMquantitative nanomechanical mapping AFM-based method for high-resolution Young's modulus measurement of polymers. *Measurement Science and Technology* **2011,** *22* (12).
(140) Heinen, S.; Cuellar-Camacho, J. L.; Weinhart, M. Thermoresponsive poly(glycidyl ether) brushes on gold: Surface engineering parameters and their implication for cell sheet fabrication. *Acta Biomater* **2017,** *59*, 117.
(141) Lorenzoni, M.; Evangelio, L.; Verhaeghe, S.; Nicolet, C.; Navarro, C.; Perez-Murano, F. Assessing the Local Nanomechanical Properties of Self-Assembled Block Copolymer Thin Films by Peak Force Tapping. *Langmuir* **2015,** *31* (42), 11630.
(142) Smolyakov, G.; Formosa-Dague, C.; Severac, C.; Duval, R. E.; Dague, E. High speed indentation measures by FV, QI and QNM introduce a new understanding of bionanomechanical experiments. *Micron* **2016,** *85*, 8.
(143) Kopycinska-Muller, M.; Geiss, R. H.; Hurley, D. C. Contact mechanics and tip shape in AFM-based nanomechanical measurements. *Ultramicroscopy* **2006,** *106* (6), 466.
(144) Michel, J. P.; Ivanovska, I. L.; Gibbons, M. M.; Klug, W. S.; Knobler, C. M.; Wuite, G. J. L.; Schmidt, C. F. Nanoindentation studies of full and empty viral capsids and the effects of capsid protein mutations on elasticity and strength. *Proceedings of the National Academy of Sciences* **2006,** *103*, 6184.
(145) Roos, W. H. AFM nanoindentation of protein shells, expanding the approach beyond viruses. *Semin Cell Dev Biol* **2018,** *73*, 145.
(146) Sirghi, L.; Rossi, F. The effect of adhesion on the contact radius in atomic force microscopy indentation. *Nanotechnology* **2009,** *20* (36), 365702.
(147) Osorio-Blanco, E. R.; Rancan, F.; Klossek, A.; Nissen, J. H.; Hoffmann, L.; Bergueiro, J.; Riedel, S.; Vogt, A.; Rühl, E.; Calderon, M. Polyglycerol-based Thermoresponsive Nanocapsules Induce Skin Hydration and Serve as Skin Penetration Enhancer. *ACS Appl Mater Interfaces* **2020**, DOI:10.1021/acsami.0c06874.
(148) Karg, M.; Wellert, S.; Prevost, S.; Schweins, R.; Dewhurst, C.; Liz-Marzán, L. M.; Hellweg, T. Well defined hybrid PNIPAM core-shell microgels: size variation of the silica nanoparticle core. *Colloid and Polymer Science* **2010,** *289* (5-6), 699.
(149) Nishizawa, Y.; Matsui, S.; Urayama, K.; Kureha, T.; Shibayama, M.; Uchihashi, T.; Suzuki, D. Non-Thermoresponsive Decanano-sized Domains in Thermoresponsive Hydrogel

Microspheres Revealed by Temperature-Controlled High-Speed Atomic Force Microscopy. *Angew Chem Int Ed Engl* **2019,** *58* (26), 8809.

(150) Steinhilber, D.; Witting, M.; Zhang, X.; Staegemann, M.; Paulus, F.; Friess, W.; Kuchler, S.; Haag, R. Surfactant free preparation of biodegradable dendritic polyglycerol nanogels by inverse nanoprecipitation for encapsulation and release of pharmaceutical biomacromolecules. *J Control Release* **2013,** *169* (3), 289.

(151) Wei, Q.; Achazi, K.; Liebe, H.; Schulz, A.; Noeske, P. L.; Grunwald, I.; Haag, R. Mussel-inspired dendritic polymers as universal multifunctional coatings. *Angew Chem Int Ed Engl* **2014,** *53* (43), 11650.

(152) Zhang, X.; Achazi, K.; Haag, R. Boronate cross-linked ATP- and pH-responsive nanogels for intracellular delivery of anticancer drugs. *Adv Healthc Mater* **2015,** *4* (4), 585.

(153) Witting, M.; Molina, M.; Obst, K.; Plank, R.; Eckl, K. M.; Hennies, H. C.; Calderón, M.; Frieß, W.; Hedtrich, S. Thermosensitive dendritic polyglycerol-based nanogels for cutaneous delivery of biomacromolecules. *Nanomedicine: Nanotechnology, Biology and Medicine 11* (5), 1179.

(154) Berto, P.; Andresen, E. R.; Rigneault, H. Background-free stimulated Raman spectroscopy and microscopy. *Phys Rev Lett* **2014,** *112* (5), 053905.

6 Appendix

6.1 Supplementary Information

6.1.1 Effect of Core Structure on the Mechanical Properties of Soft Nanoparticles

E. R. Osorio-Blanco, J. Bergueiro, B. E. Abali, S. Ehrmann, C. Böttcher, A. J. Müller, J. L. Cuéllar-Camacho, M. Calderón, *Chemistry of Materials* **2020**, *32*, 518-528.

Reprinted with permission from reference 138. Copyright 2020 American Chemical Society.
The article is electronically available:
https://pubs.acs.org/doi/10.1021/acs.chemmater.9b04258?goto=supporting-info

Effect of Core Nanostructure on the Thermomechanical Properties of Soft Nanoparticles

Ernesto Rafael Osorio-Blanco,[†] Julian Bergueiro,[†] Bilen Emek Abali,[⊥] Svenja Ehrmann, [†§] Christoph Böttcher, [§] Alejandro J. Müller, [±ϕ] José Luis Cuéllar-Camacho*[†] and Marcelo Calderón*[†‡ϕ]

†Freie Universität Berlin, Institute of Chemistry and Biochemistry, Takustr. 3, 14195 Berlin, Germany

⊥Technische Universität Berlin, Institute of Mechanics, Einsteinufer 5, 10587 Berlin, Germany

§Freie Universität Berlin, Research Center of Electron Microscopy and Core Facility BioSupraMol, Institute of Chemistry and Biochemistry, Fabeckstr. 36a, 14195 Berlin, Germany

±POLYMAT and Polymer Science and Technology Department, Faculty of Chemistry, University of the Basque Country UPV/EHU, Paseo Manuel de Lardizabal 3, 20018 Donostia-San Sebastián, Spain

‡POLYMAT and Applied Chemistry Department, Faculty of Chemistry, University of the Basque Country, UPV/EHU, Paseo Manuel de Lardizabal 3, 20018 Donostia-San Sebastián, Spain

ϕIKERBASQUE, Basque Foundation for Science, 48013 Bilbao, Spain

Materials

Ammonia solution (Roth, 25%), bisacrylamide (BIS; Sigma-Aldrich), ethanol (dry) (Acros Organics, 99.8%), potassium peroxodisulfate (KPS; Merck), sodiumdodecylsulfate (SDS; Sigma-Aldrich) sodium hydroxide (NaOH; Merck Millipore), tetraethylorthosilicate (TEOS; Sigma-Aldrich), 3-(trimethoxysilyl) propyl methacrylate (TPM; Sigma-Aldrich) were used without further purification. The monomer N-isopropylacrylamide (NIPAM; Sigma-Aldrich) was purified by recrystallization from hexane (Sigma-Aldrich). The water used during the project was purified using a Milli-Q system (Millipore).

Methods

Reactions under oxygen- and water-free conditions were performed under an argon inert gas atmosphere, using standard Schlenk techniques. Reagents and solvents were added with syringes via septum under argon flow. Solids were added as a solution or as powder under argon flow. The characterization of the nanoarchitectures was performed by ^{1}H-NMR, IR, and UV. Size and polydispersity were analyzed by DLS, NTA, TEM, SEM, and AFM.

Proton nuclear magnetic resonance (^{1}H-NMR): The spectra were recorded with Jeol ECX (400 MHz) at concentrations between 5-20 mg/mL. The samples were dissolved in deuterated solvents (D_2O, ^{1}H: 4.79 ppm; $CDCl_3$, ^{1}H: 7.26 ppm). The results were analyzed using MestReNova (version 7.1.2). The multiplicities are listed as follow: s (singlet), d (doublet), t (triplet), q (quartet), m (multiplet).

Fourier transform infra-red spectroscopy (FT-IR): FT-IR spectra were recorded on a Jasco FT/IR-410 spectrometer (4000-500 cm^{-1}) and analyzed using Omnic software.

Dynamic light scattering (DLS): Size distribution was measured at various temperatures by dynamic light scattering (DLS) using a Zetasizer Nano-ZS 90 (Malvern, UK) equipped with a He-Ne laser (λ = 633 nm) under a scattering angle of 173°. For equilibration, samples with a concentration of 1 mg/mL were incubated at the desired temperature for 5 min prior to the measurement. Particle size distributions are given as the average of three measurements from intensity distribution curves. Due to the monomodal distribution as well as single exponential decay of the autocorrelation functions of the samples, the hydrodynamic diameters are reported from the intensity distribution curves.

Nanoparticle tracking analysis (NTA): Nanoparticle size and concentration were measured by NTA using a Nanosight NS500 (Malvern Instruments, Malver, UK). Nanoparticle concentrations of 1 μg/mL were used for the analysis. Particle sizes and concentrations are given as the average of three measurements.

Synthesis and characterization of thermoresponsive nanoarchitectures (NGs, SiO_2@NGs, and NCs)

Synthesis and characterization of PNIPAM-BIS nanogels (NGs): NGs were synthesized using a precipitation polymerization technique. NIPAM (100 mg) was dissolved together with BIS (7.8 mg) and SDS (2 mg) in Milli Q water (5 mL). The solution was purged with Argon for 1 h and then heated up to 70 °C. The reaction was started by adding a solution of KPS in water (2 mg dissolved in 1 mL water) to the reaction mixture. The polymerization was stirred for 4 h at 70 °C and subsequently dialyzed for 5 d. The product was lyophilized and kept in the fridge for further analysis via ^{1}H-NMR, TEM, AFM and DLS. Yield: quantitative. ^{1}H-NMR (400 MHz, D_2O); δ: 1.19 (s, 6 H, isopropyl groups of NIPAM), 1.62 (br, 2 H, polymer backbone), 2.15 (br, 1 H, polymer backbone), 3.92 (br, 1 H, isopropyl group NIPAM).

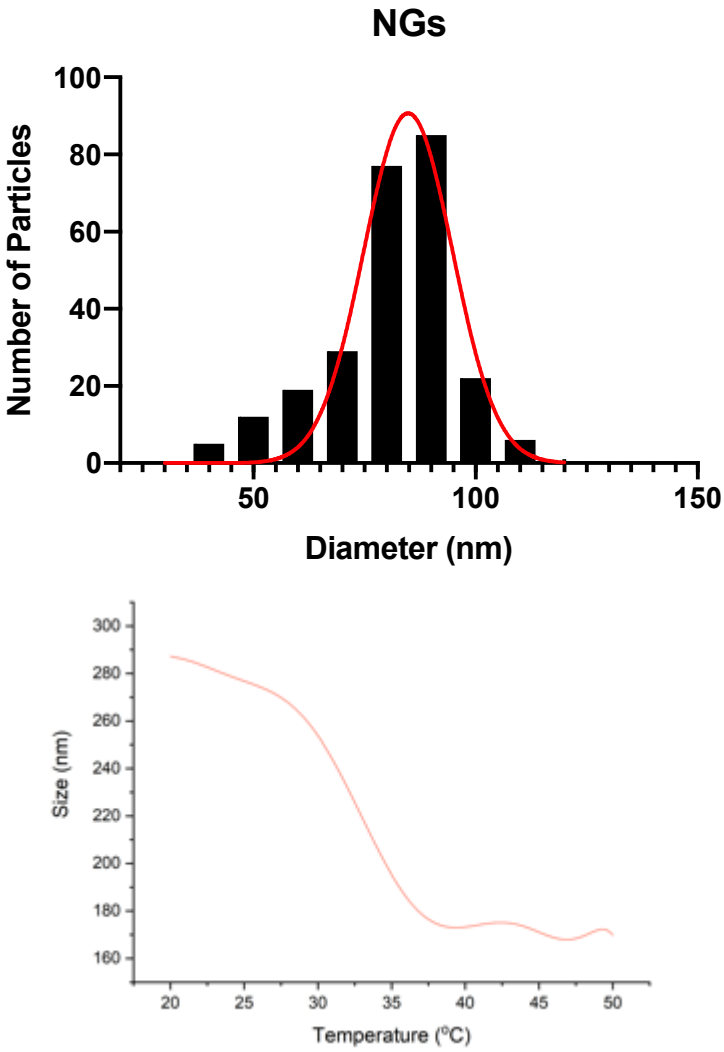

Figure 1. Size versus Temperature trend.

Synthesis and characterization of nanogels with silica nanoparticles in their core (SiO₂@NGs): Silica nanoparticles (SiO_2NPs) were synthesized using the Stöber method. A mixture of 11 mL ammonia and 130 mL extra pure ethanol was heated up to 60 °C in a 300 mL three-neck round flask equipped with a reflux condenser and a magnetic stirrer.[1] After 60 minutes equilibration time, a preheated solution of TEOS (5 mL) in ethanol (15 mL) was rapidly added. The reaction mixture became turbid within 30 minutes after the addition. The reaction was stirred for 24 hours at a constant temperature of 60 °C. Afterwards the mixture was cooled down to room temperature and TMP (5.3982×10^{-18} g TMP per SiO_2NP) was added dropwise. The dispersion was stirred for 12 hours at room temperature and then refluxed for 1 hour. Finally, the SiO_2NPs were purified by centrifugation (3 cycles of 6000 rpm, 1 hours) and re-dispersed in fresh ethanol to yield a dispersion with a concentration of 0.045 g mL^{-1}. The characterization of the product was done via IR analysis. Yield: 100%; IR (cm^{-1}): 1733 (C=O), 1652 (C=C), 945 (Si-O-Si), 791 (Si-OH).

The synthesis of SiO_2@NGs was performed following a previously reported seeded precipitation polymerization methodology.[2] NIPAM (100 mg) was dissolved together with BIS (7.8 mg) and SDS (2 mg) in Milli Q water (5 mL). The solution was purged with Argon for 1 h and then heated up to 70 °C. After 30 minutes equilibration time, a solution of modified silica NPs (10 mg) with a concentration of 45 mg/mL was added dropwise. The reaction was started by adding KPS (2 mg dissolved in 1 mL water) to the solution, becoming turbid within ten minutes. The reaction was stirred for 4 h at 70 °C. The product was purified by centrifugation

and redispersion in fresh Milli Q water and afterwards lyophilized and kept in the fridge. The characterization of the product was done via ^{1}H-NMR, TEM, AFM and DLS. Yield: 65%. ^{1}H-NMR (400 MHz, D_2O); δ: 1.14 (s, 6 H, isopropyl groups of NIPAM), 1.57 (br, 2 H, polymer backbone), 1.95 (br, 1 H, polymer backbone), 3.89 (br, 1 H, isopropyl group NIPAM).

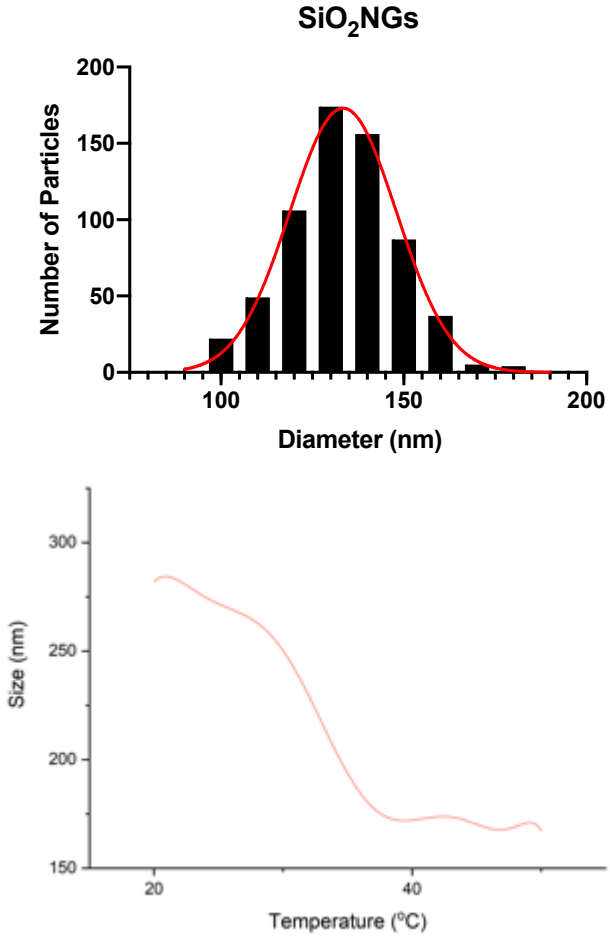

Figure 2. Size versus Temperature trend.

Synthesis and characterization of PNIPAM-BIS nanocapsules (NCs): PNIPAM-BIS SiO_2@NGs (10 mg) were dissolved in 20 mL of NaOH (0.05 M). The solution was stirred for 4 days at r.t. Finally, the NCs were purified by dialysis in water until a neutral pH was achieved. Subsequently, the NCs were lyophilized and stored in the fridge. The characterization of the product was done via ^{1}H-NMR, TEM, AFM and DLS. Yield: 100%; ^{1}H-NMR (400 MHz, D_2O); δ: 1.18 (s, 6 H, isopropyl groups of NIPAM), 1.59 (br, 2 H, polymer backbone), 1.95 (br, 1 H, polymer backbone), 3.91 (br, 1 H, isopropyl group NIPAM). The core dissolution was confirmed using TEM and AFM.

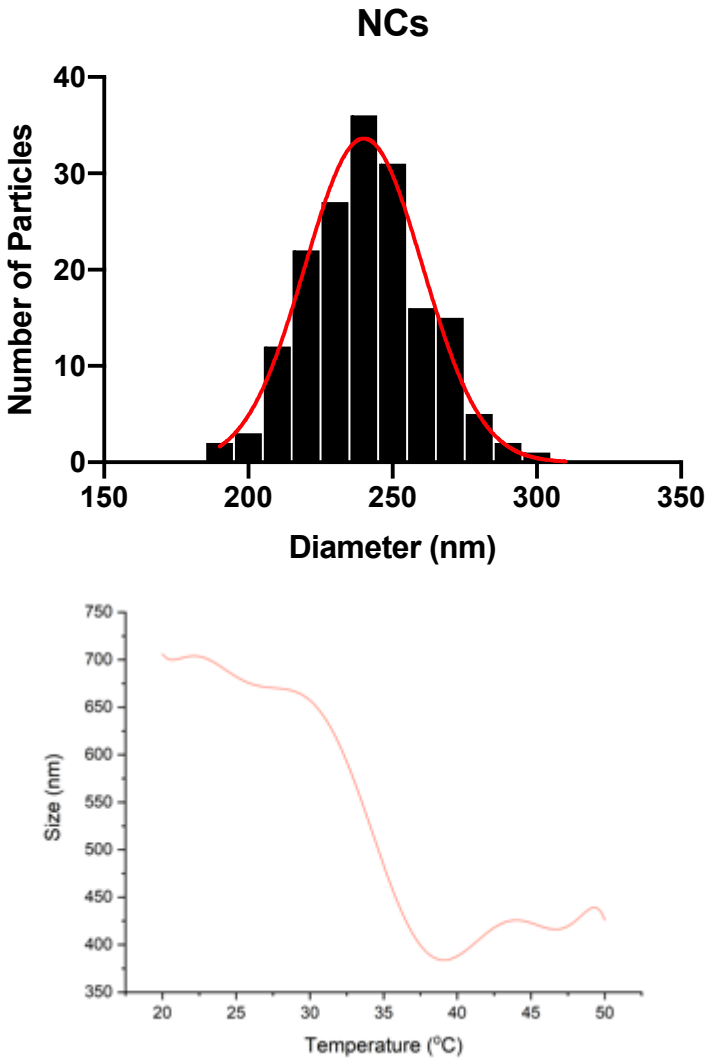

Figure 3. Size versus Temperature trend.

Cryogenic transmission electron microscopy (cryo-TEM):

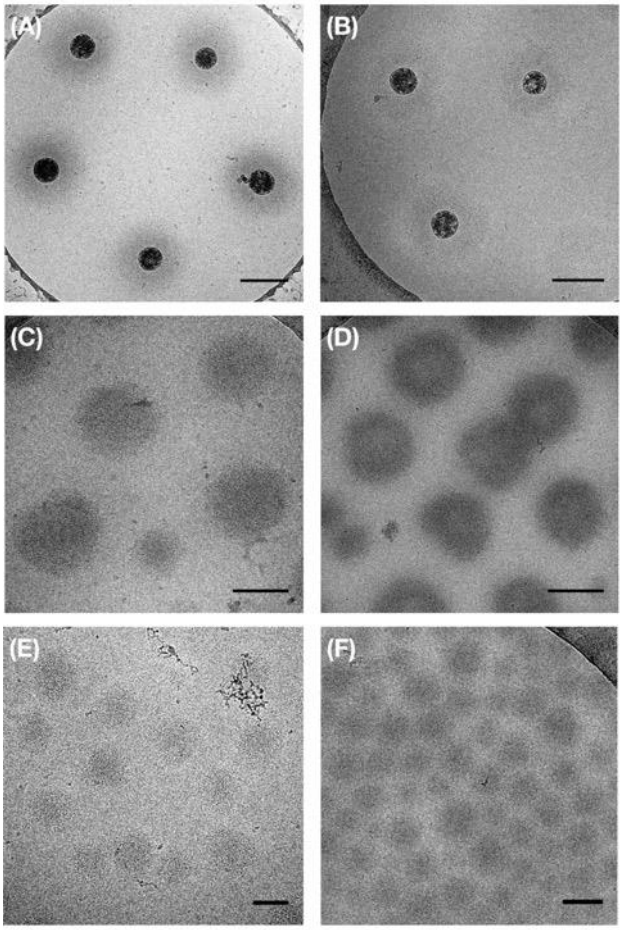

Figure 4. Cryo-TEM images of SiO_2@NG at (A) 20°C; (B) 40°C and NCs at (C) 20°C and (D) 40°C and NGs at 20 °C(E) and 40 °C (F). Scale bar represents 200 nm (A-D) in the upper and 100 nm (E and F) in the lower images.

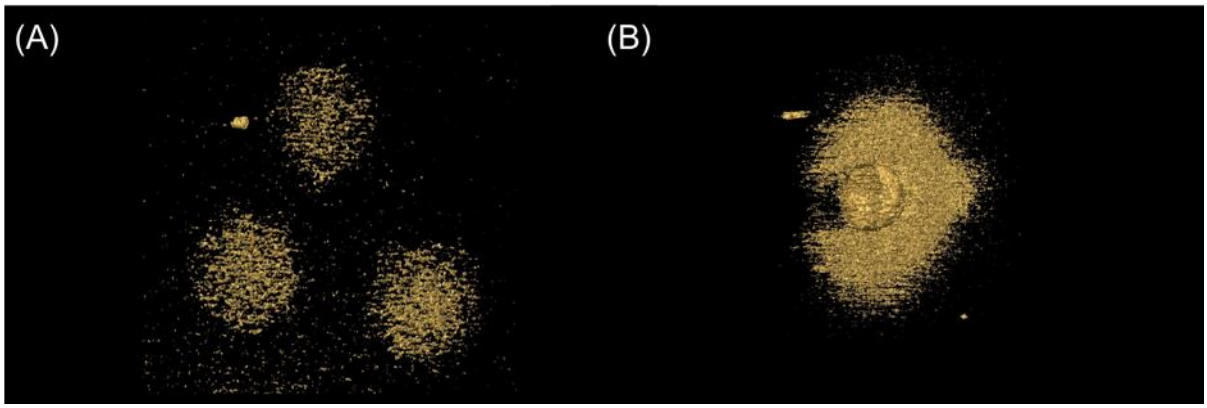

Figure 5. Isosurface representation of reconstructed cryo-ET data: **(A)** NGs and **(B)** SiO_2@NGs. For better depiction of the silica core, the volume is only shown half. (visualization by AMIRA software V 6.0.0 (Thermo Fisher Scientific Inc., Waltham, Massachusetts, USA)).

PeakForce quantitative nanomechanics (QNM):

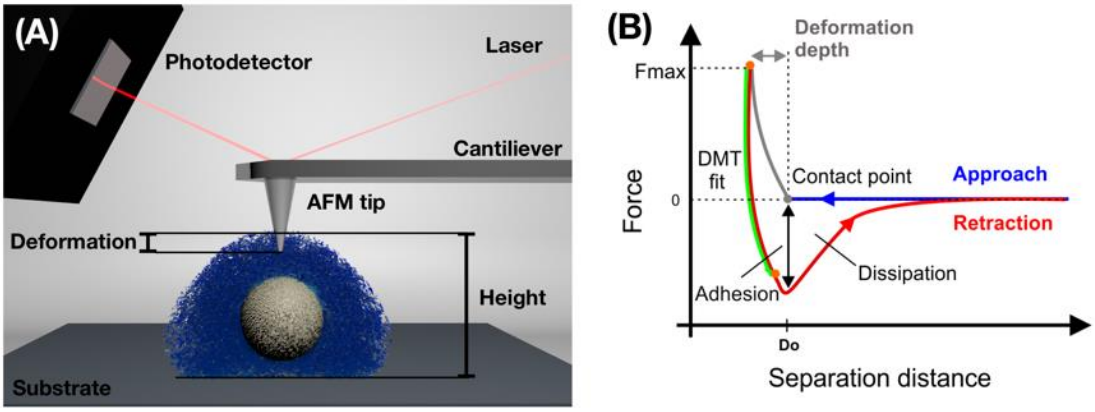

Figure 6. Schematic representation of the working principle of AFM in PeakForce QNM mode. **(A)** Key elements and parameters in the AFM tip indenting process. A very sharp tip attached at the end of a flexible cantilever indents at each point on the sample surface as the piezo is approach and retracted during a scan. If a calibrated cantilever is being used, then the vertical deflections of the cantilever can be recorded on a 4-segmented photodiode through the measurement of the reflections of a laser beam from the back of the cantilever. For the case of soft particles adhered on a hard substrate, and with a defined maximal force set point applied by the tip, a region can be scanned and the degree of deformation on soft material can be quantified. As shown in **(A)**, deformation and height of nanoparticles can be directly measured. **(B)** Representation of a typical force-separation curve from which physical parameters like height, deformation, adhesion, Young's modulus and dissipation can be obtained and mapped into 2D/3D reconstruction images. As the tip approaches the sample surface, the *contact point* defines the beginning of the interaction between tip and sample surface for a particular force set point. From the *contact point* the tip compresses the sample until it reaches the force set point at F_{max}. If a soft sample is investigated, the separation distance between *contact point* and F_{max}, is the *deformation depth* by the tip. A contrast in maps of surface topography or height and deformation is expected if a soft sample (i.e. soft nanoparticles) is imaged on a hard background (substrate). In the retraction curve from model force-separation curve, further withdrawal of the AFM tip after F_{max} has been reached, provides other useful information like *adhesion* between tip and sample and dissipation.

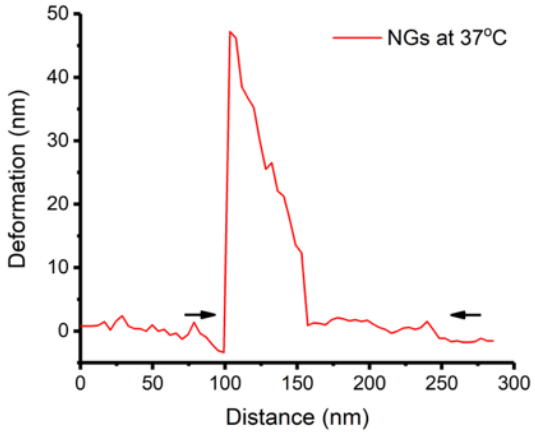

Figure 7. Cross section profile for deformation of NGs at 37 °C. The cross section is taken along a different direction as the one shown in the main text in Figure 3CIV, in order to better understand the different features of deformation on the NG. From the profile, is seems that deformation by the tip increases up to almost 50nm at the beginning of deformation by the tip and then suddenly drops almost entirely. The arrows indicate the lateral distance from where the NG response is obtained. A possible explanation for this, is that our 500pN force set point, could still be above the force threshold to damage and penetrate the NG structure.

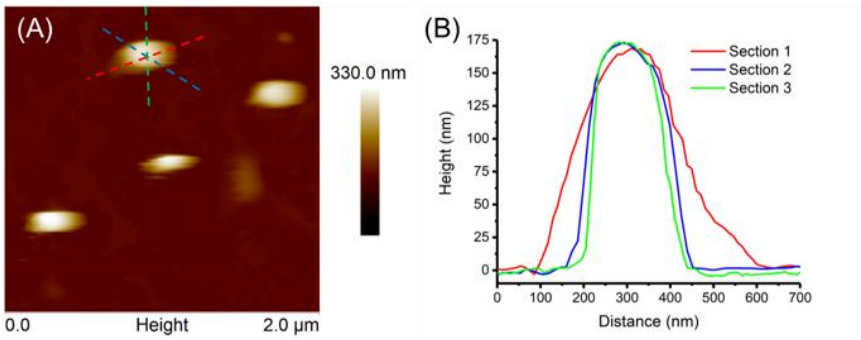

Figure 8. (A) Example of the cross-sections used for the statistic and **(B)** the corresponding profiles. In each particle, three cross-sections (always chosen in the same directions, two diagonal and one vertical to the mapping direction) were analyzed.

Nanoindentations:

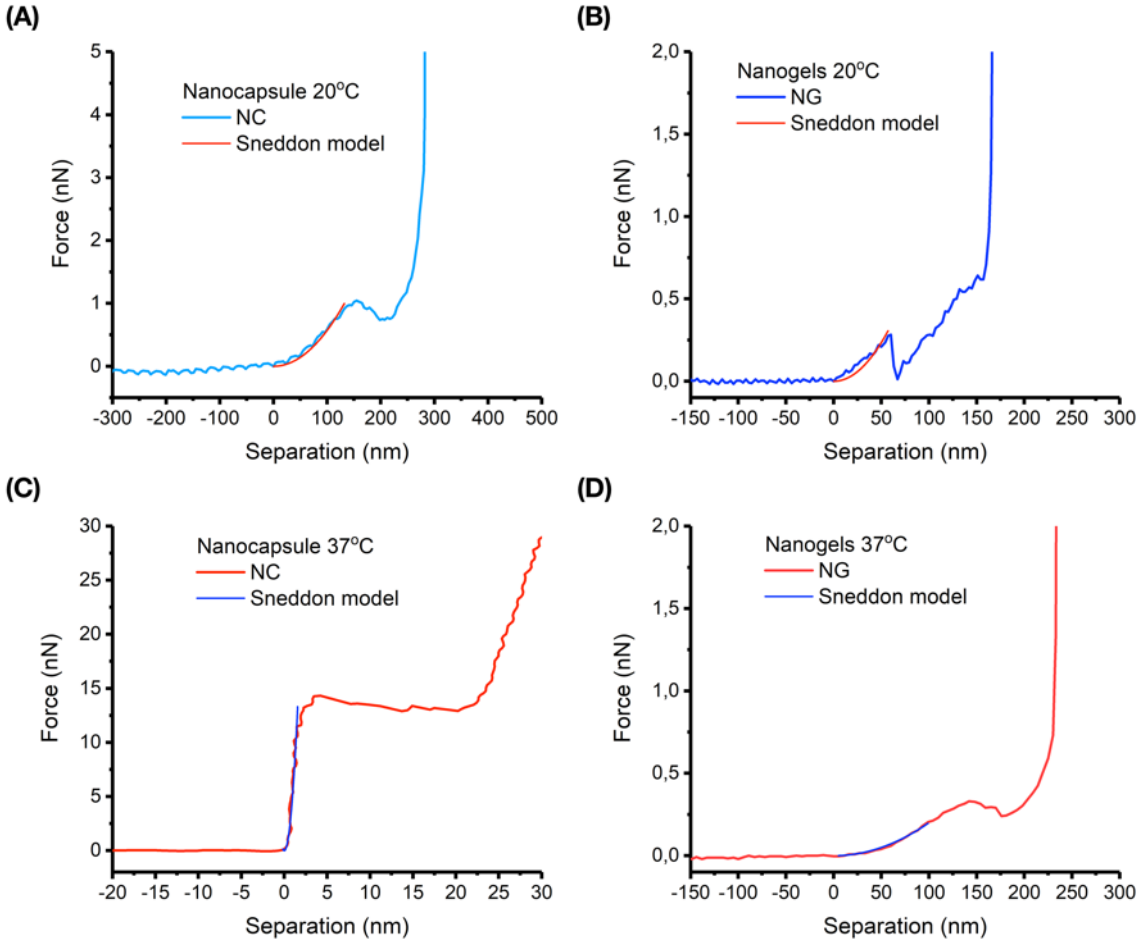

Figure 9. Force separation curves of NCs **(A, C)** and NGs **(B, D)** at 20 °C or 37 °C and their fit to the Sneddon model.

Finite element method: In order to describe the large displacement adequately, a distinction between current and reference frames needs to be done, as well as employing a continuum mechanical formulation suitable for providing accurate results under large deformations. We follow a well-established formulation and computational implementation based on the finite

element method.[3] All computations are established by using open-source packages and the codes are available to be used under the GNU public license.

The objective is to compute the displacement $\boldsymbol{u}$ in nm. As units we use kg for mass and s for time leading to nN for force and GPa for stress (energy density) as well as aJ (1 aJ = 10^{-18}J) for the energy. The displacement is a vector in space $\boldsymbol{X} \in \mathbb{R}^3$ and is used to compute the displacements of the continuum body occupying the region $\mathcal{B}$. By using an energy density, ψ in aJ/nm^3 = GPa, the structure is modeled by a scalar function. This approach is beneficial since energy, e, is a measurable quantity,

$$e = \int_{\mathcal{B}} \psi \, dV. \tag{1}$$

By using Castigliano's theorem, the force, $\boldsymbol{f}$ can be obtained, generating the displacement, $\boldsymbol{u}$, at the tip of the indenter

$$\boldsymbol{f} = \frac{\partial e}{\partial \boldsymbol{u}}. \tag{2}$$

We consider statics, i.e., the inertial effects are assumed to be negligible, since the mechanical loading is slow with respect to the response time of the material. In this case, the energy, e, needs to be minimized, this assertion is mathematically equivalent to constructing an action,

$$A = \int_{\mathcal{B}} \psi \, dV, \tag{3}$$

And setting its variation to zero, $\delta A = 0$. Furthermore, the deformation is induced by mechanical loading applied on the body. Related to the mechanical loading, effects of gravitational forces are negligible. The *variational* formulation based on the action principle in Eq. (3) can be further developed for describing the energy density by displacement. In mechanics, this energy density is called *stored* energy density indicating the reversible character of the underlying material. For the isothermal case, ψ is equivalent to the free energy density. Neglecting the viscous character of the underlying material; an elastic, brittle response in the nm length scale is expected. Moreover, this concentrated loading could lead to a sharp change in strain around the contact point. Therefore, a material model accurately capturing such a sharp change is needed, herein the so-called neo-Hookean energy density is employed

$$\psi = \frac{\lambda}{2} \ln\left(\det(F_{ij})\right)^2 + \mu\left(\frac{F_{ij}F_{ij}}{2} - \frac{\delta_{ii}}{2} - \ln\left(\det\left(F_{ij}\right)\right)\right), F_{ij} = \frac{\partial u_i}{\partial X_j} + \delta_{ij}, \tag{4}$$

With the material parameters, λ, μ. We use standard continuum mechanical notation and Einstein's summation convention over repeated indices. The deformation gradient, $\boldsymbol{F}$, gives the relation between the energy and the displacement, $\boldsymbol{u}$, defined as a function in space, $\boldsymbol{X}$, which is tantamount to the position of material particles at the "stress free" or reference frame. The simulation is started by using a spherical nanocapsule (in a collapsed state) being at the reference frame and apply a deformation along the x-axis mimicking the nanoindentation experiment. The pyramid indenter tip is approximated as a conical indenter such that the distribution of displacement at the contact point---the origin set at the contact point---between the indenter tip and material body can be approximated by using a Gaussian distribution:

$$u_x = d\exp\left(-\frac{(x^2+y^2)}{2\sigma^2}\right). \tag{5}$$

The contact radius, r_c, is used to utilize the standard deviation, $\sigma = r_c/2$. The simulation is started with a given small contact radius that is updated depending on the indentation depth, d, by means of the geometric relation for a cone, $r_c = d\tan(\alpha)$, with the constant tip angle set as $\alpha = 20\,°$ based on the specification of the indenter tip. The amplitude of the Gaussian distribution is set analogous to the experiments, in 60 s the amplitude reaches 10 nm: Implementation and computation are very challenging in the case of a so-called point force. The proposed distribution is an accurate model. For the description of the energy density in Eq. (4), the so-called Lame constants are used

$$\lambda = \frac{Ev}{(1+v)(1-2v)}, \mu = \frac{E}{2(1+v)}, \tag{6}$$

They are related to the engineering constants: Young's modulus, E, and Poisson's ratio, v. $E = 17.1$ GPa and $v = 0.45$ are used in order to mimic the experimental results (the used values are

the result from the nanoindentation of the representative NCs shown in the main article **Figure 5C**). Young's modulus is obtained with the aid of the Sneddon's solution and we expect to be able to justify the simplifications in this solution by comparing the computational and experimental results.
In order to solve $\delta A = 0$ with Eq. (3), the finite element method (FEM) is used with the aid of open-source packages developed under FEniCS project. Geometry is constructed in Salome and its triangulation is established by NetGen algorithm. Only a quarter of the spherical is used owing to the symmetry conditions. In **Figure 10**, the geometry and the regions for the symmetry conditions are shown.

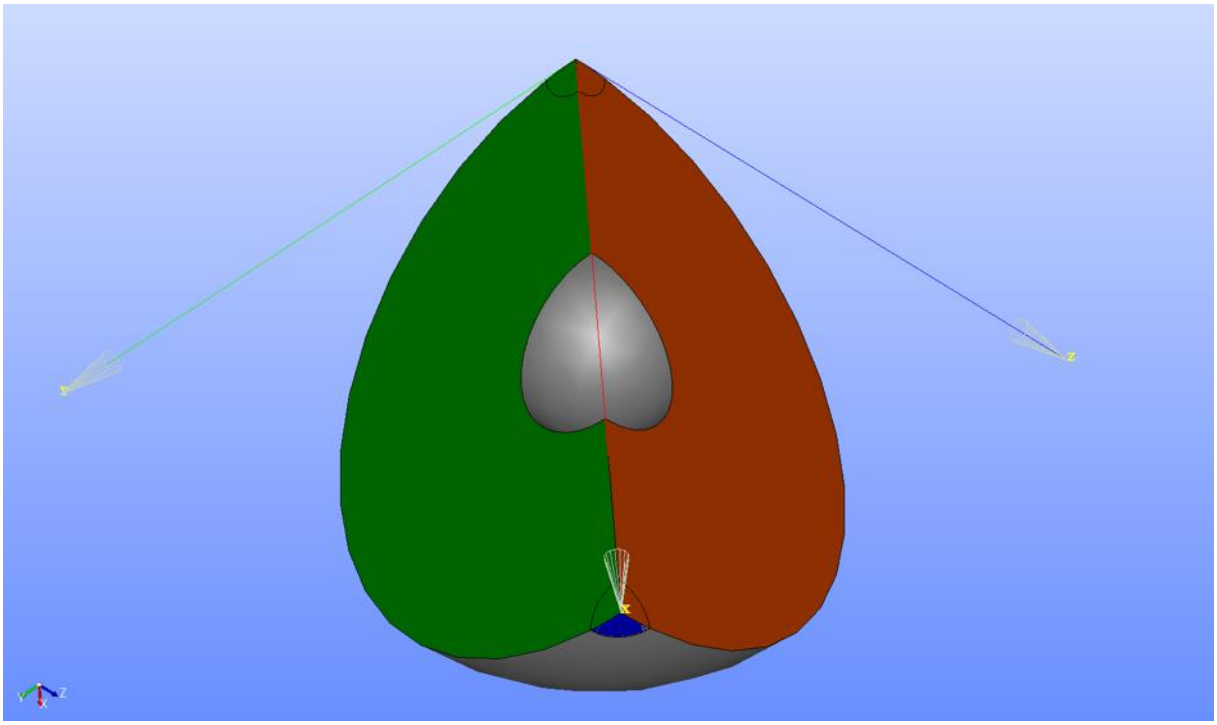

Figure 10. Geometry constructed and visualized in Salome. The quarter of the nanocapsule is simulated by applying symmetric boundary conditions along *x* on blue, along *y* on orange and along *z* on green surfaces.

The mesh out of tetrahedron elements are generated as in **Figure 11**. Around the contact point of the indentation tip, a gradually finer mesh is utilized.

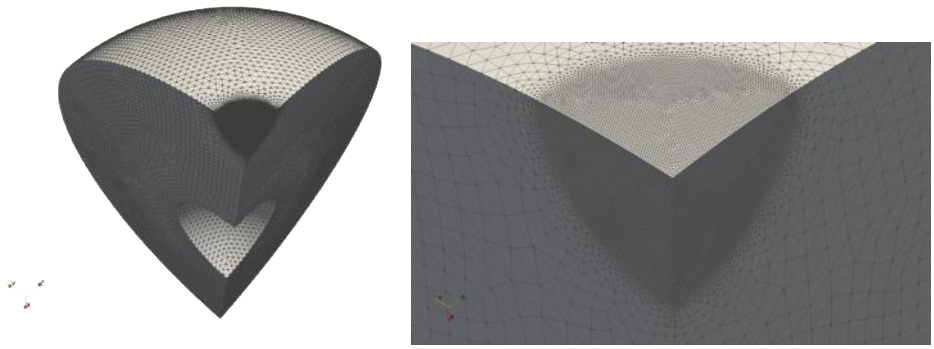

Figure 11. Mesh is generated by NetGen in Salome and visualized in ParaView. Left: computational domain. Right: a close up showing the finer mesh around the nanoindentation.

The computation of 429 531 degrees of freedom has been established in parallel on 6 Intel Xeaon E7-4850 v4 on Supermicro running Ubuntu Operating System in 2 hours of computation time by using a *conjugate gradient* type iterative solver with an *algebraic multigrid* preconditioner. For the simulation of 60 s, a time step of 0.5 s is chosen. Up to 10 nm is indented

by using the aforementioned distribution in Eq. (5). The displacement at the final time is visualized (without scaling) in **Figure 12** by using ParaView.

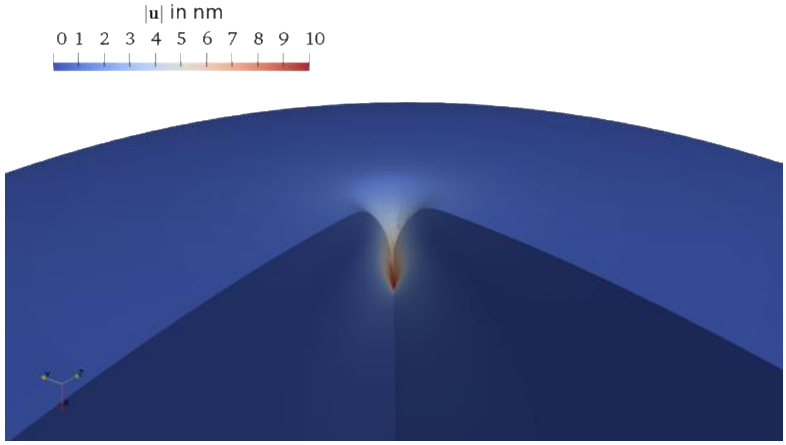

Figure 12. Displacement at the final time with amplitude of 10 nm. The close up around the origin is shown in ParaView by mirroring the solution for the sake of a better visualization. The colors denote the magnitude of displacement, whereas the displacement is shown without scaling.

The energy in the whole body is computed for each time step; the force at the contact point is extracted out of the energy by using Eq. (2).

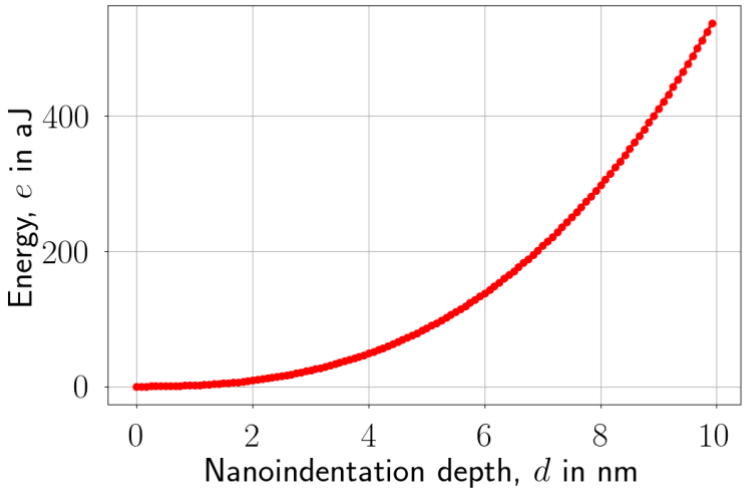

Figure 13. Energy versus nanoindentation depth.

1. Li, S.; Wang, J.; Zhao, S.; Cai, W.; Wang, Z.; Wang, S., Effect of surface modification and medium on the rheological properties of silica nanoparticle suspensions. *Ceramics International* **2016,** *42* (6), 7767-7773.
2. Dubbert, J.; Nothdurft, K.; Karg, M.; Richtering, W., Core-shell-shell and hollow double-shell microgels with advanced temperature responsiveness. *Macromol Rapid Commun* **2015,** *36* (2), 159-64.
3. Abali, B. E., *Computational Reality, Solving Nonlinear and Coupled Problems in Continuum Mechanics*. Advanced Structured Materials, Springer Nature, Singapore: 2017; Vol. 55.

6.1.2 Polyglycerol-based Thermoresponsive Nanocapsules Induce Skin Hydration and Serve as Skin Penetration Enhancer

E. R. Osorio-Blanco, F. Rancan, A. Klossek, L. Hoffmann, J. H. Nissen, J. Bergueiro, S. Hasenstab-Riedel, A. Vogt, E. Rühl, M. Calderón, *ACS Appl Mater Interfaces* **2020**.

Reprinted with permission from reference 147. Copyright 2020 American Chemical Society.
The supporting information is electronically available:
https://pubs.acs.org/doi/10.1021/acsami.0c06874?goto=supporting-info

Supporting Information

Polyglycerol-Based Thermoresponsive Nanocapsules Induce Skin Hydration and Serve as Skin Penetration Enhancer

Ernesto R. Osorio-Blanco[‡1], Fiorenza Rancan[‡2], André Klossek[3], Jan H. Nissen[4], Luisa Hoffmann[2], Julian Bergueiro[1,5], Sebastian Riedel[4], Annika Vogt[2], Eckart Rühl[3] and Marcelo Calderón*[1,6,7]

[1]Freie Universität Berlin, Institute of Chemistry and Biochemistry, Takustr. 3, 14195 Berlin, Germany.

[2]Clinical Research Center for Hair and Skin Science, Department of Dermatology and Allergy, Charité – Universitätsmedizin Berlin, Charitéplatz 1, 10117 Berlin, Germany.

[3]Freie Universität Berlin, Institute of Chemistry and Biochemistry Arnimallee 22, 14195 Berlin, Germany.

[4]Freie Universität Berlin, Institute of Chemistry and Biochemistry Fabeckstr. 34/36, 14195 Berlin, Germany.

[5]Centro Singular de Investigación en Química Biolóxica e Materiais Moleculares (CIQUS), Departamento de Química Orgánica, Universidade de Santiago de Comopostela, 15782 Santiago de Compostela, Spain.

[6]POLYMAT and Applied Chemistry Department, Faculty of Chemistry, University of the Basque Country, UPV/EHU, Paseo Manuel de Lardizabal 3, 20018 Donostia-San Sebastián, Spain.

[7]IKERBASQUE, Basque Foundation for Science, 48013 Bilbao, Spain.

‡ Authors contributed equally, co-first authorship.

*Corresponding author: marcelo.calderon@polymat.eu

Analytical Methods

Proton nuclear magnetic resonance (^{1}H-NMR)

The spectra were recorded by a Jeol ECX (400 MHz) spectrometer at concentrations between 5-20 mg/mL. The samples were dissolved in deuterated solvents (D_2O, ^{1}H: 4.79 ppm). The results were analyzed using the software MestReNova (version 7.1.2). The multiplicities are listed as follow: s (singlet), d (doublet), t (triplet), q (quartet), m (multiplet).

Fourier transform infra-red spectroscopy (FT-IR)

FT-IR spectra were recorded on a Jasco FT/IR-410 spectrometer (4000-500 cm^{-1}) and analyzed using Omnic software.

Dynamic light scattering (DLS)

Size distributions of NC were measured at various temperatures by dynamic light scattering (DLS) using a Zetasizer Nano-ZS 90 (Malvern, UK) equipped with a He-Ne laser (λ = 633 nm) under a scattering angle of 173°. For equilibration, samples with a concentration of 1 mg/mL were incubated at the desired temperature for 5 min prior to the measurement. Particle size distributions are given as the average of three measurements from intensity distribution curves.

Atomic Force Microscopy (AFM)

AFM measurements were recorded on a Multimode 8 microscope which was equipped with a Nanoscope V controller (Bruker Corporation). Freshly cleaved mica coated with 5 µL Poly-L-lysine (Sigma-Aldrich, MW: 70-150 kDa) solution was used as a substrate. After substrate preparation, 15 µL of highly diluted sample solution (10 µg/mL) was deposited on the substrate and incubated at room temperature for 15 minutes. Cantilever A, type SNL-10 from Bruker with a nominal tip radius of 2 nm and nominal spring constant of 0.35 N/m were used in these experiments to map the samples. Prior imaging, cantilevers were calibrated on the naked mica surface. A compression on mica was taken to extract the

cantilever sensitivity and then, the thermal noise method was used to derive its spring constant.[53] Imaging in soft tapping mode (sTM) was performed at room temperature in air. Imaging in PeakForce mode was carried out with a maximal applied force of 200 pN using a 512 points per line at a scan rate of 0.7 Hz. Image analysis was performed using NanoScope Analysis 1.5 software. All images were processed by the *Plane fit* program and the *flatten* tool (order 1) to correct from effects of bowing from the piezo movement. Measurements in the liquid phase were performed in a closed fluid chamber using Milli-Q water.

Cryogenic transmission electron microscopy (Cryo-TEM)

200 mesh grids covered with perforated carbon film (R1/4 batch of Quantifoil, MicroTools GmbH, Jena, Germany) were cleaned with chloroform and hydrophilized by 60 s plasma treatment at 8 W in a BAL-TEC MED 020 device (Leica Microsystems, Wetzlar, Germany). 4 µL aliquots of the sample solution were applied to the grid, blotted (blotting time: 4.5 s, drain time: 1 s) and subsequentially plunge frozen in liquid ethane by using of a Vitrobot Mark IV (Thermo Fisher Scientific Inc., Waltham, Massachusetts, USA). The vitrified samples were mounted on autogrids and transferred under liquid nitrogen into a 200 kV TALOS ARCTICA cryo transmissions electron microscope (Thermo Fisher Scientific Inc., Waltham, Massachusetts, USA) using the microscopes' autoloader system. 4096x4096 pixel images (binning 1) were acquired by a 4k Falcon III Direct Electron Detector (Thermo Fisher Scientific Inc., Waltham, Massachusetts, USA) at a nominal magnification of 29k, corresponding to a calibrated pixel size of 0.37 nm. The exposure time was 1.2 s.

Table S1: Reaction conditions of the screening for yielding dPG-PNIPAM SiO_2@NGs, the results of the reactions are described are marked with a **+** if stable SiO_2@NGs were formed and with a **-** if no SiO_2@NGs were formed. The amounts of NIPAM (67 mg), dPG (33 mg) and the initiator (3.3 mg) were kept constant throughout the screenings.

Initiator (mg)	**SDS (mg)**	**Temperature (°C)**	**Result**	**Average Size (nm); PDI**	**Yield (%)**	**Color in Figure S1**
APS	0	70	-	-	-	-
APS	1.8	70	-	-	-	-
APS/TEMED	1.8	r.t.	-	-	-	light brown
APS/TEMED	1.8	70	-	-	-	red
KPS	0	70	+	181; 0.12	35	blue
KPS	0.5	70	+	174; 0.18	20	dark green
KPS	1	70	+	169; 0.27	18	-
KPS	1.8	70	+	178; 0.24	13	green
KPS	5	70	-	-	-	light green
KPS/TEMED	0	r.t.	-	-	-	-
KPS/TEMED	1.8	r.t.	+	123; 0.31	6	-
AIBN (VA086)	1.8	r.t.	+	118; 0.26	6	magenta
AIBN (VA086)	1.8	70	-	-	-	purple

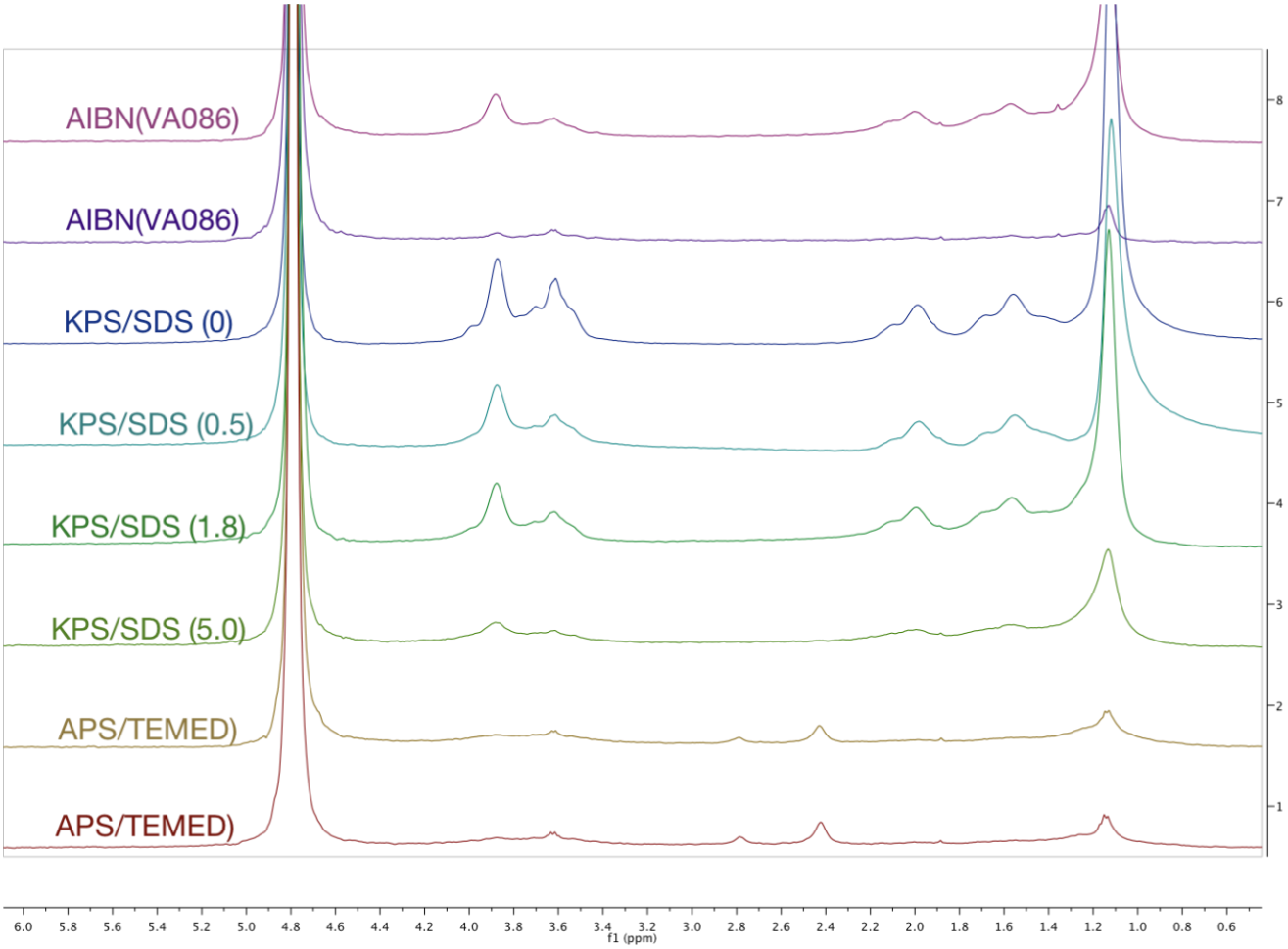

Figure S1: ^{1}H-NMR spectra from selected results from synthetic screenings: different initiator types and different SDS content (amount used is given in mg in the brackets). APS/TEMED was studied at r.t. (light brown) and at 70 °C (red). The AIBN (VA086) was used as UV-initiator at r.t. (magenta) and at 70 °C (purple).

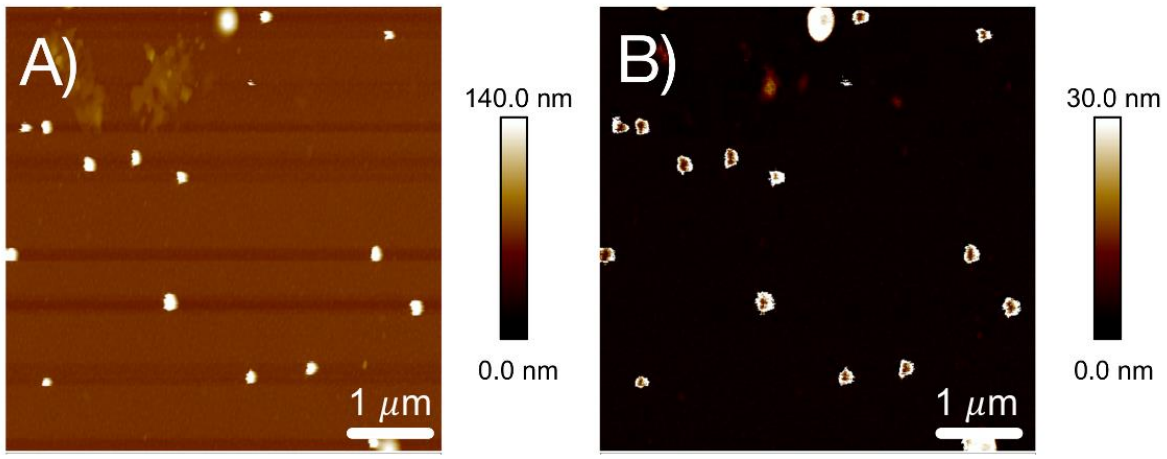

Figure S2: (A) Height image and (B) Deformation map of dPG-PNIPAM (A B) SiO_2@NGs imaged by AFM in PeakForce mode in the liquid phase.

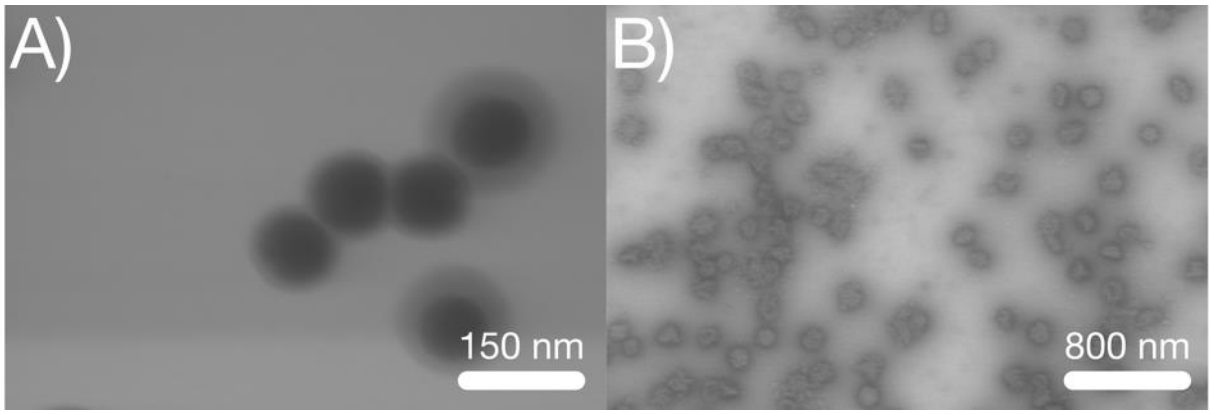

Figure S3: TEM images of dPG-PNIPAM-co-PNIPMAM (1:1) (A) SiO2@NGs and (B) NCs.

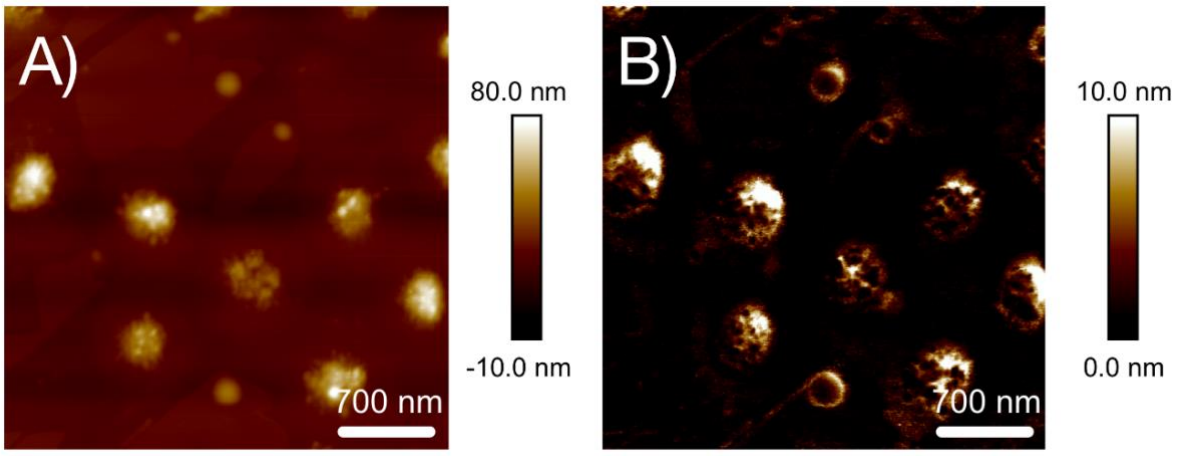

Figure S4: (A) Height image and (B) Deformation map of dPG-PNIPAM-co-PNIPMAM (1:1) NCs imaged by AFM in PeakForce mode in the liquid phase.

6.2 Publications

1. J. C. Cuggino[‡], **E. R. Osorio-Blanco**[‡], L. M. Gugliotta, C. I. Alvarez Igarzabal, M. Calderón, Crossing biological barriers with nanogels to improve drug delivery performance. *J Control Release* **2019,** *307*, 221-246.
2. **E. R. Osorio-Blanco**; J. Bergueiro; B. E. Abali; S. Ehrmann; C. Böttcher; A. J. Müller; J. L Cuéllar-Camacho; M. Calderón, Effect of Core Nanostructure on the Thermomechanical Properties of Soft Nanoparticles. *Chemistry of Materials* **2020,** *32* (1), 518-528.
3. **E. R. Osorio-Blanco**[‡], F. Rancan[‡], A. Klossek, J. H. Nissen, L. Hoffmann, J. Bergueiro, S. Riedel, A. Vogt, E. Rühl, M. Calderón, Polyglycerol-based Thermoresponsive Nanocapsules Induce Skin Hydration and Serve as Skin Penetration Enhancer. *ACS Appl Mater Interfaces* **2020**.
4. N. Tiwari, **E. R. Osorio-Blanco**, A. Sonzogni, D. Esporrin Ubieto, H. Wang, M. Calderón, Smart nanocarriers for skin applications: from basic studies to clinical development. Manuscript in preparation.

[‡]Equal contribution.

6.3 Conference Contributions

1. **E. R. Osorio-Blanco**, M. Giulbudagian, F. Rancan, A. Klossek, K. Yamamoto, J. Jurisch, F. Sahle, G. Yealland, S. Hedtrich, E. Rühl, U. Blume-Peytavi, A. Vogt, J. Lademann and M. Calderón, Thermoresponsive Nanogels as Cutaneous Delivery Systems. Wissenschaftsforum, Berlin, Germany, 2017, **Poster presentation**.
2. **E. R. Osorio-Blanco**, M. Giulbudagian, F. Rancan, K. Yamamoto, J. Jurisch, F. Sahle, G. Yealland, J. Bergueiro, S. Hedtrich, E. Rühl, A. Vogt, U. Blume-Peytavi, J. Lademann and M. Calderón, Thermoresponsive Nanogels and Nanocapsules for Dermal Delivery of Therapeutics. 6th Young Polymer Scientists Conference & 10th European Center for Nanostructured Polymers: International Conference on Nanostructured Polymers and Nanocomposites, San Sebastián, Spain, 2018, **Oral presentation and Poster presentation**.
3. **E. R. Osorio-Blanco**, S. Ehrmann, J. Bergueiro, C. Böttcher, R. Haag, J. L. Cuéllar-Camacho and Marcelo Calderón, Thermomechanical Properties of Thermoresponsive Nanogels, Core-shell Nanogels and Nanocapsules. XVI Simposio Latinoamericano de Polímeros & XIV Congreso Iberoamericano de Polímeros, Mar del Plata, Argentina, 2018. **Oral presentation**.
4. **E. R. Osorio-Blanco**, F. Rancan, A. Klossek, J. H. Nissen, J. Bergueiro, S. Riedel, A. Vogt, E. Rühl and M. Calderón, Thermoresponsive Nanocapsules for Skin Hydration. XIII Spanish-Portuguese Conference on Controlled Drug Delivery, Santiago de Compostela, Spain, 2020. **Poster Presentation**.
5. **E. R. Osorio-Blanco** and M. Calderón, Rational Development of Thermoresponsive Nanocapsules for Topical Drug Delivery. Virtual International Symposium on Nano-/Microgels, 2020. **Oral Presentation**.

6.4 Curriculum Vitae

For reasons of data protection, the curriculum vitae is not published in the electronic version.